

DRIVE SYSTEM DESIGN METHODOLOGY FOR A  
SINGLE MAIN ROTOR HEAVY LIFT HELICOPTER

A Thesis  
Presented to  
The Academic Faculty

By

Andrew T. Bellocchio

In Partial Fulfillment  
Of the Requirements for the Degree  
Masters of Science in Aerospace Engineering

Georgia Institute of Technology

December 2005

DRIVE SYSTEM DESIGN METHODOLOGY FOR A  
SINGLE MAIN ROTOR HEAVY LIFT HELICOPTER

Approved by:

Dr. Daniel P. Schrage, Advisor  
School of Aerospace Engineering  
*Georgia Institute of Technology*

Dr. Dimitri Mavris  
School of Aerospace Engineering  
*Georgia Institute of Technology*

Dr. David M. Sanborn  
School of Mechanical Engineering  
*Georgia Institute of Technology*

Date Approved: November 21, 2005

This thesis is dedicated to my wonderful and always supportive family. My beautiful wife, Katie, whose encouragement and love I treasure above all else. Her calming influence and unselfish support kept me focused throughout the school year. My daughters, Abby and Anna, are immeasurable fun and remind me to put the books down and enjoy life.

## **ACKNOWLEDGEMENTS**

Thank you to Dr. Daniel Schrage for his guidance over the past two years. I appreciate your encouragement to study a topic unique to rotorcraft design and your efforts in providing a wealth of resources to accomplish the task.

Thank you to the Committee member's Dr. Sanborn and Dr. Mavris, and all of the professors I have studied under. Their expertise and recommendations proved invaluable in the completion of course work and this thesis.

I am grateful to Dr. Robert Handschuh of the Vehicle Technology Directorate at the NASA Glen Research Center for providing resources on the Mi-26 split torque transmission and sharing his insight into the future of heavy lift rotorcraft.

Lastly, thank you to my fellow graduate students for outstanding teamwork in projects and in studying for exams. Thank you to Alex Moodie for tutoring me in the use of Model Center and system modeling.

# TABLE OF CONTENTS

<b>ACKNOWLEDGEMENTS .....</b>	<b>IV</b>
<b>LIST OF TABLES .....</b>	<b>IX</b>
<b>LIST OF FIGURES .....</b>	<b>XII</b>
<b>LIST OF SYMBOLS.....</b>	<b>XV</b>
<b>SUMMARY .....</b>	<b>XXII</b>
<b>SCOPE .....</b>	<b>1</b>
<b>MOTIVATION .....</b>	<b>3</b>
Need for a Joint Heavy Lift Helicopter .....	3
Square Cube Law .....	5
The Importance of Heavy Lift Drive Systems.....	9
<b>JHL BASELINE.....</b>	<b>11</b>
Government Furnished Baseline.....	11
Design Excursions .....	15
Design Space.....	17
<b>ASSUMPTIONS.....</b>	<b>19</b>
<b>METHODOLOGY .....</b>	<b>20</b>
Design Process.....	20
Methodology for the JHL .....	22
<b>WEIGHT ESTIMATION.....</b>	<b>25</b>
Solid Rotor Volume Method.....	25
Simple Gear Mesh.....	26
Composite Gear Systems .....	29
Boeing-Vertol Weight Formulae .....	31
RTL Weight Formulae.....	32
<b>GEARING .....</b>	<b>34</b>
Gear Fundamentals .....	34
Gear Failure Modes .....	37
Gear Types and Functions .....	41
Spur Gears in Helicopter Transmissions.....	42
Helical Gears in Helicopter Transmissions.....	43

Bevel Gears in Helicopter Transmissions .....	44
Face Gears in Helicopter Transmissions .....	47
Rating Spur and Helical Gears .....	49
Spur Gear Force Analysis .....	50
Helical Gear Force Analysis .....	52
Contact Stress .....	53
Allowable Contact Stress .....	57
Bending Stress .....	62
Allowable Bending Stress .....	65
Spur and Helical Gear Materials .....	66
Scuffing Hazard .....	68
Rating Bevel Gears .....	73
Bevel Gear Force Analysis .....	73
Contact Stress .....	76
Allowable Contact Stress .....	78
Bending Stress .....	80
Allowable Bending Stress .....	82
Bevel Gear Materials .....	82
Scuffing Hazard .....	85
<b>SHAFTING .....</b>	<b>86</b>
Simplified Shafting Model .....	86
Margin of Safety .....	89
Vibratory Bending Stress .....	90
Axial Tension Stress .....	91
Torsional shear stress .....	92
Critical Speeds .....	93
Nonuniform Shafts .....	94
Uniform Shafts .....	97
Shaft Materials .....	97
<b>GEARBOX COOLING .....</b>	<b>100</b>
<b>TRADITIONAL PLANETARY MODEL .....</b>	<b>103</b>
Drive Arrangement .....	105
Planetary Main Gearbox .....	107
Planetary Drive Modeling .....	108
Weight Estimation Results .....	110
<b>SPLIT TORQUE MODEL .....</b>	<b>112</b>
Drive Arrangement .....	113
Torque Split Drive Modeling .....	115
Weight Estimation Results .....	116
<b>RESPONSE SURFACE METHODOLOGY .....</b>	<b>120</b>
Overview .....	120
Planetary Drive RSM .....	121

Split Torque Drive RSM.....	124
<b>CONCLUSIONS .....</b>	<b>129</b>
<b>FUTURE WORK .....</b>	<b>132</b>
<b>APPENDIX A: JHL SUPPLEMENTAL PACKAGE EXTRACTS .....</b>	<b>134</b>
<b>APPENDIX B: SPUR-HELICAL GEAR RATING CALCULATIONS .....</b>	<b>140</b>
Spur-Helical Gear Summary.....	141
User Inputs and Selections.....	143
AGMA Stress Equations.....	145
Scuffing (Scoring) Summary .....	150
Lubrication Analysis.....	155
Material Properties.....	156
Bending Stress Geometry Factor .....	158
<b>APPENDIX C: BEVEL GEAR RATING CALCULATIONS.....</b>	<b>162</b>
Bevel Gear Summary.....	163
User Inputs and Selections.....	164
AGMA Stress Equations.....	165
Force Analysis .....	169
Bevel Gear Geometry .....	170
Material Properties.....	173
Bending Strength Geometry Factor .....	174
Pitting Resistance Geometry Factor .....	179
<b>APPENDIX C: SHAFT DESIGN CALCULATIONS.....</b>	<b>182</b>
Summary of Results.....	183
User Inputs and Selections.....	184
Margin of Safety .....	185
Critical Speed (Uniform Shaft).....	187
Critical Speed (Nonuniform Shaft).....	189
Total Load and Moments.....	194
Material Properties.....	195
<b>APPENDIX D: PLANETARY DRIVE CALCULATIONS.....</b>	<b>196</b>
Design Calculations .....	197
Weight Equations.....	201
Modified Solid Rotor Volume Weight Estimation .....	202
Force Feed Oil Cooling.....	204
Minimum Weight Solution .....	205
<b>APPENDIX E: SPLIT TORQUE DRIVE CALCULATIONS .....</b>	<b>206</b>
Design Calculations .....	207
Weight Equations.....	210
Modified Solid Rotor Volume Weight Estimation .....	211

<b>APPENDIX F: MODEL FIT FOR PLANETARY DRIVE.....</b>	<b>212</b>
<b>APPENDIX G: MODEL FIT FOR SPLIT TORQUE DRIVE .....</b>	<b>216</b>
<b>REFERENCES.....</b>	<b>220</b>



## LIST OF TABLES

Table 1: Design Excursions E1-E3 .....	16
Table 2: Design Excursions E4-E7 .....	16
Table 3: Design Space .....	18
Table 4: K Factors for Gears.....	28
Table 5: Gear Types and Applications.....	41
Table 6: Overload Factor Values .....	55
Table 7: Spur-Helical Gear Steels.....	67
Table 8: MIL Lubricant Mean Scuffing Temperatures.....	72
Table 9: Scuffing Risk .....	73
Table 10: Bevel Gear Load Face .....	74
Table 11: Bevel Gear Reliability Factors.....	80
Table 12: Spur-Helical Gear Steels.....	84
Table 13: Shaft Material Properties .....	98
Table 14: Sample Cooler Design .....	101
Table 15: Planetary Drive Weight Estimate Results.....	110
Table 16: Planetary Baseline Design Summary.....	111
Table 17: Split Torque Drive Weight Estimate Results.....	118
Table 18: Split Torque Baseline Design Summary.....	119
Table 19: Baseline Planetary Drive RSE Input Variables .....	123

Table 20: Split Torque RSE Baseline Inputs .....	126
Table 21: Split Torque Model Fit Comparison.....	127
Table 22: Total Drive System Weight Method Summary .....	131
Table 23: JHL Baseline Aircraft Data .....	135
Table 24: Example JHL Substantiation .....	136
Table 25: JHL Baseline Tabulated Data .....	137
Table 26: JHL Baseline Power vs. Airspeed Data 0 to 110 knots .....	138
Table 27: JHL Baseline Power vs. Airspeed Data 120 knots or more.....	139
Table 28: Spur-Helical Gear Summary.....	141
Table 29: Spur-Helical User Inputs and Selections .....	143
Table 30: Spur-Helical AGMA Stress Equations .....	145
Table 31: Spur-Helical Gear Scuffing .....	150
Table 32: Spur-Helical Lubrication Analysis .....	155
Table 33: Spur-Helical Gear Properties.....	156
Table 34: Spur-Gear Bending Strength Geometry Factor for Pinion .....	158
Table 35: Spur Gear Bending Strength Geometry Factor for Gear .....	160
Table 36: Bevel Gear User Inputs and Selections .....	163
Table 37: Bevel Gear AGMA Stress Equations .....	165
Table 38: Bevel Gear Force Analysis .....	169
Table 39: Bevel Gear Geometry .....	170
Table 40: Bevel Gear Material Selection.....	173
Table 41: Bevel Gear Bending Strength Geometry Factor .....	174
Table 42: Bevel Gear Pitting Resistance Geometry Factor .....	179

Table 43: Shafting Summary of Results .....	183
Table 44: Shafting User Inputs and Selections .....	184
Table 45: Shafting Margin of Safety Calculations .....	185
Table 46: Shafting Critical Speed Calculations (Uniform Shaft) .....	187
Table 47: Shafting Critical Speed Calculations (Nonuniform Shaft) .....	189
Table 48: Shafting Total Load and Moments Calculations .....	194
Table 49: Shafting Material Properties Database .....	195
Table 50: Planetary Design Calculations .....	197
Table 51: Planetary Drive Weight Equations .....	201
Table 52: Planetary Drive Solid Rotor Volume Weight Estimations .....	202
Table 53: Planetary Drive Force Feed Oil Cooling .....	204
Table 54: Planetary Drive Minimum Weight Solution .....	205
Table 55: Split Torque Drive Design Calculations .....	207
Table 56: Split Torque Weight Equations .....	210
Table 57: Split Torque Modified Solid Rotor Volume Weight Estimation .....	211
Table 58: RSE Model Fit for Planetary Drive .....	213
Table 59: RSE Model Fit for Split Torque Drive .....	217

## LIST OF FIGURES

Figure 1: The Future Combat System.....	4
Figure 2: Square Cube Law Block.....	5
Figure 3: Square-Cube Law Predictions of Weight verse Torque.....	8
Figure 4: Single Main Rotor JHL .....	12
Figure 5: Single Main Rotor JHL 3-View Drawing .....	14
Figure 6: Design Process .....	20
Figure 7: Furnished Baseline Drive System Configuration.....	24
Figure 8: Gear Nomenclature.....	34
Figure 9: Tooth Action.....	37
Figure 10: Bending Stress.....	38
Figure 11: Compressive Stress .....	39
Figure 12: Gear Tooth Stress vs. Power .....	40
Figure 13: Example Spur Gear .....	42
Figure 14: Example Helical Gear .....	43
Figure 15: Helical Gear Terminology.....	44
Figure 16: Bevel Gear Terminology .....	46
Figure 17: Example Spiral Bevel Gear .....	46
Figure 18: Face Gear Terminology.....	47
Figure 19: Example Face Gear .....	48

Figure 20: Free Body Diagram of a Simple Gear Train .....	50
Figure 21: Helical Gear Free Body Diagram.....	53
Figure 22: Dynamic Factor .....	56
Figure 23: Pitting Resistance Stress Cycle Factor, $Z_N$ .....	59
Figure 24: Minimum J Along the Involute Profile .....	63
Figure 25: Geometry Factor for Helical Gears .....	64
Figure 26: Modifying Factor for J for Different Mating Gears .....	65
Figure 27: Bending Strength Stress Cycle Factor, $Y_N$ .....	66
Figure 28: Contact Temperature Along the Line of Action.....	69
Figure 29: Calculated Flash Temperature Along the Line of Action .....	71
Figure 30: Bevel Gear Tooth Forces.....	74
Figure 31: Finding the Bevel Gear Geometry Factor, I.....	78
Figure 32: Loading Diagram for y-Direction.....	87
Figure 33: Sample Shaft Moment Diagram.....	88
Figure 34: Mathematical Model of Nonuniform Shaft.....	95
Figure 35: Nonuniform Shaft Bending .....	95
Figure 36: Typical Main Gearbox Lubrication System .....	102
Figure 37: HLH Drive System Arrangement.....	103
Figure 38: HLH Aft Transmission.....	104
Figure 39: Drive System Components.....	105
Figure 40: Example Optimized 2-Stage Planetary Gearbox.....	107
Figure 41: Planetary Drive in Model Center.....	109
Figure 42: Mi-26 Main Gearbox.....	113

Figure 43: Mi-26 Main Gearbox Arrangement.....	114
Figure 44: Split Torque in Model Center.....	116
Figure 45: Drive System Weight vs. Final Reduction Ratio .....	117
Figure 46: Planetary Drive Screening Test Pareto Chart.....	122
Figure 47: Planetary Drive RSE Model Fit.....	124
Figure 48: Split Torque Screening Test Pareto Chart.....	125
Figure 49: Initial Split Torque RSE Model Fit .....	127
Figure 50: Split Torque Final RSE Model Fit .....	128

## LIST OF SYMBOLS

$a, A$	Area
$A$	Distance along an involute tooth profile
Access	Accessory Drive
$a_{mr}$	Adjustment factor for main rotor
$a_{tr}$	Adjustment factor for tail rotor
$B$	Bearing
$b$	Number of planets
BH	Brinnell Hardness
$b_i$	Coefficient for first order terms
$b_{ii}$	Coefficients for pure quadratic terms
$b_{ij}$	Coefficients for cross-product terms
$c$	Application factor or radius where stress is calculated
$C$	Gear constant
$C_f$	Surface condition factor
$C_H$	Hardness ratio factor
$C_p$	Elastic coefficient
$C_p$	Specific heat of oil
$C_{xc}$	Crowning factor for bevel contact stress
$d$	Pinion pitch diameter or inner shaft diameter
$D$	Gear pitch diameter or outer shaft diameter
$d_G$	Gear diameter

$d_p$	Pinion diameter
$d_s$	Drive system
$d_{sh}$	Drive shafting
$E$	Modulus of elasticity
Eng	Engine
$F$	Force or net face width
$f_a$	Axial tension stress
$f_b$	Vibratory bending stress
$F_{en}$	Endurance limit stress
fpm	Feet per minute
$f_s$	Torsional shear stress
$F_{sy}$	Shear yield stress
$F_{ty}$	Tensile yield stress
$G$	Gear
$g$	gravity acceleration
gb	Gearbox
HP	Horsepower
$HP_{rated}$	Rated horsepower
$HP_{ratedDrive}$	Drive System Rated Power
$HP_{req}$	Horsepower Required
HRC	Hardness Rockwell C
$I$	Geometry factor for pitting resistance
$I$	Moment of inertia



in	Inch
J	Geometry factor for bending stress
J	Polar moment of inertia
K	Surface durability factor
k	Total endurance factor
$K_b$	Bending stress concentration factor
$K_B$	Rim thickness
$K_m$	Load distribution factor
$K_o$	Overload factor
$K_R$	Reliability factor
$K_s$	Size factor
$K_s$	Torsional stress concentration factor
$k_t$	Configuration factor
$K_T$	Temperature factor
$K_v$	Dynamic factor
L	Desired life or shaft length
$L_{ab}$	Line of action
lb	Pound
$L_{dr}$	Horizontal distance between rotor hubs
M	Bending moment or oil flow
max	Maximum
$m_c$	Contact ratio
$m_G$	Gear reduction ratio

$m_N$	Load sharing ratio
$M_o$	Overall ratio
MR	Main Rotor
MS	Margin of Safety
$m_s$	Ratio of planet to sun gear
N	Number of teeth
n	Speed (rpm)
$N_c$	Critical speed
$N_{cycles}$	Number of cycles
$n_{dsh}$	Number of drive shafts excluding rotor shaft
$n_{gb}$	Number of gearboxes
$n_p$	Pinion speed
OC	Oil Cooler
p	Circular pitch
P	Diametral pitch or planet gear
$P_{nd}$	Normal diametral pitch
psi	Pounds per square inch
$p_x$	Axial pitch
Q	Heat generated
q	Number of contacts per revolution
$Q_v$	Transmission quality number
r	radial distance of the desired stress point on shaft
R	Ring gear or response of interest

$r, R$	Pinion and gear pitch radii
$R_{99}$	Reliability constant for 1 failure in 100
$R_c$	Rockwell Hardness (C)
Redux	Stage Reduction Ratio
$R_{el}$	Reliability constant
rpm	Rotations per minute
S	Sun gear
$s_{ac}$	Allowable contact stress
$s_{at}$	Allowable bending stress
$s_c$	Contact stress
$S_F$	Safety factor for bending stress
$S_H$	Safety factor for contact stress
$s_t$	Bending stress
$S_{ut}$	Ultimate tensile strength
T	Torque or kinetic energy
$t_c$	Contact temperature
$t_{fl}$	Flash temperature
Th	Thrust
$t_M$	Bulk temperature
$T_{mrgb}$	Ratio of transmission hp to main rotor rpm
$t_{oil}$	Oil temperature
$T_{oilavg}$	Average oil temperature
$T_{oilin}$	Oil in temperature

$T_{oilout}$	Oil out temperature
TR	Tail Rotor
$T_{trgb}$	Ratio of tail rotor power to tail rotor rpm
V	Potential energy
v	Volume
W	Weight or total force
$W_a$	Axial force or thrust load
$w_i$	Lumped weight
$W_r$	Radial force
$W_t$	Tangential force or transmitted load
$x_{ij}$	Independent variable
y	Shaft deflection
$y_i$	Element deflection
$Y_N$	Stress cycle factor for bending stress
$z_{mr}$	Number of stages in main rotor drive
$Z_N$	Stress cycle factor
$\Delta T$	Temperature rise across gearbox
$\mu$	Poisson's ratio
v	Coefficient of variation
$\phi$	Pressure angle
$\phi_t$	Transverse pressure angle
$\psi$	Helix angle
$\Delta T$	Temperature rise

$\varepsilon$	Error term
$\eta$	Efficiency
$\omega$	shaft frequency

## SUMMARY

The transformation of Joint forces to be lighter, more lethal, and capable of deploying from multiple dispersed locations free of prepared landing zones will widen a capability gap that cannot be met by the current fleet of Joint aircraft. In order to close this capability gap, a dedicated heavy lift VTOL aircraft must rapidly deliver large payloads, such as the 20 to 26 ton Future Combat System, at extended ranges in demanding terrain and environmental conditions.

Current estimates for a single main rotor configuration place the design weight over 130,000 pounds with an installed power of approximately 30,000 horsepower. Helicopter drive systems capable of delivering torque of this magnitude succeeded in the Russian Mi-26 helicopter's split-torque design and the Boeing VERTOL Heavy Lift Helicopter (HLH) prototype's traditional multi-stage planetary design. The square-cube law and historical trends show that the transmission stage weight varies approximately as the two-thirds power of torque; hence, as the size and weight of the vehicle grows, the transmission's weight becomes an ever-increasing portion of total gross weight. At this scale, optimal gearbox configuration and component design holds great potential to save significant weight and reduce the required installed power.

The presented drive system design methodology creates a set of integrated tools to estimate system weight and rapidly model the preliminary design of drives system components. Tools are provided for gearbox weight estimation and efficiency, gearing, shafting, and lubrication and cooling. Within the same architecture, the designer may add

similar tools to model subcomponents such as support bearings, gearbox housing, freewheeling units, and rotor brakes.

Measuring the relationships between key design variables of these components and system performance metrics reveals insight into the performance and behavior of a heavy lift drive system. A parametric study of select design variables is accomplished through an intelligent Design of Experiments that utilizes Response Surface Methodology to build a multivariate regression model. The model permits visualization of the design space and assists in optimization of the drive system preliminary design.

This methodology is applied to both the Boeing HLH and the Russian Mi-26. Both designed in the late 1970's, the tandem rotor HLH fails to take full advantage of the tremendous benefits gained by dividing the input torque into multiple, high speeds paths and then recombining the split paths at the final stage. The Mi-26 has successfully employed a split torque gearbox in the field for over 20 years. This study applies the drive system design methodology to compare the split-torque gearbox over a multi-stage planetary gearbox in a single main rotor heavy lift helicopter.

## **SCOPE**

The scope of this thesis includes the furnished single main rotor baseline design and drive system requirements, drive system configuration for a multi-stage planetary main gearbox and a split-torque main gearbox, weight estimation, and preliminary design tools for the following drive components:

1. Gearboxes
2. Shafting
3. Gearbox cooling
4. Accessory accommodation

A designer has the freedom to incorporate additional analysis into the model.

Some recommended elements that should be included for a complete preliminary design include:

1. Bearings
2. Housing
3. Keyways
4. Seals
5. Couplings
6. Structural integration
7. Failure warning and health systems

The thesis obtains the impact of excursions through a Design of Experiments (DoE) and utilizes Response Surface Methodology (RSM) to explore the response behavior of the drive system through the



design space defined by excursions (E1, E2, E4, E5, and E6). The thesis limits the study to:

1. Single main rotor helicopter
2. Specified design space
3. Simplified rotor loads
4. Accessory accommodation

# MOTIVATION

## *Need for a Joint Heavy Lift Helicopter*

The military and commercial industries have great need for a heavy lift VTOL aircraft capable of transporting large payloads over longer distances and at a high rate of speed. Current transport fixed wing aircraft require large runways and support facilities, thus severely restricting a military commander's or commercial operations officer's freedom. The heavy lift VTOL aircraft fills a capability gap by providing heavy lift capability at high speeds independent of large runways.

For the military, the transport of large payloads is possible with fixed wing aircraft such as the C-130, C-141, or C-5. These assets, however, have their limitations as they are tied to fixed-base operations and large runways. A commercial airline experiences the same trade off within its fleet of commercial transport airplanes. The modern V-22 achieves a new degree of freedom through its vertical take-off capability and high-speed cruise though it cannot lift large payloads. The largest heavy lift helicopter in the world, the Mi-26, is capable of transporting the requisite 20-ton payload but is restricted from shipboard operations and reaches only 150 knots. There is not an aircraft in existence that can couple the freedom gained by VTOL, a high cruise speed, and a high payload capacity.

This mission is further detailed in the Draft Version 6.1 of the Initial Capabilities Document of the Joint Heavy Lift (JHL) Supplemental Package and is summarized by the associated Statement of Objectives:

“The JHL is expected to overcome enemy anti-access strategies, execute joint-enabled operational maneuver, and leverage sea basing in order to expand Expeditionary Maneuver Warfare capabilities. It [JHL] is also expected to achieve positional advantage to maintain operational momentum; enable SOF infiltration & exfiltration operations; conduct mounted and dismounted vertical envelopment; and perform aerial delivery operations.”<sup>1</sup>

The military is searching for new ways to provide a rapid, flexible response in a hostile environment without being dependent upon runways. Furthermore, the military is looking for a way to bypass traditional points of embarkation in exchange for the flexibility to operate directly from ships. The overall goal is to transport light combat vehicles at payloads, ranges, and speeds beyond what is considered feasible for traditional helicopters. The heaviest payload includes the Future Combat System (FCS) at a weight of 20-26 tons (see Figure 1). Despite the Mi-26’s success, there exists no shipboard capable rotorcraft with the payload capacity, cruise speed and range to accomplish this mission.



**Figure 1: The Future Combat System**

---

<sup>1</sup> Aviation Applied Technology Directorate, “Joint Heavy Lift Supplemental Package: Statement of Objectives” (Fort Eustis: AATD, 4 November, 2004), 1.

## Square Cube Law

The square-cube is a mathematic principle of proportion that is often applied to engineering and biomechanics. The square-cube law states “when an object undergoes a proportional increase in size, its new volume is proportional to the cube of the multiplier and its new surface area is proportional to the square of the multiplier.”<sup>2</sup> This proportional increase is illustrated in Figure 2.

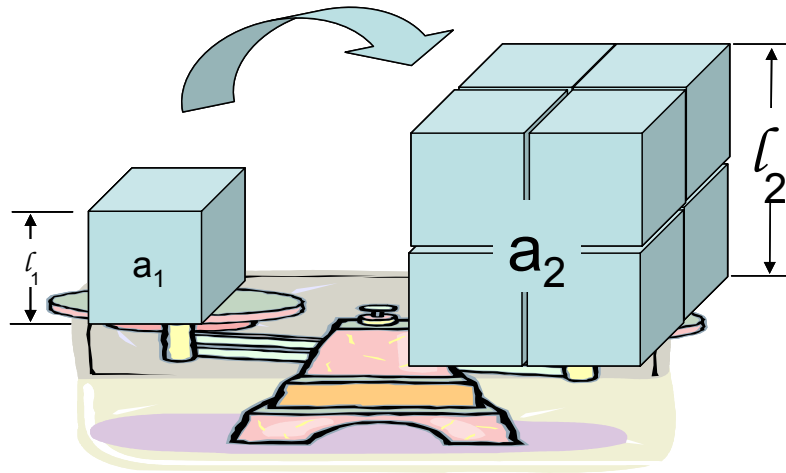


**Figure 2: Square Cube Law Block**

Relating volume to area will mathematically express this law as:

$$v_2 = v_1 \left( \frac{\lambda_2}{\lambda_1} \right)^3 \quad \text{and} \quad a_2 = a_1 \left( \frac{\lambda_2}{\lambda_1} \right)^2$$

### **Equation 1**

where

$l_1$  is the original length and  $l_2$  is the new length

$v_1$  is the original volume and  $v_2$  is the new volume

---

<sup>2</sup> Wikipedia website, [http://en.wikipedia.org/wiki/Square-cube\\_law](http://en.wikipedia.org/wiki/Square-cube_law), 1 August, 2005.

$a_1$  is the original surface area and  $a_2$  is the new surface area

For example, if the length,  $l_1$ , of a cube shown in Figure 2 is doubled in length to  $l_2$ , the cube's surface area is increased by  $2^2$  or by a factor of 4. For volume, if  $l_2$  is doubled, then volume increases by  $2^3$  or 8 times the cube's original volume.

By equating the expressions in Equation 1 and considering constant material, uniform density, and constant speed (for rotating components such as gears, shafts, and bearings) the square-cube law may be expressed as:

$$W_2 = W_1 \left( \frac{T_2}{T_1} \right)^{3/2}$$

**Equation 2**

where

$W_1$  is the original weight and  $W_2$  is the new weight  
 $T_1$  is the original torque and  $T_2$  is the new torque required

This relationship has a tremendous impact on the engineering of structures and mechanical systems such as mechanical power transmitting drive trains. As the size or torque transmitted of the drive system increases, the system mass will outpace the torque change at an exponential rate. This application of the square-cube law provides a general guideline to the resizing of mechanical systems as a function of the torque of 1.50 (Equation 2). In fact, the AMCP 706-201 predicts new gear stage weight as a power of 1.43.<sup>3</sup>

---

<sup>3</sup> Headquarters, U.S. Army Material Command, AMC Pamphlet 706-201 Engineering Design Handbook: Helicopter Engineering (Part One: Preliminary Design) (Alexandria: GPO, 1974), 4-66.

The AMCP approximates gear stage weight as:

$$W_{stage_2} = W_{stage_1} \left( \frac{T_2}{T_1} \right)^{1.43}$$

**Equation 3**

According to the AMCP, the change in shafting weight is an even more dramatic power of 2.63:

$$W_{shaft_2} = W_{shaft_1} \left( \frac{T_2}{T_1} \right)^{2.63}$$

**Equation 4**

An increase in weight against the change in torque required is shown graphically for Equation 2, Equation 3, and Equation 4 in Figure 3.

At higher and higher relative torque, a drive system grows enormous in size and especially weight. If carried to the extreme, the size of a system will reach a practical limit where the system will be unable to support itself and buckle under its own massive weight. Such limits are common in the civil engineering of a skyscraper's structure. For aerospace engineering, the aircraft structure or drive system may never reach such an extreme point, but the design will certainly reach a practical limit where the generated lift cannot sustain flight of the aircraft's large gross weight.

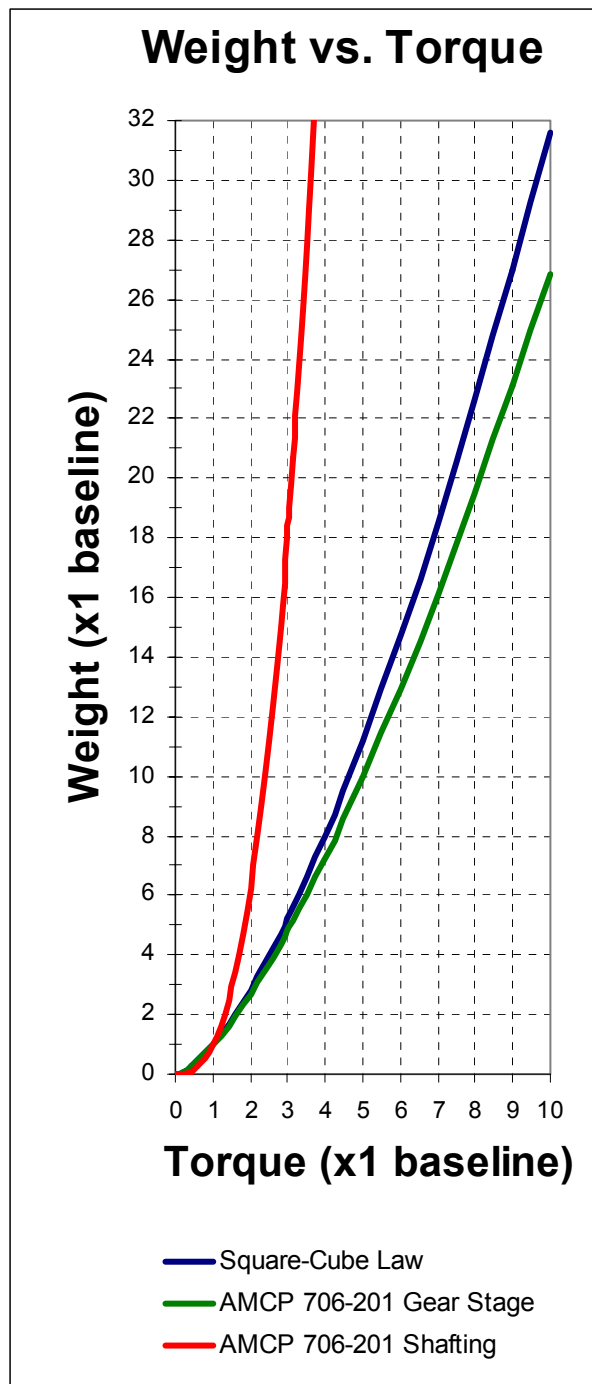


Figure 3: Square-Cube Law Predictions of Weight verse Torque

## **The Importance of Heavy Lift Drive Systems**

Current estimates for a single main rotor heavy lift configuration place the design weight over 130,000 pounds with an installed power of approximately 30,000 horsepower. At such high gross weights and loads, the drive system becomes an ever-increasing percentage of the aircraft gross weight.

For heavy lift rotorcraft and drive systems, increasing total lift exacerbates this exponential weight increase. To generate sufficient lift, the rotorcraft requires a larger power plant and either more lifting rotors or larger rotor blades. Either condition increases drive system weight. Adding more rotors is an alternative method to avoiding high single torque values and excessively heavy components; however, much of this benefit is lost by duplicate gearing and heavy cross shafting.

Increasing the rotor blade radius presents a different set of problems in the quest for additional lift. With the tip speed of rotor blades fixed constant by compressible flow limits, a larger rotor demands slower rotor rotational speed (rpm). Slower rotational speed requires a greater drive system reduction ratio and results in higher torque values at the end of the drive train. Drive systems capable of higher torque values demand larger and heavier gears, shafting, and bearings. Dividing the torque into multiple paths and combining the torque at the end of the drive train may avoid a portion of this gear and shafting weight gain. Such a system is called a split-torque design and is explored in this study as an alternative to traditional planetary gearing. Despite the benefits of a split-torque, a final reduction to the slower rotation speed is inevitable. Split-torque designs cannot eliminate the heavy gearing and support bearings at the last stage but may lessen the severity of the total system weight gain.



The use of face gearing to combine the split torque paths, however, does hold promise to further mitigate the weight gain in the last stage. Unfortunately, the gearing community has yet to standardize face gear stress formulas<sup>4</sup>—removing face gear drives from consideration for this preliminary design model. Despite the current immaturity of face gear standardization, an optimized split-torque drive utilizing spur and bevel gears still holds great potential to save significant weight and reduce the required installed power.

---

<sup>4</sup> F.L. Litvin et al, NASA/CR-2000-209909 Handbook on Face Gear Drives With a Spur Involute Pinion (NASA, March 2000), 48.

## **JHL BASELINE**

As part of the JHL's Concept Design and Analysis (CDA) effort, the government has solicited industry to assist in "the conceptual design of a baseline VTOL platform configuration and the exploration of the technical trade space associated with that concept."<sup>5</sup> The CDA's focus is on "the substantiation of viable design concepts" within the desired trade space that "have a reasonable chance of achieving TRL 6 by 2012."<sup>6</sup> The aircraft's trade space shall meet the desired capabilities described in the Draft Initial Capabilities Document (ICD) and the design flight profile as defined in the Model Performance Specification (MPS). Additionally, the CDA will assess the impact of a set of excursions from the design baseline. This thesis strives to provide insight into the performance and behavior of a heavy lift drive system within the CDA bounds.

### **Government Furnished Baseline**

To assist in the CDA development and to provide a common starting point, the government has furnished conceptual sizing and performance data for a single main rotor helicopter configuration (extracted information relative to the thesis is included in APPENDIX A: JHL SUPPLEMENTAL PACKAGE EXTRACTS). The work of this

---

<sup>5</sup> Aviation Applied Technology Directorate, "Joint Heavy Lift Supplemental Package: Statement of Objectives," (Fort Eustis: AATD, 4 November, 2004).

<sup>6</sup> Aviation Applied Technology Directorate, "Joint Heavy Lift Supplemental Package: Statement of Objectives," (Fort Eustis: AATD, 4 November, 2004).

study is to provide a preliminary design and optimization of the drive system as defined by the furnished single main rotor baseline. This baseline aircraft is a traditional single main rotor helicopter design with a five-bladed main rotor and classic anti-torque tail rotor as shown in Figure 4.



**Figure 4: Single Main Rotor JHL<sup>7</sup>**

The power plant consists of three scaleable turbine engines with the drive system combining engine torque at the main gearbox. A long, segmented shaft transmits torque to the tail rotor intermediate gearbox that supplies a direction change at the base of the

---

<sup>7</sup> Wayne Johnson, "Heavy Lift Rotorcraft Plans and Status" (Ames Research Center: NASA, 8 June, 2004).

vertical tail. A shorter shaft connects the intermediate gearbox with the tail rotor gearbox. Figure 5 on the next page shows the 3-view drawing of the furnished, single main rotor baseline aircraft.

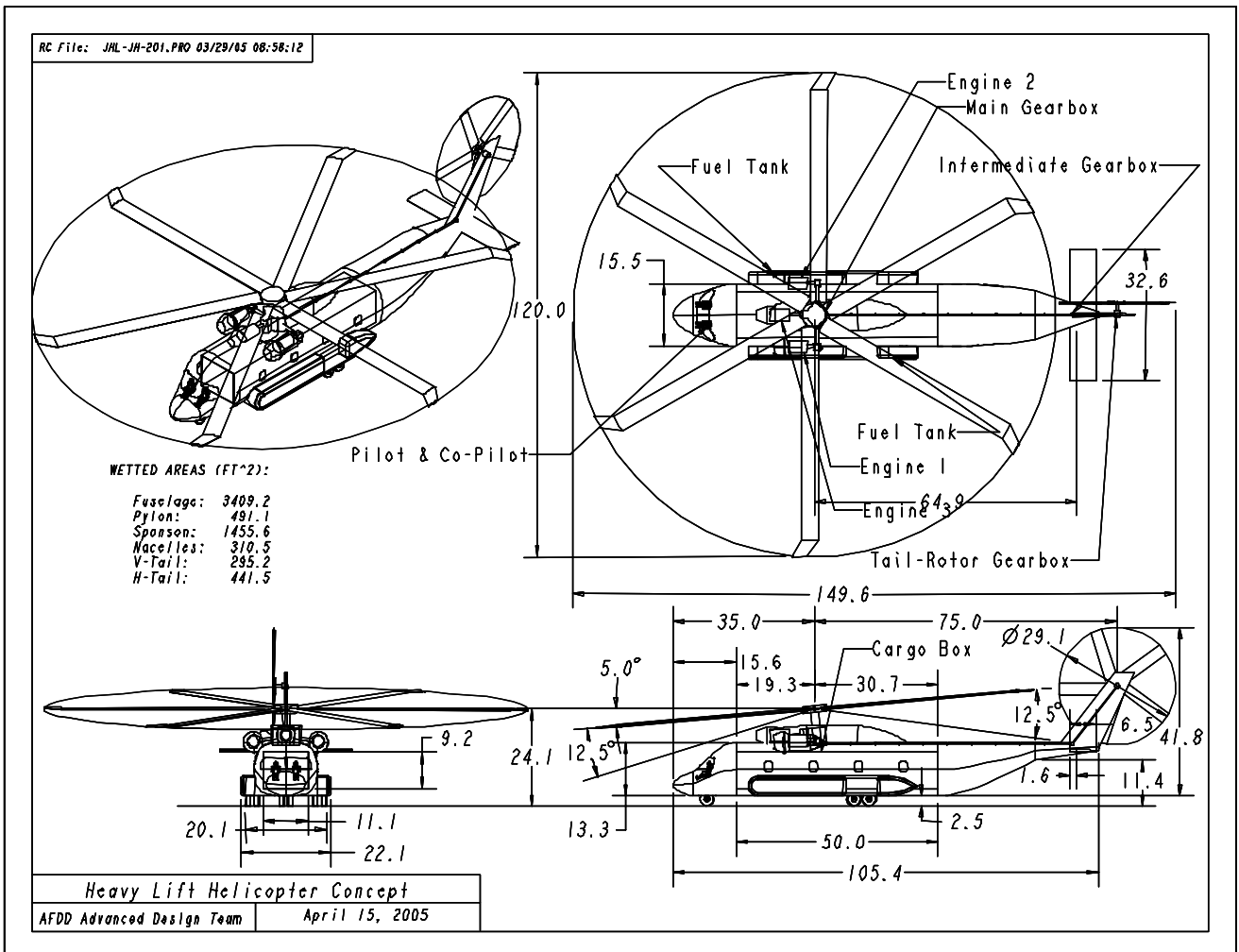


Figure 5: Single Main Rotor JHL 3-View Drawing<sup>8</sup>

<sup>8</sup> Aviation Applied Technology Directorate, "Joint Heavy Lift Supplemental Package: Government Furnished Information Listing, Sample Data Formats, JHL Baseline Drawings," (Fort Eustis: AATD, November 4, 2004).

## **Design Excursions**

Seven design excursions or alternate sizes from the baseline shall assist in the understanding of varying user design requirements. The purpose of the excursions is to provide trade space information to assess the impact of changing user requirements. The design excursions vary one mission parameter at a time (underline variables represent the baseline design values):<sup>9</sup>

1. Design Payload Excursion: 16 ton, 20 ton, 26 ton
2. Design Radius Excursion, 210 nm, 250 nm, 400 nm, 500 nm
3. Design Hi/Hot Excursion: 4,000'/95°F, 6,000'/95°F

These excursions serve as the basis to the formulation of the design space for the drive system design in this thesis. The seven excursions are summarized in Table 1 and Table 2 below. Further information is in found throughout APPENDIX A: JHL SUPPLEMENTAL PACKAGE EXTRACTS and especially in Table 23 and Table 24.

---

<sup>9</sup> Aviation Applied Technology Directorate, "Joint Heavy Lift Supplemental Package: Contract Data Requirements List A005 Block 16 Remarks Continuation Sheet," (Fort Eustis: AATD, November 4, 2004).

**Table 1: Design Excursions E1-E3<sup>10</sup>**

Design	Baseline	E1	E2	E2A*	E3
Payload	20	<i>16</i>	<i>26</i>	<i>26</i>	20
Radius	250	250	250	250	<i>210</i>
High/Hot, 1000ft/deg F	4k/95	4k/95	4k/95	4k/95	4k/95
Design Gross Weight	138,868	<i>114,035</i>	177,392	xxx,xxx	xxx,xxx
Engine Size, shp	10,985	<i>9,114</i>	13,912	xxx,xxx	xxx,xxx
Drive Rating (TO rpm), shp	25,964	<i>21,420</i>	33,011	xx,xxx	xx,xxx

\*E2A has larger cargo box size to fit FCS Full Combat Configuration. All others have standard cargo box size to fit FCS Essential Combat Configuration.

*Italics* are variation from baseline design variable. *Blue* is low variation. *Red* is high variation.

**Table 2: Design Excursions E4-E7**

Design	Baseline	E4	E5	E6	E7*
Payload	20	20	20	20	20
Radius	250	<i>400</i>	<i>500</i>	250	250
High/Hot, 1000ft/deg F	4k/95	4k/95	4k/95	<i>6k/95</i>	4k/95
Design Gross Weight	138,868	172,197	<i>206,501</i>	148,606	xxx,xxx
Engine Size, shp	10,985	13,495	<i>16,066</i>	13,113	xx,xxx
Drive Rating (TO rpm), shp	25,964	30,642	<i>35,469</i>	27,567	xx,xxx

\*E7 must be shipboard compatible. All others are shipboard capable.

*Italics* are variation from baseline design variable. *Blue* is low variation. *Red* is high variation.

---

<sup>10</sup> Aviation Applied Technology Directorate, "Joint Heavy Lift Supplemental Package: Government Furnished Information Listing, Sample Data Formats, JHL-Design Excursions Description Capabilities," (Fort Eustis: AATD, November 4, 2004).

The baseline, E1, E2, E3, E4, E5, and E6 provide valid trade space on changing payload, radius, and hi/hot atmosphere. For simplicity, the study will omit excursions E2A (larger cargo box) and E7 (shipboard capable), as it does not measure payload, radius, or atmospheric performance. E3 is also excluded, as sufficient data is unavailable.

### **Design Space**

The Joint Heavy Lift Supplemental Package provides sufficient information to establish a baseline drive system specific design space. Data arises from the tables in APPENDIX A: JHL SUPPLEMENTAL PACKAGE EXTRACTS or from calculations from the same data. A few calculations are:

1. A constant tip speed of 725 ft/s and rotor diameter allowed the calculation of the main rotor speed.
2. Main rotor thrust is the product of the constant disc loading at 12.3 lb/ft<sup>2</sup> and the provided effective disk area.
3. An examination of the scaleable NASA high tech turbine engine for heavy lift gave an approximate speed range from 10,000 to 20,000 rpm.



**Table 3: Design Space**

<b>Symbol</b>	<b>Metric</b>	<b>Units</b>	<b>Low</b>	<b>Baseline</b>	<b>High</b>
$HP_{reqMR}$	Main Rotor Power Required	hp	<i>14,000</i>	22,247	<i>27,000</i>
$HP_{reqTR}$	Tail Rotor Power Required	hp	<i>1,500</i>	1,989	<i>3,200</i>
$HP_{engMRP}$	Engine Maximum Rated Power	hp	9,114	10,985	16,066
$HP_{reqAccess}$	Accessory Power Required	hp	<i>60</i>	120	<i>180</i>
$n_{MR}$	Main Rotor Speed	Rpm	90	115	130
$n_{TR}$	Tail Rotor Speed	Rpm	375	476	530
$n_{eng}$	Engine Speed	Rpm	<i>10,000</i>	<i>15,000</i>	<i>20,000</i>
$Th_{MR}$	Main Rotor Thrust	lb	111,156	139,113	206,480

*Italics indicate estimates.*

When data was lacking, estimated values were selected to best represent a feasible range. Estimates originate from a comparison to other aircraft (mainly the Boeing HLH and Mi-26), extrapolation using the square cube law, and engineering judgment. The design space as shown in Table 3 established the bounds for the analysis conducted in the remaining sections.

# ASSUMPTIONS

Major assumptions for the thesis include:

1. Scaling for aircraft excursions follows square-cube law
2. Design space extremes are in appropriate and valid ranges
3. Reference Heavy Lift NASA High Tech Engine deck for engine output speed
4. Tail rotor tip speed equals main rotor tip speed (725 ft/s)
5. Design of excluded components (bearings, splines, keyways, seals, etc) does not significantly impact the transmission design
6. Estimate accessory power requirements
7. Simplified model for rotor loads on main and tail rotor drive shafts
8. Detailed geometry complies with baseline drawings
9. Shipboard compatible and folding/stowage shall not impact drive system design with the exception of a rotor brake
10. Main rotor and tail rotor shafts are nonuniform while all others are uniform with bearings to absorb loading

# METHODOLOGY

## Design Process

The preliminary design and optimization is a three step process (Figure 6) of:

1. Drive System Configuration
2. Drive System Weight Estimate
3. Capture Responses and Conclusions

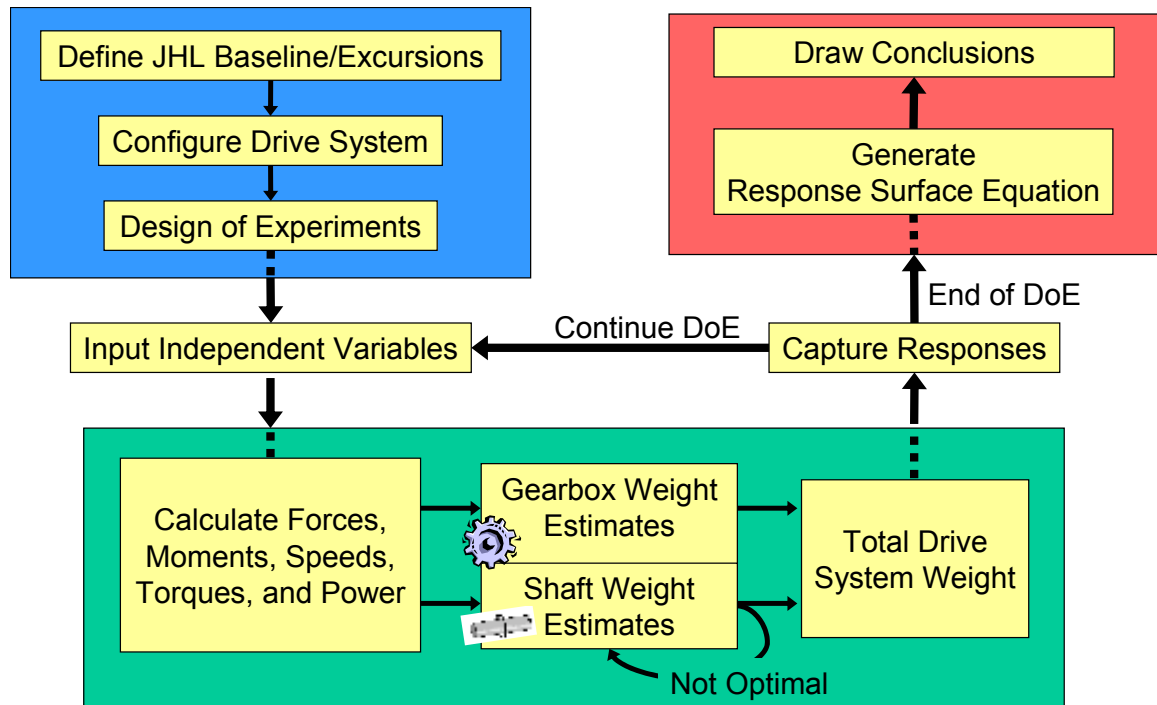


**Figure 6: Design Process**

The first step, Drive System Configuration (upper left box), involves defining the supplied Single Main Rotor (SMR) JHL configuration. Associated with this is a

component layout to include selection of gearboxes and shafting connecting gearboxes. Next, a screening test selected the major design parameters that most influence the drive system behavior. Once identified, the combinations of key design parameters constitute a Design of Experiments (DoE). Each independent design parameter is varied within the defined design space and in accordance with the DoE.

The middle step (shown as a bottom box), models the actual drive system response for a particular set of inputs. The Weight Estimates section contains three drive system weight estimate methods (modified solid rotor volume, Boeing-Vertol, and Research Technology Laboratories). Here, a designer has the option to model all drive system components similar to the gearing, shafting, and gearbox cooling tools in the Appendices. The accuracy of the weight estimates and the integration of each toolbox to provide a functional, weight-optimized design is the most crucial step in generating realistic solutions.

The final step, Capture Responses and Conclusions (upper right box), captures the output responses for each configuration and uses Response Surface Methodology to determine system behavior. For every set of design parameters, output responses for the solution shall be captured and used to generate a Response Surface Equation (RSE). With the RSE constructed, a family of optimized solutions maybe provided for the drive system. The RSE shall also enable the design to quickly evaluate the impact of changing design parameters through the design process. The accuracy of the weight RSE maybe judged against the two well establish weight estimates as well as compared to similar aircraft like the Mi-26 or CH-53.







## **Methodology for the JHL**

According to Lynwander, “the function of a gearbox is to transmit rotational motion from a driving prime mover to a driven machine.”<sup>11</sup> In the case of a helicopter, the driver is one or more turbine engines and the driven members include lifting rotors, anti-torque device, and any mechanically driven accessories. A drive system is composed of a series of gears linked together by shafting, supported by bearings, enclosed and mounted by housing, and lubricated and cooled by oil.

The following key principles support the drive system design:

1. Transmission loads are a function of power and speed: ( $T = \text{HP}/\text{rpm}$ )
2. Input rpm is fixed by output speed of engine
3. Rotor speed is a function of blade tip speed and rotor diameter
4. Best to take largest reductions in the final stage

Most of the transmission elements can be broken down into:

1. Gears 
2. Shafting 
3. Bearings 
4. Freewheel units (clutches) and Rotor Brake 
5. Lubrication systems 
6. Housing 

---

<sup>11</sup> Peter Lynwander, Gear Drive Systems Design and Application (New York: Marcel Dekker, 1983), iii.

Each of these components can be designed into toolboxes, represented by an icon, that will analyze forces, size the component, and select the correct configuration. For the demonstration of this methodology in the planetary and split torque gearboxes, only gearing, shafting, and gearbox cooling are included. The designer has the freedom to integrate toolboxes as needed. The above list is the suggested minimum for a complete preliminary design.

For the included toolboxes, gear capacity is derived from American Gear Manufacturer's Association (AGMA) standards and includes gear type selection in a variety of external and internal arrangements, evaluation of axial and radial loading, sizing for bending and compressive stress (pitting), and reduced scoring hazard. Shafting withstands simultaneous axial tension stress, vibratory bending stress, and torsional shear stress while ensuring appropriate operation away from critical speeds. Lubrication absorbs gearbox-generated heat through a series of independent splash and force feed oil systems.

The overall system configuration is defined in the government furnished JHL baseline. Figure 7 shows the drive system layout as derived from the furnished 3-view drawings. Included are suggested toolboxes for a complete preliminary design.

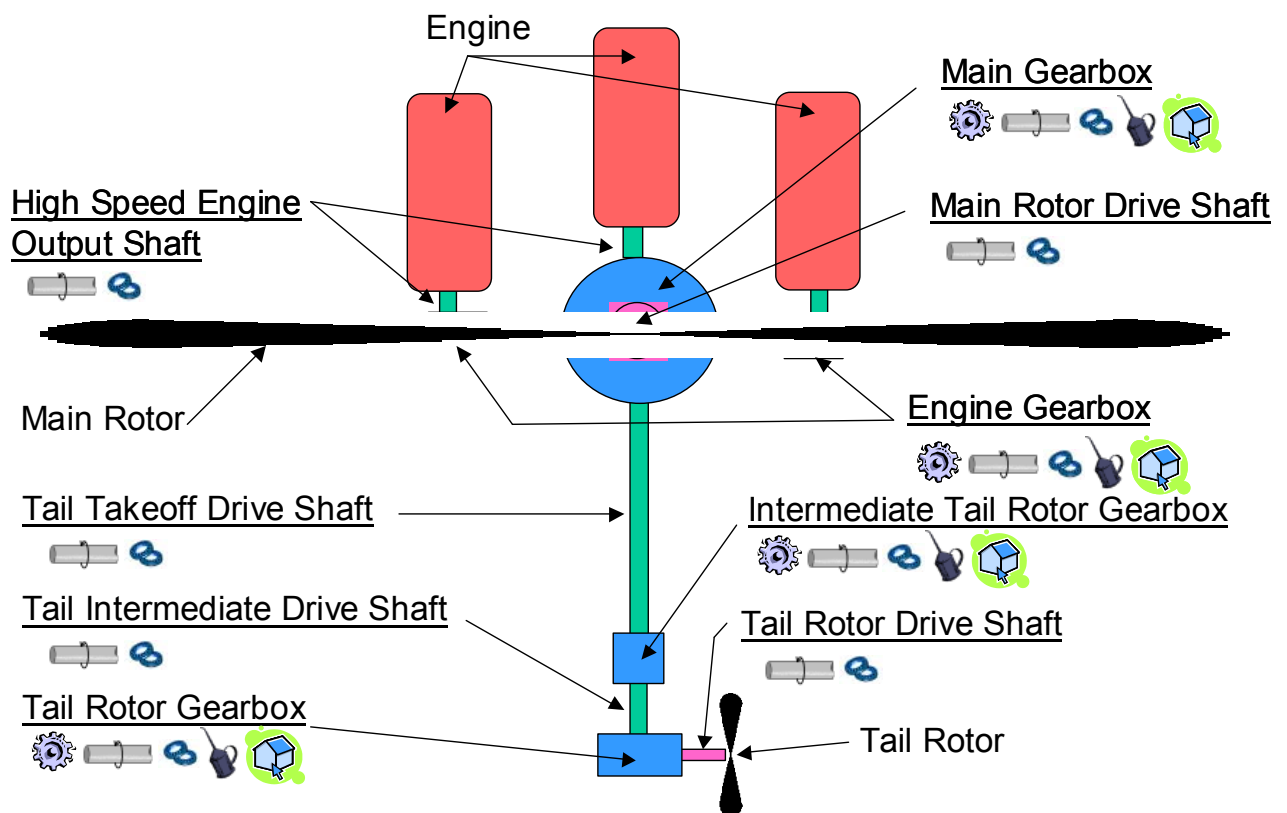


**Figure 7: Furnished Baseline Drive System Configuration**

## WEIGHT ESTIMATION

Three different weight estimation methods are calculated for iterations in the planetary and split torque gearbox model. The solid rotor volume by Willis assumes gear weight is proportional to the solid rotor volume ( $Fd^2$ ) and uses the surface durability factor K for computation.<sup>12</sup> The next two methods are weight equations taken from a NASA sponsored comparative study of Soviet vs. Western helicopters (1983).<sup>13</sup> The weight equations are from Boeing-Vertol and Research Technology Laboratories (RTL) as cited in the NASA study. The comparative study's Soviet set of equations were from Tishchenko's Soviet Weight Formulae; however, his estimation had to be excluded because the formulae as shown were for tandem helicopters only.

### **Solid Rotor Volume Method**

R.J. Willis's solid rotor volume weight estimation method provides a simple way to estimate gearbox weight and select the optimal reduction ratio in multiple stage drives. The method assumes the weight of a gear drive is "proportional to the solid rotor volume

---

<sup>12</sup> R.J. Willis, "New Equations and Chart Pick Off Lightest-weight Gears," Product Engineering v. 34, n.s. 2 (January 21, 1963): 64.

<sup>13</sup> W.Z. Stepniewski and R.A. Shinn, NASA TR 82-A-10 A Comparative Study of Soviet vs. Western Helicopters: Part 2-Evaluation of Weight, Maintainability and Design Aspects of Major Components (Ames Research Center: AVRADCOM Research and Technology Laboratories, 1983).



( $Fd^2$ ) of the individual gears in the drive”<sup>14</sup> and that a surface durability factor,  $K$ , of each mesh is constant. The method is explained in Willis’s “Lightest-weight Gears” published in *Product Engineering* in 1963.<sup>15</sup> Similar methods are outlined in Dudley’s Handbook of Practical Gear Design (1994) and in AGMA 911-A94, *Information Sheet-Design Guidelines for Aerospace Gearing* (1994).

## Simple Gear Mesh

The solid rotor volume maybe expressed as:

$$Fd_p^2 = \frac{126,000HP}{Kn_p} \left( \frac{m_G + 1}{m_G} \right) = \frac{2T}{K} \left( \frac{m_G + 1}{m_G} \right)$$

### Equation 5

where

$F$  is pinion face  
 $d_p$  is pinion diameter  
 $HP$  is horsepower  
 $K$  is surface durability factor  
 $n_p$  is the pinion speed  
 $m_G$  is reduction ratio  
 $T$  is torque

The solid rotor volume of the gear is proportional to the gear ratio squared:

$$Fd_G^2 = Fd_p^2 m_G^2$$

### Equation 6

---

<sup>14</sup> R.J. Willis, “New Equations and Chart Pick Off Lightest-weight Gears,” *Product Engineering* v. 34, n.s. 2 (January 21, 1963): 64.

<sup>15</sup> R.J. Willis, “New Equations and Chart Pick Off Lightest-weight Gears,” *Product Engineering* v. 34, n.s. 2 (January 21, 1963): 64-75.

The total weight of a gearbox is a function of the sum of solid rotor volume of each gear. For a simple pinion-gear mesh:

$$\sum Fd^2 = Fd_p^2 + Fd_G^2$$

**Equation 7**

Combining Equation 5, Equation 6, and Equation 7 yields:

$$\sum Fd^2 = \frac{2T}{K} \left( \frac{m_G + 1}{m_G} \right) + \frac{2T}{K} \left( \frac{m_G + 1}{m_G} \right) m_G^2$$

**Equation 8**

For ease of notation, let:  $C = 2T / K$ . Equation 8 can reduce to:

$$\sum \frac{Fd^2}{C} = 1 + \frac{1}{m_G} + m_G + m_G^2$$

Values for the surface durability factor, K, are listed in Table 4.

**Table 4: K Factors for Gears**

Application	Service Characteristics		Hardness		PLV	Accuracy	K factor lb/in <sup>2</sup>
	Driver	Driven	Pinion	Gear			
Aircraft* (single pair)	Engine	Auxiliary Drive	58 Rc	58 Rc	10,000	High ground	1,000
Aircraft* Planetary	Engine	Propeller	58 Rc	58 Rc	3,000 – 10,000	Ground	600
Carburized Aerospace Gears <sup>#</sup>			58 Rc	58 Rc	10,000 and beyond	Ground	500-600

\* for helical and spur gears listed by Willis

<sup>#</sup> listed by AGMA 911-A94 for aerospace carburized and case hardened gears

According to Willis, estimating actual weight is possible by multiplying the total gearbox solid rotor volume by an application factor, c, where c is 0.25 to 0.30 for aircraft application.<sup>16</sup> This weight factor assumes magnesium or aluminum casings, limited life design, high stress levels, and rigid weight controls—all properties that are included in the drive system design of the JHL.

$$W_{gearbox} = c \sum Fd^2$$

**Equation 9**

One of the advantages of the solid rotor method is that the estimated weight includes the entire gearbox with housing, bearings, oil, and gear shafting; thus, the weight of an entire drive system maybe quickly calculated by the sum of the gearbox weights

---

<sup>16</sup> R.J. Willis, “New Equations and Chart Pick Off Lightest-weight Gears,” Product Engineering v. 34, n.s. 2 (January 21, 1963): 70.

and the total shafting weight (as calculated in section SHAFTING on page 86). The accuracy of the weight estimation is a product of the accuracies of the K factor and the application weight factor, c.

## **Composite Gear Systems**

In addition to the weight estimation, Willis details a means to determine the optimal stage reduction ratio that provides the lightest overall weight for the gear system. Most of the stage reduction ratio optimization employs a series of graphs that is not conducive to computer modeling.

Epicyclic or planetary systems may also be optimized with the solid rotor volume method. For a planetary gearset, let:

$$m_s = \frac{d_p}{d_s} = \frac{M_o}{2} - 1$$

**Equation 10**

where

$m_s$  is ratio between planet and sun gear  
 $M_o$  is overall ratio  
P is planet gear subscript  
S is sun gear subscript  
R is ring gear subscript

If  $b$  represents the number of planets (or branches) in the gearset, then the sun gear volume is:

$$Fd_s^2 = \frac{2T}{bK} \left( \frac{m_{G1} + 1}{m_{G1}} \right)$$

**Equation 11**

From Equation 10, one can deduce:

$$bFd_p^2 = bFd_s^2 m_s^2$$

**Equation 12**

The relationship between the ring gear and the sun gear is:

$$Fd_r^2 = Fd_s^2 \left( \frac{d_r}{d_s} \right)^2 0.4$$

**Equation 13**

where

0.4 is an adjustment to account for weight of the cage structure and housing

The total weight of the planetary gear system is sum of the sun gear weight, number of planets times the gear weight, and the ring gear weight.

$$\sum Fd^2 = Fd_s^2 + bFd_p^2 + Fd_r^2$$

**Equation 14**

Substituting Equation 12 and Equation 13 into Equation 14 yields:

$$\sum Fd^2 = Fd_s^2 + Fd_s^2 m_s^2 + Fd_s^2 \left( \frac{d_r}{d_s} \right)^2 0.4$$

**Equation 15**

After simplification, the following expression is reached:

$$\sum \frac{Fd^2}{C} = \frac{1}{b} + \frac{1}{bm_s} + m_s + m_s^2 + \frac{0.4(M_o - 1)^2}{b} + \frac{0.4(M_o - 1)^2}{bm_s}$$

**Equation 16**

### **Boeing-Vertol Weight Formulae**

The following weight equations (Equation 17 to Equation 19) are taken from NASA Technical Report 82-A-10, *A Comparative Study of Soviet vs. Western Helicopters Part 2*.<sup>17</sup>

The weight of the main rotor drive system is:

$$(W_{ds})_{mr} = 250a_{mr} \left[ (HP_{mr} / rpm_{mr}) z_{mr}^{0.25} k_t \right]^{0.67}$$

**Equation 17**

where

$a_{mr}$  is an adjustment factor (assumed to be 1)

$HP_{mr}$  is drive system horsepower

$rpm_{mr}$  is main rotor rpm

---

<sup>17</sup> W.Z. Stepniewski and R.A. Shinn, NASA TR 82-A-10 A Comparative Study of Soviet vs. Western Helicopters: Part 2-Evaluation of Weight, Maintainability and Design Aspects of Major Components (Ames Research Center: AVRADCOM Research and Technology Laboratories, 1983), 61-4.

$z_{mr}$  is number of stages in main rotor drive  
 $k_t$  is configuration factor ( $k_t = 1$  for single main rotor)

The weight of the tail rotor drive train with shafting is:

$$(W_{ds})_{tr} = 300a_{tr} [1.1(HP_{tr}/rpm_{tr})]^{0.8}$$

**Equation 18**

where

$a_{tr}$  is an adjustment factor ( $a_{tr} = 0.9$ )  
 $HP_{tr}$  is tail rotor horsepower  
 $rpm_{tr}$  is tail rotor speed

The total drive system weight is the sum of the main rotor drive and tail rotor drive weight:

$$W_{ds} = (W_{ds})_{mr} + (W_{ds})_{tr}$$

**Equation 19**

**RTL Weight Formulae**

The following weight equations (Equation 20 to Equation 22) are taken from NASA Technical Report 82-A-10, *A Comparative Study of Soviet vs. Western Helicopters Part 2*.<sup>18</sup>

---

<sup>18</sup>, W.Z. Stepniewski and R.A. Shinn, NASA TR 82-A-10 A Comparative Study of Soviet vs. Western Helicopters: Part 2-Evaluation of Weight, Maintainability and Design Aspects of Major Components (Ames Research Center: AVRADCOM Research and Technology Laboratories, 1983), 66.

The RTL formulae take the drive system components as a function of transmitted power and speed. The total gearbox weight is predicted with:

$$W_{gb} = 172.7 T_{mrgb}^{0.7693} T_{trgb}^{0.079} n_{gb}^{0.1406}$$

### Equation 20

where

$W_{gb}$  is total gearbox weight

$T_{mrgb} = HP_{trmr} / rpm_{mr}$  ratio of transmission hp to main rotor rpm

$T_{trgb} = 100(HP_{tr} / rpm_{tr})$  ratio of tail rotor power to its rpm

$n_{gb}$  is the number of gearboxes

The total shafting weight is:

$$W_{dsh} = 1.152 T_{mrgb}^{0.4265} T_{trgb}^{0.0709} L_{dr}^{0.8829} n_{dsh}$$

### Equation 21

where

$W_{dsh}$  is total drive shafting weight

$L_{dr}$  is the horizontal distance between rotor hubs (feet)

$n_{dsh}$  is the number of drive shafts excluding rotor shaft

Total drive system weight is the sum of gearbox and shafting weight:

$$W_{ds} = W_{gb} + W_{dsh}$$

### Equation 22



# GEARING

## **Gear Fundamentals**

This section includes a brief outline of fundamental gear geometry and properties that will be referenced throughout the remainder of the thesis. For further information, consult any machine design textbook such as Shigley and Mischke's Mechanical Engineering Design.<sup>19</sup> Another excellent source is the Handbook of Practical Gear Design by Dudley.<sup>20</sup> Figure 8 from Shigley and Mischke shows basic gear layout for the simplest of gearing types, the spur gear.

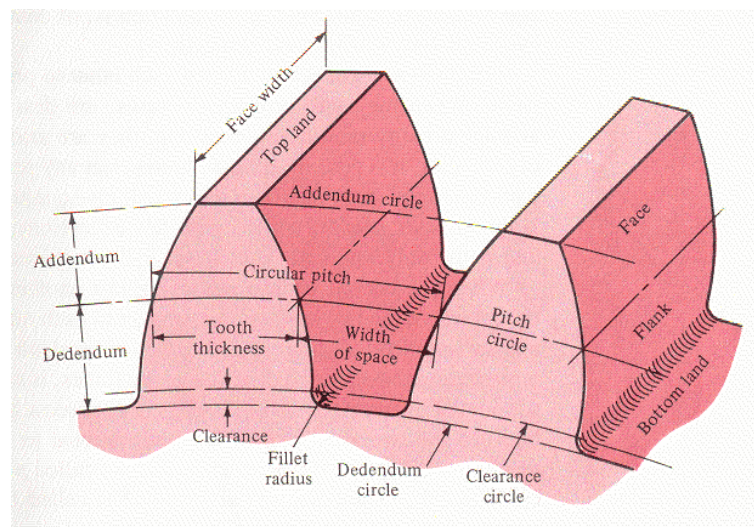


**Figure 8: Gear Nomenclature<sup>21</sup>**

---

<sup>19</sup> Joseph Shigley and Charles Mischke, Mechanical Engineering Design, 5<sup>th</sup> ed (New York: McGraw-Hill, 1989).

<sup>20</sup> Darle Dudley, Handbook of Practical Gear Design (Lancaster: Technomic, 1994).

<sup>21</sup> Figure extracted Joseph Shigley and Charles Mischke, Mechanical Engineering Design, 5<sup>th</sup> ed (New York: McGraw-Hill, 1989), 529.

The *reduction ratio* or gear ratio,  $m_G$ , of a pair of gears is describes the ratio of pitch diameters of the larger gear to the smaller pinion.

$$m_G = \frac{N_2}{N_1} = \frac{d_2}{d_1} = \frac{n_1}{n_2}$$

**Equation 23**

where

$m_G$  is the reduction ratio  
 $N$  is the number of teeth  
 $d$  is the pitch diameter  
 $n$  is the rotational speed

The typical reduction ratio is from 1:1 to 10:1 for most gearing. Modern face gear designs can reach even higher ratios. As gears mesh, the larger gear has a slower rotational speed,  $n$ , than the smaller gear. This speed ratio is the same as the gear or reduction ratio and is also expressed in Equation 23.

Even though different size gears rotate at different speeds, the peripheral speed, or *pitch line velocity* (PLV), of a meshing gear pair is the same:

$$PLV = \frac{\pi d n}{12}$$

**Equation 24**

The *diametral pitch*,  $P$ , measures the size of the teeth with respect to the size of the gear and has units of teeth per inch.

$$P = \frac{N}{d}$$

**Equation 25**

The *circular pitch*,  $p$ , is the arc distance from one tooth width and space to the next tooth and has units of inches per tooth.

$$p = \frac{\pi d}{N} = \frac{\pi}{P}$$

**Equation 26**

The most common tooth shape is the *involute profile*. The involute profile creates a conjugate action similar to cams in order to maintain a steady torque over the meshing gear pair despite the fact that the load on an individual tooth constantly changes magnitude and direction. As involute teeth mesh, the point of contact between them changes. The line in which resultant forces act along is called the *line of action*,  $L_{cd}$ , and is shown as line  $cd$  in Figure 9. The *pressure angle*,  $\phi$ , is the angle formed between the line of action and the tangency of the pitch circles. This tooth action is also showed in Figure 9.



A higher contact ratio provides better load sharing, smoother meshing, and reduced noise.

Aerospace gearing is sized on three considerations: bending fatigue, surface compression (Hertz stress), and scuffing (scoring) resistance. A design must include adequate ability to resist all three types of failures. Of the three failures modes, tooth bending has “the most severe consequences . . . whereas pitting and scoring are durability type failures.”<sup>23</sup>

<sup>23</sup> American Gear manufacturers Association, *AGMA 911-A94, Information Sheet-Design Guidelines for Aerospace Gearing* (Alexandria: AGMA, 1994), 41.

*Bending stress* is concentrated tensile stress at the base of the tooth on the loaded side. A gear tooth can be thought of as a short cantilever beam with a force pushing at the end of the beam. The highest point of stress concentration will occur at the base of the beam, or for gears, at the root fillet (see Figure 10). The ability of a particular gear to resist this stress is called *allowable bending strength* and “is a function of the hardness and residual stress near the surface of the root fillet and at the core.”<sup>24</sup> To determine failure, allowable bending stress is derated by factors such as dynamic loading, overloading, and reliability. This number is then compared to the bending stress.

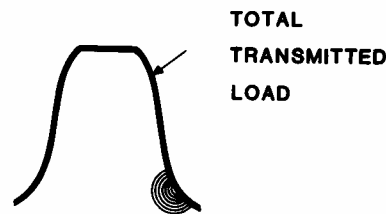


**Figure 10: Bending Stress**<sup>25</sup>

*Compressive or contact stress* causes pitting that weakens the gear surface by increasing local stress concentrations. Gear teeth undergo compression and tension as the tooth rolls through the mesh with the mating tooth.<sup>26</sup> Over the life of a gear, this repetitive cycle progressively pits the surface until it eventually leads to a fatigue failure. Figure 11 shows the compressive stress point on a tooth. *Allowable Compressive*

---

<sup>24</sup> American Gear manufacturers Association, *AGMA 911-A94, Information Sheet-Design Guidelines for Aerospace Gearing* (Alexandria: AGMA, 1994), 6.

<sup>25</sup> Figure extracted from Peter Lynwander, *Gear Drive Systems Design and Application* (New York: Marcel Dekker, 1983), 96.

<sup>26</sup> American Gear manufacturers Association, *AGMA 911-A94, Information Sheet-Design Guidelines for Aerospace Gearing* (Alexandria: AGMA, 1994), 42.

*strength* measures the tooth surface's resistance to pitting. To increase compressive strength, aerospace gears are usually strengthened through carburized, case hardening. To determine failure, allowable compressive strength is derated by factors such as surface condition, hardness, and dynamic factors. This value is then compared to the contact stress.

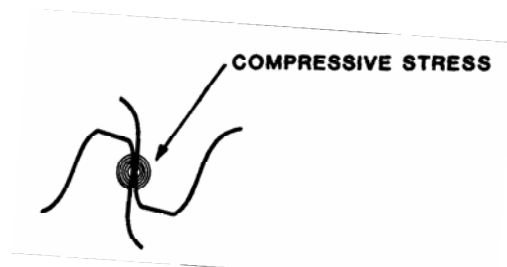


**Figure 11: Compressive Stress<sup>27</sup>**

As transmitted power increases, the bending stress increases linearly while compressive strength increase as the square root of transmitted power (Figure 12). For the same gear geometry and design, compressive stress will be the higher stress in regions of lower transmitted power while bending stress often dominates the higher power regions.

---

<sup>27</sup> Figure extracted from Peter Lynwander, Gear Drive Systems Design and Application (New York: Marcel Dekker, 1983), 103.

## Gear Tooth Stress vs Power

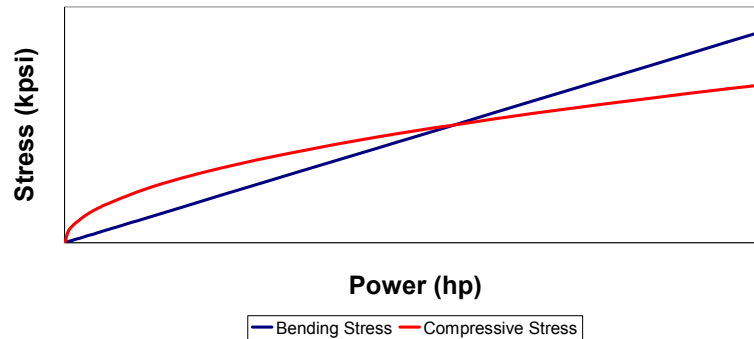


**Figure 12: Gear Tooth Stress vs. Power**

The Preliminary Design Handbook recommends that a well balanced design occurs where the bending stress to allowable compress stress ratio and the compressive stress to allowable compressive stress are relatively equal and at the desired factor of safety.

*Scuffing* (scoring) failure occurs when the mating gear welds the metal surface of the mated gear. Although scoring is not a fatigue failure, excessive compressive stress over a period of time will create radial scratch lines in the surface that promotes the onset of scoring.<sup>28</sup> Scuffing is a durability failure that may occur instantaneously.<sup>29</sup> Heavily loaded, high-speed gears such as aircraft gears tend to fail by scoring.<sup>30</sup> The probability of a gear pair to resist scoring is called *scuffing resistance*.

---

<sup>28</sup> Darle Dudley, Handbook of Practical Gear Design (Lancaster: Technomic, 1994), 2.24.

<sup>29</sup> American Gear Manufacturers Association, *AGMA Standard 2001-C95, Fundamental Rating Factors and Calculation Method for Involute Spur and Helical Gear Teeth* (Alexandria: AGMA, 1995), 9.

<sup>30</sup> Darle Dudley, Handbook of Practical Gear Design (Lancaster: Technomic, 1994), 2.24.

## **Gear Types and Functions**

In a drive system, gears serve to reduce or increase speed, change the direction of drive, and split or combine torque paths. A designer has several different types of gears to select from in order to best achieve the intended function. Spur, helical, and planetary gears transmit torque along a parallel axis. Bevel, worm, and face gears transmit torque along intersecting axis. Crossed helicals or hypoids are used for nonparallel axis gears. For helicopter transmissions, the nonparallel axis gears are not normally used because their efficiency “decreases rapidly as the helix angle increases.”<sup>31</sup> A low inefficiency also applies to worm gears. Table 5 outlines the gear types, functions, and typical uses in helicopter transmissions.

**Table 5: Gear Types and Applications**

<b>Gear Type</b>	<b>Axis Type</b>	<b>Function</b>	<b>Typical Use</b>
Spur	Parallel	Speed reducer Combine/split paths	Planetary gearing Accessory gearing Tail rotor gearbox
Helical	Parallel	Speed reducer Combine/split paths	Low noise gearing High speed, high load
Bevel	Intersecting	Speed reducer Direction change Combine/split path	Change drive direction Intermediate gearboxes Crown/collector gear
Face	Intersecting	Speed reducer Combine/split paths 90° direction change	High gear ratio Crown/collector gear

---

<sup>31</sup> Headquarters, U.S. Army Material Command, AMC Pamphlet 706-201 Engineering Design Handbook: Helicopter Engineering (Part One: Preliminary Design) (Alexandria: GPO, 1974), 7-5.



## Spur Gears in Helicopter Transmissions

The simplest and “most commonly used” gear in helicopter transmissions is the spur gear.<sup>32</sup> The spur gear has straight teeth and transmits torque between parallel axis (Figure 8). Spur gears tend to have lower contact ratios than other types of gears and, therefore, generate more noise. The advantage of spur gears is that they do not develop axial loads or thrust like helical or bevel gears. This eliminates the need for thrust bearings and permits a lighter gearbox weight. Although not traditionally a high-speed gear, aerospace spur gears can operate at high pitch velocities up to 20,000 feet per minute<sup>33</sup> but do generate significant noise. The lack of an axial load makes spur gears well suited for planetary configurations and where permitted.

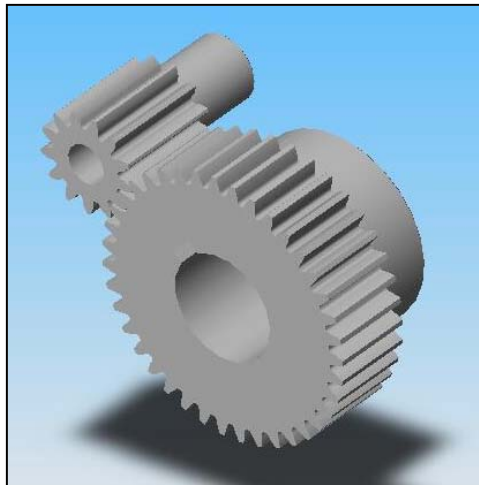


**Figure 13: Example Spur Gear**

---

<sup>32</sup> Headquarters, U.S. Army Material Command, AMC Pamphlet 706-201 Engineering Design Handbook: Helicopter Engineering (Part One: Preliminary Design) (Alexandria: GPO, 1974), 7-5.

<sup>33</sup> Headquarters, U.S. Army Material Command, AMC Pamphlet 706-201 Engineering Design Handbook: Helicopter Engineering (Part One: Preliminary Design) (Alexandria: GPO, 1974), 7-5.

## Helical Gears in Helicopter Transmissions

Helical gears have teeth angled or twisted to the axis of rotation. This helix angle,  $\psi$ , varies from 15 to 30 degrees and generates radial and axial loads on associated bearings. Spur gears are a special form of helical gear with a  $0^\circ$  helix angle.

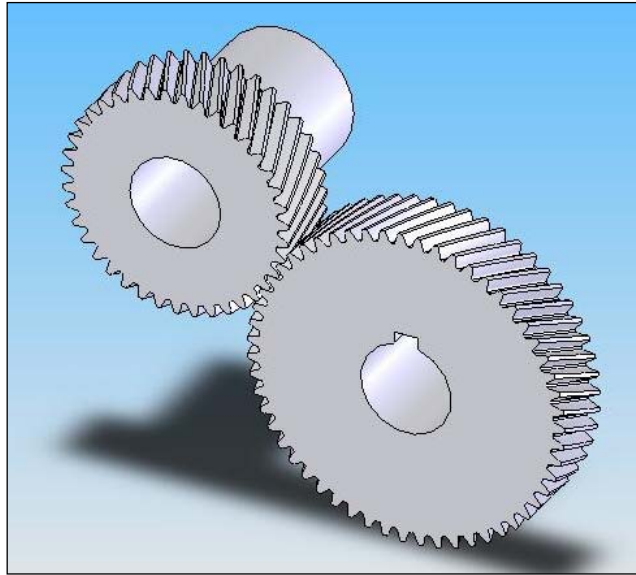


**Figure 14: Example Helical Gear**

Relative to a spur gear, the effective face width and line of contact in a helical mesh is longer due to the angled nature of the tooth face as shown in Figure 15. This generates higher contact ratios than spur gears and improves load sharing. This improved load sharing permits smoother meshing, reduces noise, and better handles higher speeds and horsepower.

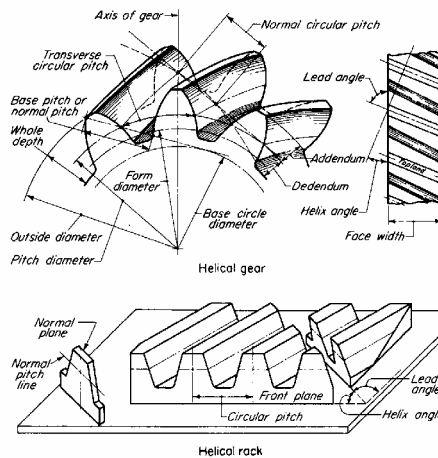


**Figure 15: Helical Gear Terminology<sup>34</sup>**

Despite the higher load capacity, the Helicopter Engineering Preliminary Design Handbook cautions against the employment of helical gears in helicopter transmissions:

“For the same face width, helical gears have more load carrying capacity than spur gears of equal size, are quieter, and have approximately the same efficiency. The overall design is not necessarily lighter; however, because the effect of thrust upon the mounting bearings must be considered. In general, helical gears designed for helicopters use do not offer a tremendous advantage over spur gears of the same size.”<sup>35</sup>

## Bevel Gears in Helicopter Transmissions

Bevel gears are the primary means to change direction between intersecting axis. The shaft angle created between the intersecting axis is typically between 0° and 115°, with 90° being the most common angle. Straight bevel gears have radial teeth while spiral bevel gears have curved teeth. Figure 16 shows the bevel gear terminology.

<sup>34</sup> Figure extracted from Darle Dudley, Handbook of Practical Gear Design (Lancaster: Technomic, 1994), 1.31.

<sup>35</sup> Headquarters, U.S. Army Material Command, AMC Pamphlet 706-201 Engineering Design Handbook: Helicopter Engineering (Part One: Preliminary Design) (Alexandria: GPO, 1974), 7-7.

Straight bevel gears are limited to pitch line velocity less than 1,000 fpm while spiral bevel gears operate beyond 30,000 fpm.<sup>36</sup> Due to the restrictive pitch line velocity, straight bevel gears are generally not feasible for primary power paths in helicopter drive systems. Compared to straight bevel gears, spiral bevel gears form a contact area that permits smaller gear pitch for the same contact stress. This allows the use of coarser gears (lower diametral pitch) to increase bending strength.<sup>37</sup> The three dimensional curve of spiral bevel gears creates three-dimensional loads requiring multiple bearing restraints. Other forms of bevel gears such as Zerol are possible, but the high speed, high power applications found in helicopter drives best suit spiral bevel gears.

---

<sup>36</sup> Headquarters, U.S. Army Material Command, AMC Pamphlet 706-201 Engineering Design Handbook: Helicopter Engineering (Part One: Preliminary Design) (Alexandria: GPO, 1974), 7-8.

<sup>37</sup> Headquarters, U.S. Army Material Command, AMC Pamphlet 706-201 Engineering Design Handbook: Helicopter Engineering (Part One: Preliminary Design) (Alexandria: GPO, 1974), 7-8.

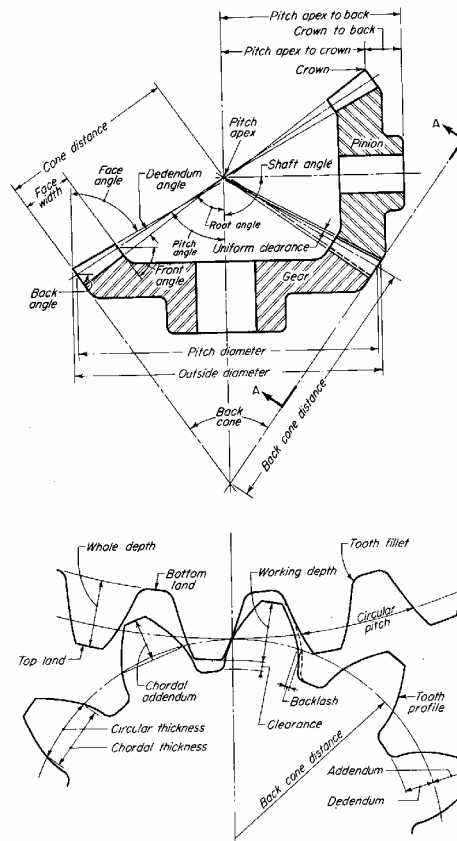


**Figure 16: Bevel Gear Terminology<sup>38</sup>**

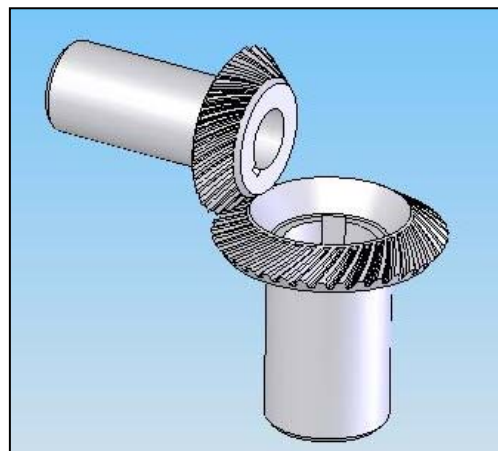


**Figure 17: Example Spiral Bevel Gear**

<sup>38</sup> Figure extracted from Darle Dudley, Handbook of Practical Gear Design (Lancaster: Technomic, 1994), 134.

## Face Gears in Helicopter Transmissions

Face gears have the teeth cut on top of gear instead of at the outer edge. The face gear tooth changes shape radially. The outside end of the gear limits the outer edge thickness and the pointed tooth limits the inner thickness. They are most similar to straight bevel gears but mate with a standard spur pinion. Gear and pinion have intersecting axis that normally creates a  $90^\circ$  shaft angle. Figure 18 shows the basic geometry for a face gear. Figure 19 shows a face gear-spur pinion mesh.

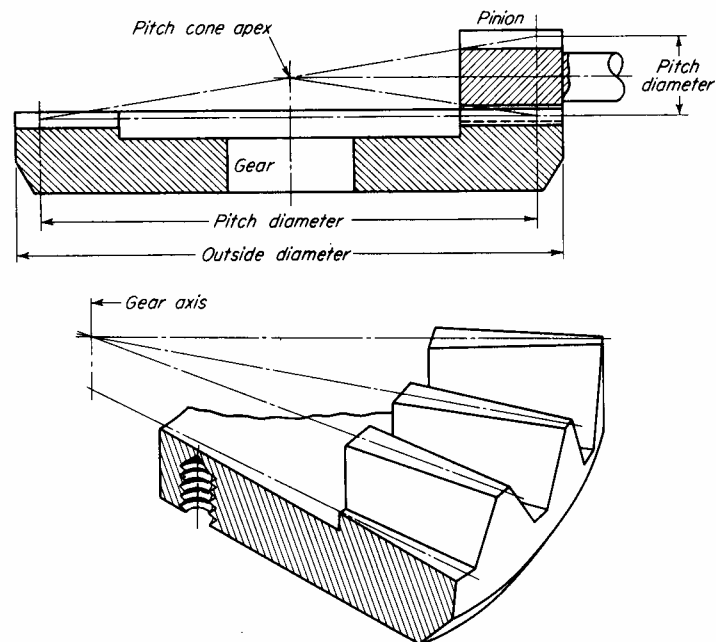


**Figure 18: Face Gear Terminology<sup>39</sup>**

---

<sup>39</sup> Figure extracted from Darle Dudley, Handbook of Practical Gear Design (Lancaster: Technomic, 1994), 1.40.

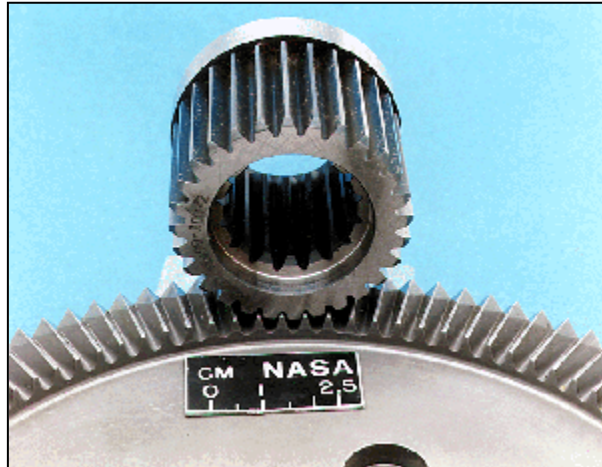


**Figure 19: Example Face Gear<sup>40</sup>**

In 2004, the Rotorcraft Drive System for the 21<sup>st</sup> Century (RDS-21) demonstrated that a 5,100 hp face gear, split torque gearbox potentially increases horsepower to weight ratio by 35%, reduces noise by 12 dB, and reduces cost by 20%.<sup>41</sup> Unfortunately, no standardized formulas to rate face gear stresses exist. All current face gear design accomplished with the partial use of Finite Element Analysis (FEA).<sup>42</sup> The level of design involved with FEA is beyond the scope of this thesis and; therefore, face gears cannot be considered for this model's split-torque transmission. Dudley (1994) does suggest a possible means to preliminary estimate of face gear size. According to Dudley:<sup>43</sup>

“Face gears may be handled somewhat similarly to straight bevel gearsets. Generally it will be necessary to use less face width for the face gear than would be allowed as a maximum for the same ratio of bevel gears.”

---

<sup>40</sup> NASA Research and Technology website, <http://www.grc.nasa.gov/WWW/RT1995/2000/2730h.htm>, November 1, 2005.

<sup>41</sup> Yuriy Gmirya, et al, “Design and Analysis of 5100 HP RDS-21 Demonstrator Gearbox” 60<sup>th</sup> Annual Forum Proceedings, vol 2, (Alexandria: AHS International, 2004), 1221.

<sup>42</sup> F.L. Litvin et al, NASA/CR-2000-209909 Handbook on Face Gear Drives With a Spur Involute Pinion (NASA, March 2000), 48.

<sup>43</sup> Darle Dudley, Handbook of Practical Gear Design (Lancaster: Technomic, 1994), 2.51.

In the future, as face gear analyses improves and the gearing community accepts standards, face gears will likely be the gear of the choice for high reduction ratio transmissions found in heavy lift helicopters.

### **Rating Spur and Helical Gears**

In preliminary design, prior to Finite Element Analysis, the rating methods used by most helicopter gear design engineers are from the American Gear Manufacturers Association (AGMA) standards.<sup>44</sup> Spur gears are a special case of helical gears where the helix angle,  $\psi$ , is zero. As such, the bending strength, compressive strength, and scuffing hazard calculations for both spur and helical gears are found using helical gear calculations. Equating  $\psi$  to zero reduces the helical equations to the set of spur equations.

The following force analysis, bending strength analysis, compressive strength analysis, and scuffing risk judgment are derived from Standard ANSI/AGMA 2001-C95 *Fundamental Rating Factor and Calculation Methods for Involute Spur and Helical Gear Teeth*. Additionally, much helicopter specific information and recommendations originates from AGMA 911-A94 *Information Sheet-Design Guidelines for Aerospace Gearing*.

---

<sup>44</sup> Headquarters, U.S. Army Material Command, AMC Pamphlet 706-201 Engineering Design Handbook: Helicopter Engineering (Part One: Preliminary Design) (Alexandria: GPO, 1974), 7-18.



## Spur Gear Force Analysis

In general, the stresses on the gear tooth are a function of the transmitted tooth load. In its simplest form, the transmitted load is:

$$W_t = \frac{T}{r} = \frac{2T}{d}$$

**Equation 27**

where

$W_t$  is the transmitted load on a tooth

$T$  is torque

$r$  is the pitch radius or  $d$  is the pitch diameter

The total force or load between the driving tooth and the driven tooth is not tangent to the contact point, but is instead along the line of action as measured by the pressure angle. The resultant, total load is typically broken into tangential and radial components as shown in Figure 20.

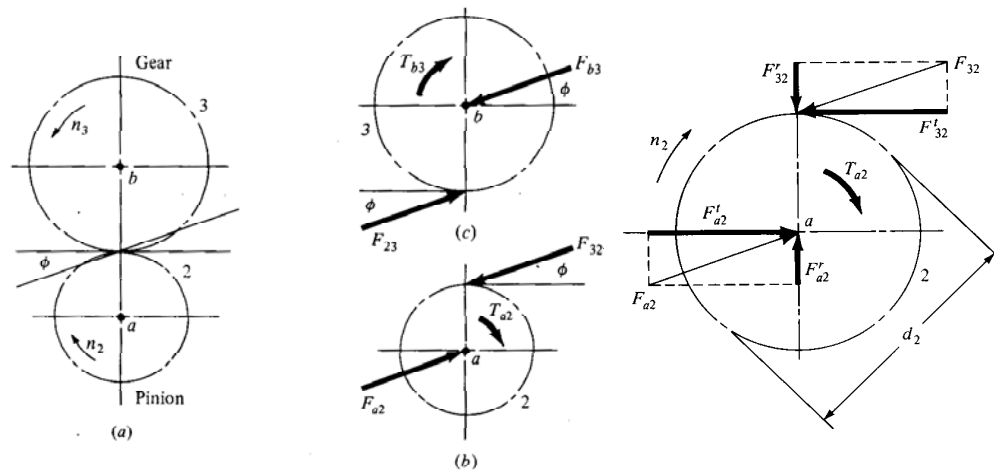


**Figure 20: Free Body Diagram of a Simple Gear Train<sup>45</sup>**

<sup>45</sup> Figure extracted from Joseph Shigley and Charles Mischke, Mechanical Engineering Design, 5<sup>th</sup> ed (New York: McGraw-Hill, 1989), 557.

In Figure 20, the total, resultant load on the larger gear is  $F_{23}$  while the load on the smaller pinion is  $F_{32}$ . The tangential component of  $F_{32}$  is  $F_{32}^t$  and the radial component is  $F_{32}^r$ . The reaction forces transferred to the gear are  $F_{a2}^t$  and  $F_{a2}^r$ . These reaction forces must be supported by bearings connected to the gearbox housing.

The tangential load serves to transfer the torque between the mating gears. The radial load “serves no useful purpose”<sup>46</sup> and must be reacted to by supporting bearings to hold the gear in mesh. The tangential and radial components of the total force,  $W$ , are:

$$W_r = W \sin \phi$$

$$W_t = W \cos \phi$$

#### Equation 28

where

$W$  is total force

$W_r$  is the radial force

$W_t$  is the tangential force or transmitted load

$\phi$  is the pressure angle

The relationships between the transmitted load, torque, speed, and power are shown in Equation 29 and Equation 30:

$$HP = \frac{W_t PLV}{(550)(60)} = \frac{2\pi nT}{(550)(60)(12)}$$

#### Equation 29

---

<sup>46</sup> Joseph Shigley and Charles Mischke, Mechanical Engineering Design, 5<sup>th</sup> ed (New York: McGraw-Hill, 1989), 557.

$$T = \frac{dW_t}{2} = \frac{HP(550)(60)(12)}{2\pi n}$$

**Equation 30**

where

$HP$  is power (hp)  
 $PLV$  is pitch line velocity (fpm)  
 $T$  is torque (in lb)  
 $W_t$  is transmitted load (lb)  
 $n$  is rotational speed (rpm)  
 $d$  is pitch diameter (in)

### Helical Gear Force Analysis

The axial and component forces mentioned by the Preliminary Design Handbook are drawn in Figure 21 and calculated with:

$$\begin{aligned} W_r &= W \sin \phi_n \\ W_t &= W \cos \phi_n \cos \psi \\ W_a &= W \cos \phi_n \sin \psi \end{aligned}$$

**Equation 31**

where

$W$  is total force  
 $W_r$  is the radial force  
 $W_t$  is the tangential force or transmitted load  
 $W_a$  is the axial force or thrust load  
 $\phi_n$  is the normal pressure angle  
 $\psi$  is the helix angle

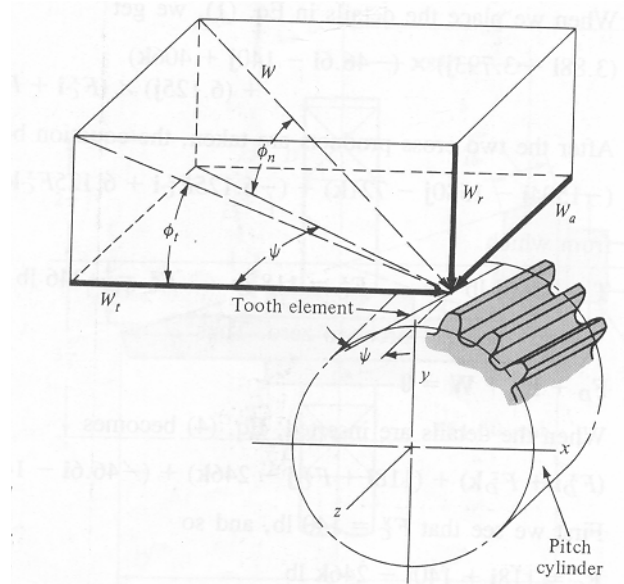


**Figure 21: Helical Gear Free Body Diagram<sup>47</sup>**

## Contact Stress

The fundamental formula for compressive or contact stress is:

$$s_c = C_p \sqrt{W_t K_o K_v K_s \frac{K_m}{dF} \frac{C_f}{I}}$$

### Equation 32

where

$s_c$  is contact stress (lb/in<sup>2</sup>)

$C_p$  is elastic coefficient (lb/in<sup>2</sup>)<sup>0.5</sup>

$W_t$  is transmitted tangential load (lb)

$K_o$  is overload factor

$K_v$  is dynamic factor

$K_s$  is size factor

$K_m$  is load distribution factor

$C_f$  is surface condition factor for pitting resistance

$F$  is net face width (in)

$I$  is geometry factor for pitting resistance

$d$  is operating pitch diameter of pinion (in)

<sup>47</sup> Figure extracted from Joseph Shigley and Charles Mischke, Mechanical Engineering Design, 5<sup>th</sup> ed (New York: McGraw-Hill, 1989), 562.

For a complete detailing of each factor, refer to ANSI/AGMA 2001-C95. A sample calculation of a planetary spur gear is shown in Table 30. A brief outline of the contact stress equation is listed below as it pertains to helicopter gears.

### **Elastic Coefficient, $C_p$**

The elastic coefficient is a function of the material's Poisson's ratio and modulus of elasticity. Values for steel are approximately  $2300 \text{ (lb/in}^2\text{)}^{0.5}$ . The elastic coefficient is:

$$C_p = \sqrt{\frac{1}{\pi \left[ \left( \frac{1 - \mu_p^2}{E_p} \right) + \left( \frac{1 - \mu_G^2}{E_G} \right) \right]}}$$

### **Equation 33**

where

$\mu_p$  and  $\mu_G$  is Poisson's ratio for pinion and gear, respectively  
 $E_p$  and  $E_G$  is Modulus of Elasticity for pinion and gear

### **Overload Factor, $K_o$**

The overload factor accounts for externally applied loads beyond the tangential load. According to AGMA, "overload factors can only be established after considerable field experience."<sup>48</sup> In place of field experience, a preliminary value may be located from Table 6. Considering turbines as uniform prime mover and the changing torque values of the rotors as light shock derives an overload factor of 1.25.

---

<sup>48</sup> AGMA Standard 2003-B97, *Rating the Pitting Resistance and Bending Strength of Generated Straight Bevel, Zerol Bevel and Spiral Bevel Gear Teeth*. (AGMA: Alexandria), 1997.

**Table 6: Overload Factor Values<sup>49</sup>**

Character of prime mover	Character of load on driven machine			
	Uniform	Light shock	Medium shock	Heavy shock
Uniform	1.00	1.25	1.50	1.75 or higher
Light shock	1.10	1.35	1.60	1.85 or higher
Medium shock	1.25	1.50	1.75	2.00 or higher
Heavy shock	1.50	1.75	2.00	2.25 or higher

**Dynamic Factor,  $K_v$** 

The dynamic factor accounts for vibration of gear masses and resulting dynamic forces.  $K_v$  maybe approximated from Figure 22. Aerospace gears are usually precision ground gears with a high degree of accuracy. High accuracy gears are equivalent to AGMA  $Q_v$  12 to 13.<sup>50</sup> A value of  $Q_v = 12$  promotes successful operation at high pitch line velocities to and beyond 10,000 fpm. From Figure 22, this yields a value from 1.00 to 1.10.

---

<sup>49</sup> Extracted with permission from AGMA Standard 2003-B97, *Rating the Pitting Resistance and Bending Strength of Generated Straight Bevel, Zerol Bevel and Spiral Bevel Gear Teeth*. With the permission of the publisher, American Gear Manufacturers Association, 1500 King Street, Suite 201, Alexandria, Virginia 22314., p. 35.

<sup>50</sup> Darle Dudley, Handbook of Practical Gear Design (Lancaster: Technomic, 1994), 3.107.

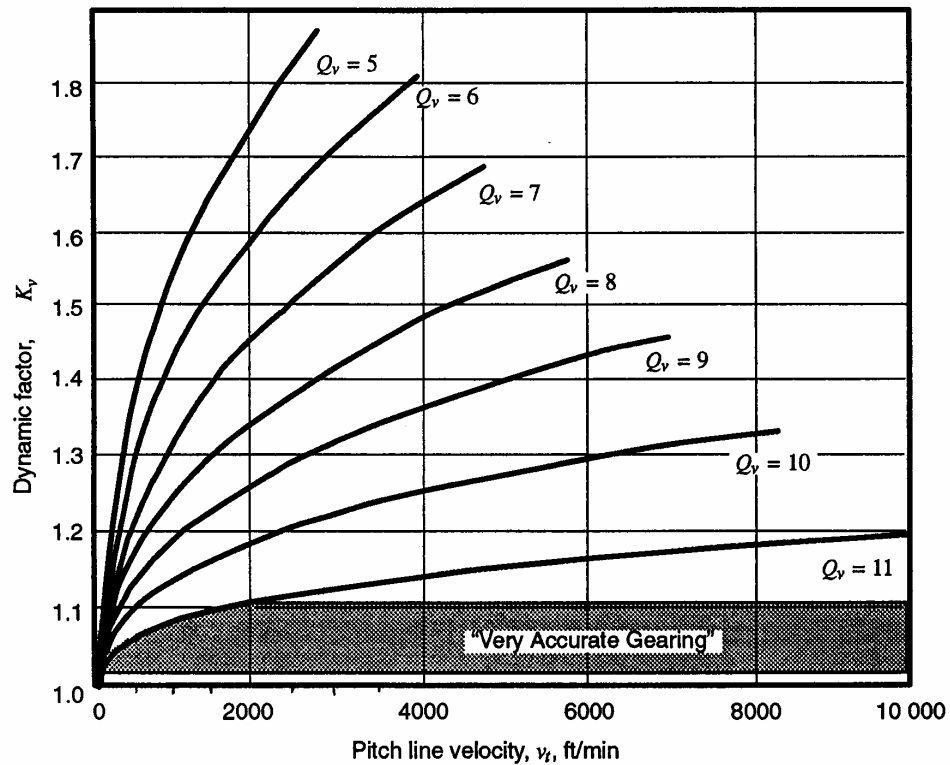


Figure 22: Dynamic Factor<sup>51</sup>

### Size Factor, $K_s$

A size factor of unity is taken for properly heat-treated material.

### Load Distribution Factor, $K_m$

The load distribution factor captures the impact of non-uniform load along the lines of contact. Several conditions influence the load distribution factor to include unmodified or properly modified leads, straddle mounted or overhung pinions, and adjusted gearing at assembly or improved compatibility by lapping. Values range from

<sup>51</sup> Extracted with permission from AGMA Standard 2001-C95, *Fundamental Rating Factors and Calculation Methods for Involute Spur and Helical Gear Teeth*. With the permission of the publisher, American Gear Manufacturers Association, 1500 King Street, Suite 201, Alexandria, Virginia 22314., p. 14.

1.10 to 1.20 for this design. Calculations for the load distribution factor may be found in Table 30.

### **Surface Condition Factor, $C_f$**

The surface condition factor is unity for properly ground gears.

### **Geometry Factor, $I$**

The geometry factor,  $I$ , measures the radii of curvature of contacting tooth profiles in order to evaluate the Hertzian contact stress in the tooth. The equation for the geometry factor is:

$$I = \begin{cases} \frac{\cos \phi_t \sin \phi_t}{2m_n} \frac{m_G}{m_G + 1} & \text{external gears} \\ \frac{\cos \phi_t \sin \phi_t}{2m_n} \frac{m_G}{m_G - 1} & \text{internal gears} \end{cases}$$

### **Equation 34**

where

$\phi_t$  is the transverse pressure angle  
 $m_N$  is load sharing ratio (1 for spur gears)  
 $m_G$  is the gear ratio

### **Allowable Contact Stress**

The allowable contact stress adjusted for stress cycles, temperature effects, and reliability must be greater than the calculated contact stress. The relationship between



contact stress and the allowable contact stress is:

$$s_c \leq \frac{s_{ac}}{S_H} \frac{Z_N}{K_T} \frac{C_H}{K_R}$$

where

$s_{ac}$  is allowable contact stress (lb/in<sup>2</sup>)

$Z_N$  is stress cycle factor

$C_H$  is hardness ratio factor

$S_H$  is safety factor

$K_T$  is temperature factor

$K_R$  is reliability factor

### **Stress Cycle Factor, $Z_N$**

Allowable contact stress for a given material is rated to  $10^7$  load cycles yet most aerospace gears often must last  $10^9$  cycles. The stress cycle factor adjusts the material contact stress for the required increased in fatigue life. The number of required cycles is:

$$N_{cycles} = 60Lnq$$

### **Equation 35**

where

$N_{cyc}$  is the number of stress cycles

$L$  is required life (hours)

$n$  is speed (rpm)

$q$  is number of contacts per revolution

A typical gear pair only experiences one contact per revolution; however, if a gear mates with  $q$  other gears it will experience  $q$  contacts per revolution. This often occurs in accessory drives and especially in planetary gearboxes. The stress cycle factor for pitting resistance can be found in Figure 23. For cycles beyond  $10^7$ ,  $Z_N$  was assumed to be the mean of the shaded value.

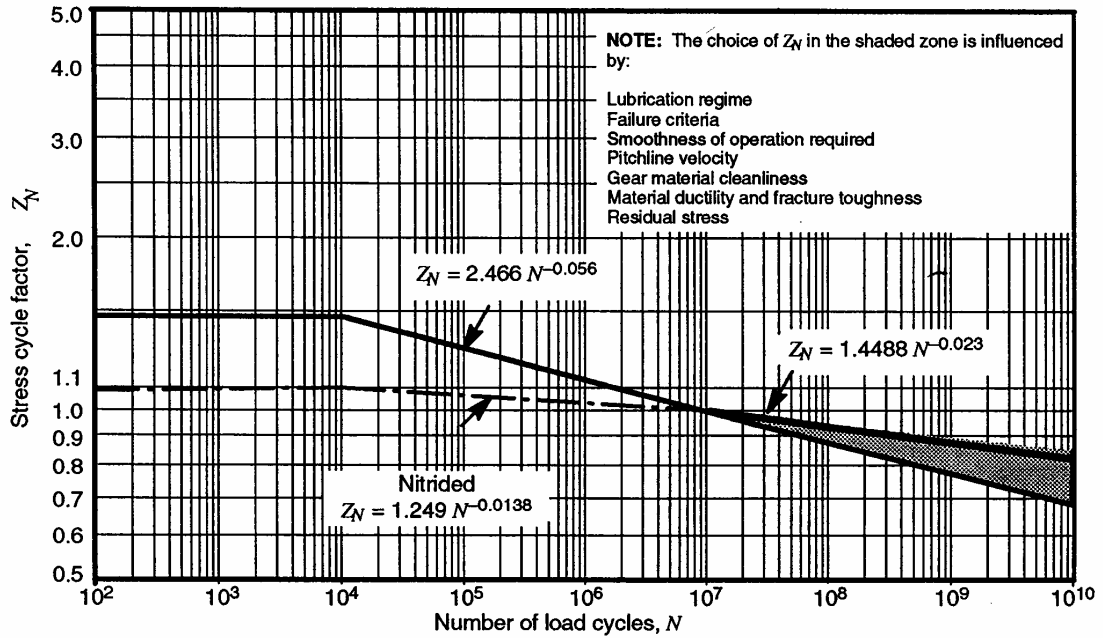


Figure 23: Pitting Resistance Stress Cycle Factor,  $Z_N$ <sup>52</sup>

### Hardness Ratio Factor, $C_H$

Gear capacity increases when the pinion is substantially harder than the gear.

This factor applies to the gear not the pinion.

$$C_H = 1.0 + A(m_G - 1.0)$$

### Equation 36

where

$$A = 0.00898 \left[ \frac{H_{BP}}{H_{BG}} \right] - 0.00829$$

$H_{BP}$  is pinion Brinell hardness number

$H_{BG}$  is gear Brinell hardness number

For  $H_{BP}/H_{BG} < 1.2$ ,  $A = 0$

For  $H_{BP}/H_{BG} > 1.7$ ,  $A = 0.00698$

<sup>52</sup> Extracted with permission from AGMA Standard 2001-C95, *Fundamental Rating Factors and Calculation Methods for Involute Spur and Helical Gear Teeth*. With the permission of the publisher, American Gear Manufacturers Association, 1500 King Street, Suite 201, Alexandria, Virginia 22314., p. 37.

### **Safety Factor $S_H$**

The safety factor is added to include uncertainties in design analysis, material characteristics and manufacturing tolerances as well as human and economic risk. For the purposes of preliminary design, measuring these factors is beyond the scope of study and a value of unity is used.

### **Temperature Factor, $K_T$**

For gear blank temperatures below 250°F, the temperature factor is unity. For gear blank temperatures above 250°F, values above 1.0 should be used. To maintain gear strength, sufficient lubrication is included to ensure temperatures do not exceed the 250°F and a value of unity may be used.

### **Reliability Factor, $K_R$**

The reliability factor relates the statistic variations in material to a normal probability distribution. For this normal distribution, the reliability constant is:

$$R_{el} = 1 - nv$$

#### **Equation 37**

where

$R_{el}$  is the reliability constant

$n$  is the number of standard deviations

$v$  is the coefficient of variation (standard deviation/mean),  $v = 0.1$  for spur and helical gears

“For highly reliable aerospace design, a reliability of 3 standard deviations has been used in the past (or  $3\sigma$ ).”<sup>53</sup> Three standard deviations ( $n = 3$ ) yields a reliability of 0.99875 and a constant of  $R_{el} = 0.7$ . AGMA reliabilities on material properties are listed at a failure of 1 in 100 for a standard deviation of  $n = 2.326$ , and a  $R_{99} = 0.7674$ . The reliability factor is:

$$K_R = \frac{R_{99}}{R_{desired}}$$

**Equation 38**

where

$R_{99}$  is the reliability constant for 99% (0.7674)

$R_{desired}$  is the reliability constant

For a  $3\sigma$  aerospace design,  $K_R$  is 1.096. The spur-helical model shown in Table 30 of APPENDIX B: SPUR-HELICAL GEAR RATING CALCULATIONS permits user input for other reliabilities from 1 in 10 failures up to 1 in 10,000 failures. This is calculated through a numerical approximation of:

$$R_{el} = \int_{-\infty}^n \frac{e^{-\frac{n^2}{2}}}{\sqrt{2\pi}} dn$$

**Equation 39**

---

<sup>53</sup> American Gear manufacturers Association, *AGMA 911-A94, Information Sheet-Design Guidelines for Aerospace Gearing* (Alexandria: AGMA, 1994), 44.

## Bending Stress

The fundamental formula for bending stress is:

$$s_t = W_t K_o K_v K_s \frac{P_d}{F} \frac{K_m K_B}{J}$$

### Equation 40

where

$s_t$  is bending stress number (lb/in<sup>2</sup>)

$K_B$  is rim thickness factor

$J$  is geometry factor for bending strength

$P_d$  is transverse diametral pitch (in<sup>-1</sup>)

$P_d$  is  $P_{nd}$  for spur gears

$P_d = \frac{\pi}{p_x \tan \psi_s} = P_{nd} \cos \psi_s$  for helical gears

$P_{nd}$  is normal diametral pitch (in<sup>-1</sup>)

$p_x$  is axial pitch (in)

$\psi_s$  is helix angle at standard pitch diameter

For a complete detailing of each factor, refer to ANSI/AGMA 2001-C95. A complete detailed calculation of a planetary spur gear is in Table 30. A brief outline of the bending stress equation is listed below as it pertains to helicopter gears. Values for  $W_t$ ,  $K_o$ ,  $K_v$ ,  $K_s$ ,  $F$ , and  $K_m$  are the same as those for the contact stress formula Equation 32.

### Rim Thickness Factor, $K_B$

The rim thickness factor is a stress concentration factor when the rim thickness cannot fully support the tooth root. All gears in this analysis are designed to ensure sufficient tooth support ( $K_B = 1$ ).

## Geometry Factor, J

The bending strength geometry factor accounts for stress concentration from tooth bending and compression from the radial load. For calculations of spur gear geometry factor consult AGMA 911-A94, *Information Sheet-Design Guidelines for Aerospace Gearing*. The guideline includes the geometry factor for both internal and external gears. This method finds the geometry factor, J, by calculating the value at discrete intervals along the edge, A, of the tooth. The point of lowest J value occurs where the bending stress is at its maximum. Associated calculations are in Table 34 and Table 35 of APPENDIX B: SPUR-HELICAL GEAR RATING CALCULATIONS. This is graphically shown in Figure 24.

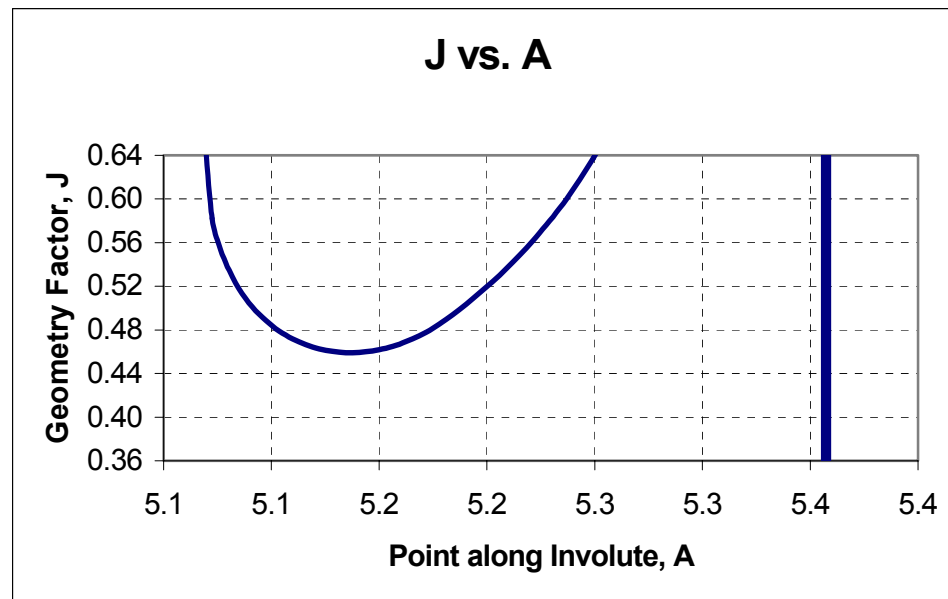


**Figure 24: Minimum J Along the Involute Profile**

For helical gears, the solution becomes lengthy and is beyond the level of detail required for a preliminary design. Typically, J for helical gears is found in a series of

tables. To automate this table look up, the geometry factor for helical gears is estimated by means of least squares regression from the I and J Factor Tables found in AGMA Standard 908-B89, INFORMATION SHEET, *Geometry Factors for Determining the Pitting Resistance and Bending Strength of Spur, Helical, and Herringbone Gear Teeth*.<sup>54</sup> The estimated J factor lies within  $\pm 5$  percent of actual values. Figure 25 and Figure 26 are replicas of graphs shown in Shigley and Mischke (1989) and show graphically J for a standard pressure angle of 20°.

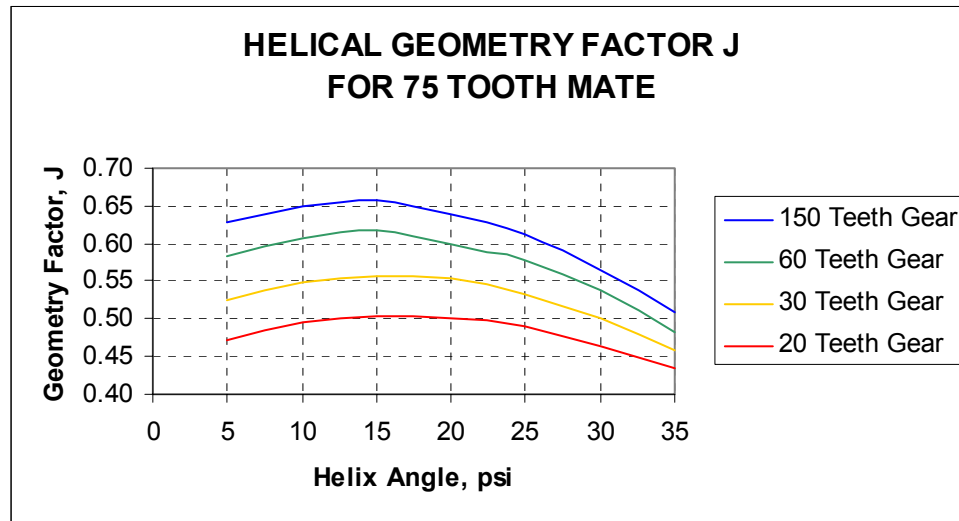


**Figure 25: Geometry Factor for Helical Gears**

<sup>54</sup> American Gear Manufacturers Association, *AGMA Standard 908-B89, Information Sheet, Geometry Factors for Determining the Pitting Resistance and Bending Strength of Spur, Helical and Herringbone Gear Teeth* (Alexandria: AGMA, 1989).

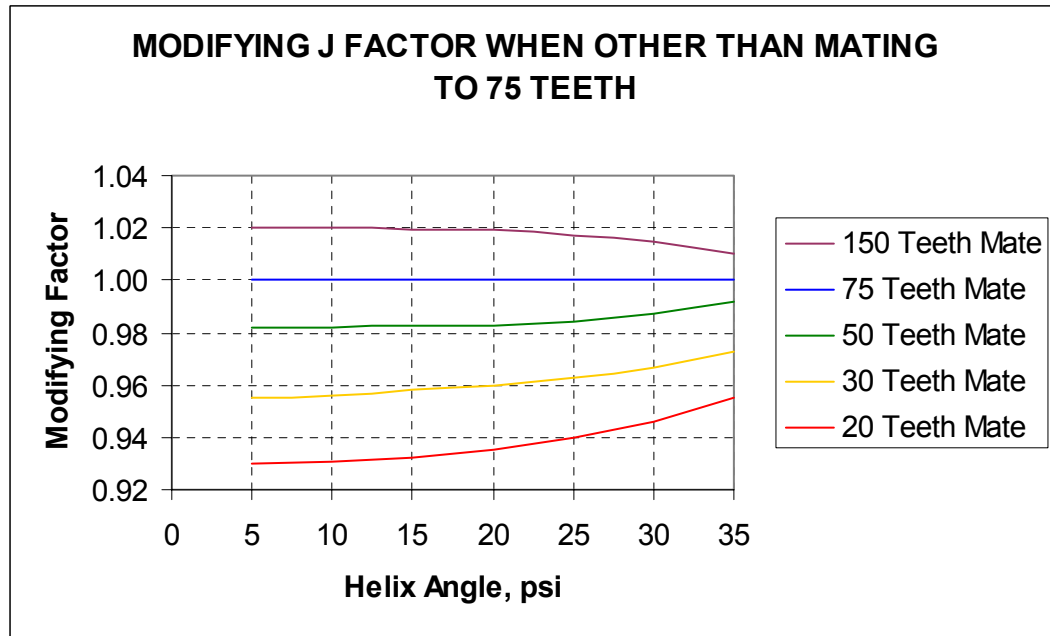


**Figure 26: Modifying Factor for J for Different Mating Gears**

### Allowable Bending Stress

The allowable bending stress (adjusted for stress cycles, temperature effects, and reliability) must be greater than the calculated bending stress. The correlation between bending stress to allowable bending stress is:

$$s_t \leq \frac{s_{at} Y_N}{S_F K_T K_R}$$

#### Equation 41

where

$s_{at}$  is allowable bending stress (lb/in<sup>2</sup>)

$Y_N$  is stress cycle factor

$S_F$  is safety factor

The values for  $K_T$  and  $K_R$  are the same as those used in section Allowable Contact Stress. Safety factor,  $S_F$ , is evaluated in the same method as  $S_H$ .



## Stress Cycle Factor, $Y_N$

The stress cycle factor for bending strength is found similarly as the stress cycle factor for pitting resistance. Cycles are calculated from Equation 35 in section Allowable Contact Stress. Figure 27 applies to the bending stress cycle factor.

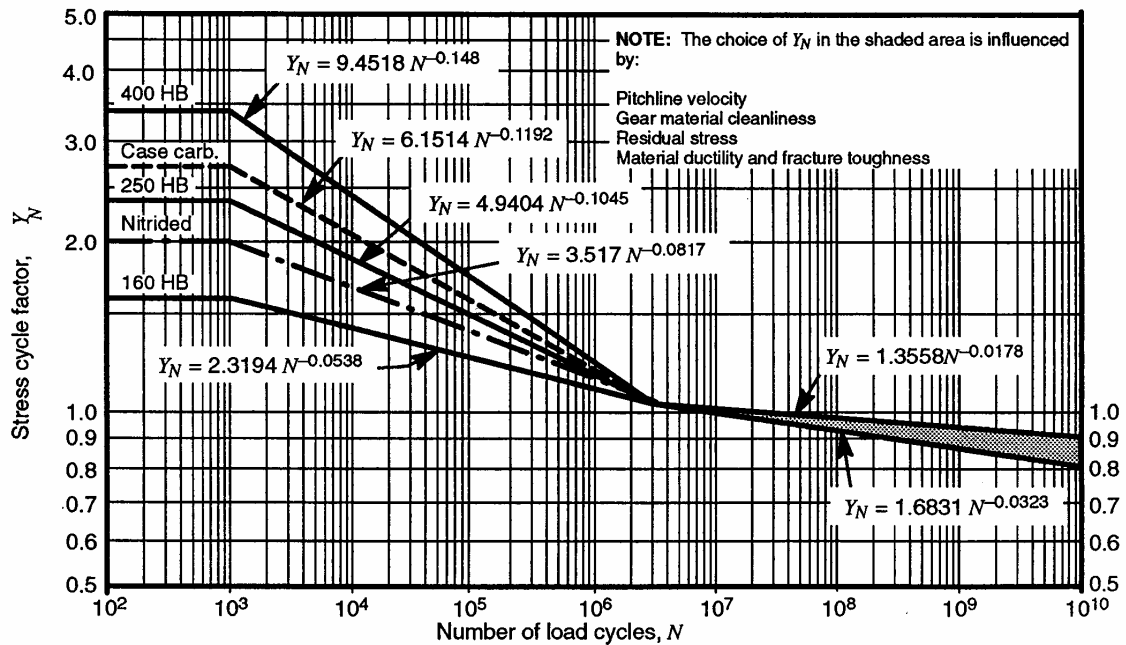


Figure 27: Bending Strength Stress Cycle Factor,  $Y_N$ <sup>55</sup>

## Spur and Helical Gear Materials

High performance aerospace gears require high tensile strength to endure high bending stresses and high surface hardness to resist pitting from high contact stresses.

<sup>55</sup> Extracted with permission from AGMA Standard 2001-C95, *Fundamental Rating Factors and Calculation Methods for Involute Spur and Helical Gear Teeth*. With the permission of the publisher, American Gear Manufacturers Association, 1500 King Street, Suite 201, Alexandria, Virginia 22314., p. 37.

The majority of helicopter gearing are produced from “heat treated alloy steels and surface hardened.”<sup>56</sup> Aerospace gears are carburized and case hardened to increase the surface hardness. For alloy steel processing, gas carbon is infused into the steel at high temperature, cooled slowly, and repeated at specified levels and temperatures. The carburizing and hardening cycles “produce a very hard, martensitic layer on the surface with a less hard, tough core.”<sup>57</sup> Five different high strength steels are listed in Table 7. Typical applications and relevant material properties are included.

**Table 7: Spur-Helical Gear Steels**

<b>Description</b>	<b>Units</b>	<b>AISI 9310</b>	<b>VASCO X2M</b>	<b>PYRO-WEAR 53</b>	<b>CBS 600</b>	<b>AISI 4340</b>
<b>AMS Spec</b>		6265/ 6260		6308	6255	6414
<b>Heat Treatment</b>		C-H	C-H	C-H	C-H	TH-N
<b>Main drive Application</b>		X	X	X		
<b>Accessory application</b>		X				X
<b>High Temp. Application</b>			X	X	X	
<b>Case Hardness</b>	<b>HRC</b>	61	62	62	60	50.5
<b>Core Hardness</b>	<b>HRC</b>	37	40	40	38	31
<b>Brinell Hardness</b>	<b>BH</b>	632	647	647	617	488
<b>Allowable Contact Stress</b>	<b>psi</b>	244,897	250,145	250,145	239,736	195,086
<b>Allowable Bending Stress</b>	<b>psi</b>	52,102	51,990	51,990	52,149	49,966
<b>Poisson’s Ratio</b>		0.292	0.300	0.292	0.296	0.82
<b>Modulus of Elasticity</b>		29.00E6	29.64E6	30.00E6	29.30E6	29.50E6
<b>Density (weight)</b>	<b>lb/in3</b>	0.283	0.280	0.282	0.282	0.283

*C-H is Case Hardened. TH-N is Through Harden and Nitride.*

<sup>56</sup> American Gear manufacturers Association, *AGMA 911-A94, Information Sheet-Design Guidelines for Aerospace Gearing* (Alexandria: AGMA, 1994), 41.

<sup>57</sup> American Gear manufacturers Association, *AGMA 911-A94, Information Sheet-Design Guidelines for Aerospace Gearing* (Alexandria: AGMA, 1994), 41.

The bending fatigue strength and compressive strength of case hardened steels (AISI 9310, VASCO X2M, PYROWEAR 53, CBS600) are generally the same; however VASCO X2M and PYROWEAR 53 also have high temperature capability to resist scuffing. This makes these two carburized steels the best choice for the scuffing critical main gearbox. In addition to VASCO X2M's high strength, high hardness, high temperature capability, it is also the lightest of the steels. Due to these advantages, the power gears were evaluated using VASCO-X2M. The spur-helical model shown in Table 33 of APPENDIX B: SPUR-HELICAL GEAR RATING CALCULATIONS includes user options to select any of the six listed steels. In accordance with the Preliminary Design Handbook for Helicopter Engineering, "primary gear drives should be made from electrode vacuum melt (CEVM) processed steel" in order to be less vulnerable to fatigue failure than air-processed steel.<sup>58</sup>

## Scuffing Hazard

Scuffing (scoring) failure occurs when the mating gear welds and tears the metal surface of the mated gear. Scuffing risk is a function of oil viscosity, operating bulk temperature of gear blanks, sliding velocity, surface roughness, gear materials, and surface pressure.<sup>59</sup> Following Blok's contact temperature theory as outlined by AGMA, scuffing will occur when the maximum contact temperature ( $t_{cmax}$ ) exceeds a critical

---

<sup>58</sup> Headquarters, U.S. Army Material Command, AMC Pamphlet 706-201 Engineering Design Handbook: Helicopter Engineering (Part One: Preliminary Design) (Alexandria: GPO, 1974), 7-2.

<sup>59</sup> American Gear Manufacturers Association, *AGMA Standard 2001-C95, Fundamental Rating Factors and Calculation Method for Involute Spur and Helical Gear Teeth* (Alexandria: AGMA, 1995), 9.

temperature known as the scuffing temperature ( $t_s$ ).<sup>60</sup> The contact temperature is the sum of the flash temperature ( $t_f$ ) and the bulk oil temperature ( $t_M$ ).

$$t_c = t_M + t_f$$

#### Equation 42

where

$t_M$  is bulk temperature

$t_f$  is the flash temperature

Figure 28 shows the variation of local temperature (y-axis) along the line of contact (x-axis) where:

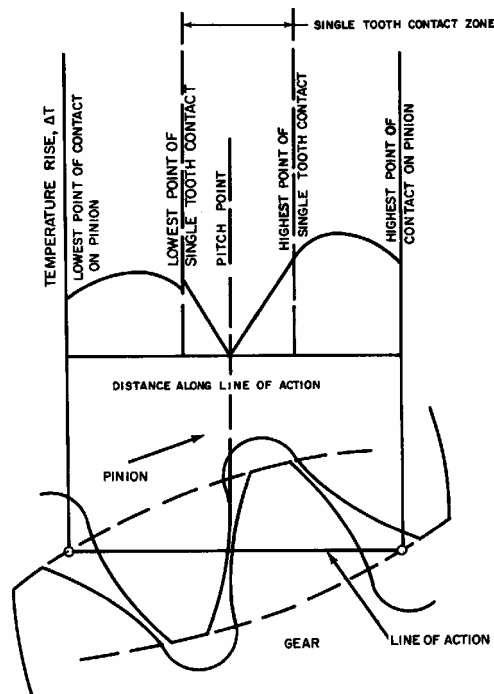


**Figure 28: Contact Temperature Along the Line of Action<sup>61</sup>**

<sup>60</sup> Blok, H. *Les temperatures de Surface dans les Conditions de graissage Sans Pression Extreme*, Second World Petroleum Congress, Paris, June, 1937 as outlined in AGMA Standard 2001-C95, *Fundamental Rating Factors and Calculation Methods for Involute Spur and Helical Gear Teeth*. (American Gear Manufacturers Association: Alexandria), 1995, Appendix A.

<sup>61</sup> Figure extracted from Peter Lynwander, *Gear Drive Systems Design and Application* (New York: Marcel Dekker, 1983), 127.

The flash temperature is the local rise in temperature at a specified contact point along a tooth's line of action. Steps to find the flash temperature along the line of contact are detailed in Annex A of AGMA Standard 2001-C95, *Fundamental Rating Factors and Calculation Methods for Involute Spur and Helical Gear Teeth*. The full set of calculations for the flash temperature is shown in Table 31: Spur-Helical Gear Scuffing. The fundamental formula for flash temperature is:

$$t_{fl} = K\mu_m \frac{X_\Gamma w_{Nr}}{B_M (b_H)^{0.5}} |(v_{r1})^{0.5} - (v_{r2})^{0.5}|$$

**Equation 43**

where

- $K$  is 0.80, numerical factor for frictional heat over the contact band
- $\mu_m$  is mean coefficient of friction
- $X_\Gamma$  is load sharing factor
- $w_{Nr}$  is normal unit load
- $v_{r1}$  is rolling velocity of pinion
- $v_{r2}$  is rolling velocity of gear
- $B_M$  is thermal contact coefficient
- $b_H$  is semi-width of Hertzian contact band

Figure 29 graphs the results from the calculations in Equation 43. The maximum flash temperature ( $t_{flmax}$ ) used to measuring the scuffing risk is the highest temperature along the line of contact. This compares favorably to Figure 28.

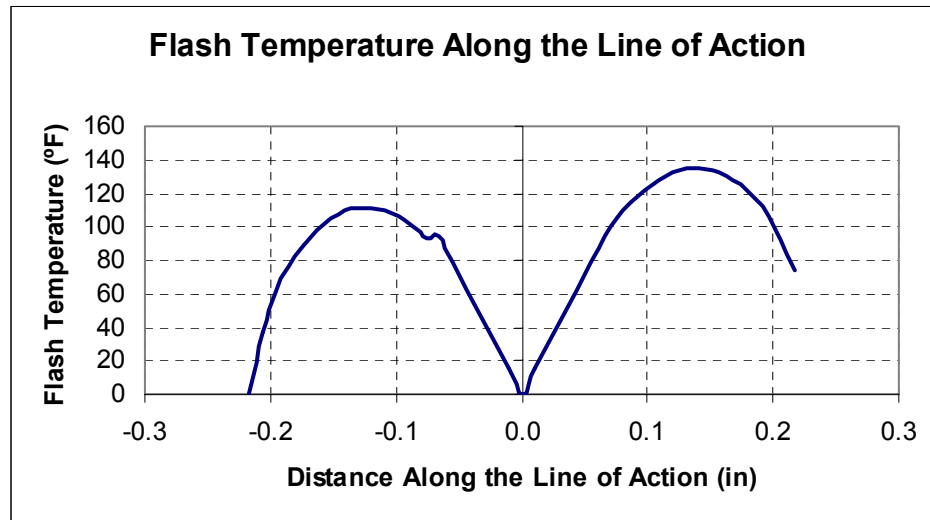


**Figure 29: Calculated Flash Temperature Along the Line of Action**

The oil temperature is taken to be the average of the cooler incoming oil and the outgoing hotter oil. The inlet temperature is assumed to be 125° F<sup>62</sup> while the maximum rise ( $\Delta T$ ) is limited to 45° F.<sup>63</sup>

$$t_{oil} = \frac{t_{oilin} + t_{oilout}}{2} = t_{oilin} + \frac{\Delta T}{2}$$

**Equation 44**

The bulk temperature maybe roughly approximated as:

$$t_M = -24 + 1.2t_{oil} + 0.56t_{flmax}$$

**Equation 45**

where

$t_{oil}$  is oil temperature (°F)

$t_{flmax}$  is maximum flash temperature

<sup>62</sup> Peter Lynwander, Gear Drive Systems Design and Application (New York: Marcel Dekker, 1983), 228.

<sup>63</sup> Darle Dudley, Handbook of Practical Gear Design (Lancaster: Technomic, 1994), 3.129.

The maximum contact temperature is the sum bulk temperature and the maximum flash temperature.

$$t_{c \max} = t_M + t_{fl \max}$$

#### Equation 46

Helicopters mostly use synthetic oils to provide protection in a wider temperature range (approximately –50 to 400° F) than mineral oils. For MIL lubricants, the scuffing temperature is taken as a constant value with a normal distribution. Table 8 shows the MIL lubricants mean and standard deviation. The Boeing HLH aircraft had great success using MIL-L-23699 with VASCO X2M steel gears. For the lowest scuffing risk, the main gearbox shall use VASCO X2M with MIL-L-23699.

**Table 8: MIL Lubricant Mean Scuffing Temperatures**

<b>Lubricant</b>	<b>Mean Scuffing Temperature °F</b>	<b>Standard Temperature Deviation °F</b>
MIL-7808 <sup>64</sup>	366	56.6
MIL-L-6081 <sup>65</sup> (grade 1005)	264	74.4
MIL-L-23699 <sup>66</sup>	391	58.65
MIL-L-23699 with VASCO X2M <sup>67</sup>	459	31

For synthetic oils, the scuffing risk is the probability the maximum contact temperature exceeds the lubricant scuffing temperature. Probabilities for scuffing

<sup>64</sup> American Gear Manufacturers Association, *AGMA Standard 2001-C95, Fundamental Rating Factors and Calculation Method for Involute Spur and Helical Gear Teeth* (Alexandria: AGMA, 1995), 50.

<sup>65</sup> American Gear Manufacturers Association, *AGMA Standard 2001-C95, Fundamental Rating Factors and Calculation Method for Involute Spur and Helical Gear Teeth* (Alexandria: AGMA, 1995), 50.

<sup>66</sup> Headquarters, U.S. Army Material Command, *AMC Pamphlet 706-201 Engineering Design Handbook: Helicopter Engineering (Part One: Preliminary Design)* (Alexandria: GPO, 1974).

<sup>67</sup> Mack, J.C., *USAAMRDL-TR-77-38: HLH Drive System* (Boeing Vertol: Philadelphia, 1977).

guidelines are mentioned in AGMA Standard 2001-C95.<sup>68</sup> Due to the critical nature aerospace gearing, only a low risk should be considered acceptable.

**Table 9: Scuffing Risk**

<b>Probability of Scuffing</b>	<b>Scuffing Risk</b>
<10%	Low
10 to 30%	Moderate
>30%	High

### **Rating Bevel Gears**

Bevel gears stresses and allowables closely follow the procedure for spur and helical gears (section Rating Spur and Helical Gears, p. 49). The AGMA standard for bevel rating is ANSI/AGMA 2003-B97, *Rating the Pitting Resistance and Bending Strength of Generated Straight Bevel, Zerol Bevel, and Spiral Bevel Gear Teeth* and ANSI/AGMA 2005-C96, *Design Manual for Bevel Gears*. All formulas in the section are based upon AGMA 2003-B97. Bevel gear sample calculations are enclosed in Table 36 through Table 42 of APPENDIX C: BEVEL GEAR RATING CALCULATIONS.

### **Bevel Gear Force Analysis**

A bevel gear creates a resultant force that has three components: tangential, radial, and axial loading as shown in Figure 30.

---

<sup>68</sup> American Gear Manufacturers Association, *AGMA Standard 2001-C95, Fundamental Rating Factors and Calculation Method for Involute Spur and Helical Gear Teeth* (Alexandria: AGMA, 1995), 50.



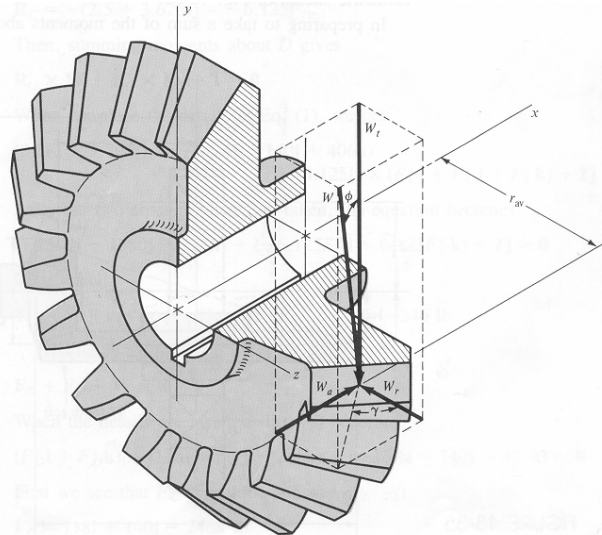


**Figure 30: Bevel Gear Tooth Forces<sup>69</sup>**

The direction of the radial and axial forces depends upon the type of load face: concave or convex. Load face is a function of the hand of spiral, rotation of gear, and whether the gear drives or is driven. Table 10 lists the combinations for load face.

**Table 10: Bevel Gear Load Face<sup>70</sup>**

Pinion hand of spiral	Gear hand of spiral	Rotation of driver	Rotation of driven	Load face	
				Driver	Driven
Right	Left	Clockwise	Counterclockwise	Convex	Concave
		Counterclockwise	Clockwise	Concave	Convex
Left	Right	Clockwise	Counterclockwise	Concave	Convex
		Counterclockwise	Clockwise	Convex	Concave

<sup>69</sup> Figure extracted from Joseph Shigley and Charles Mischke, *Mechanical Engineering Design*, 5<sup>th</sup> ed (New York: McGraw-Hill, 1989), 559.

<sup>70</sup> The majority of the information in this table is extracted from ANSI/AGMA 2005-C96, *Design Manual for Bevel Gears*, with the permission of the publisher, the American Gear Manufacturers Association, 1500 King Street, Suite 201, Alexandria, Virginia 22314.

The axial or thrust load is different for a concave and convex load face. A positive sign indicates a load away from the pitch apex. A negative sign indicates a load towards the pitch apex.

$$W_a = \frac{W_t}{\cos \psi} (\tan \phi \sin \gamma + \sin \psi \cos \gamma) \quad \text{concave load face}$$

$$W_a = \frac{W_t}{\cos \psi} (\tan \phi \sin \gamma - \sin \psi \cos \gamma) \quad \text{convex load face}$$

#### Equation 47

where

$W_a$  is the axial force or thrust load

$W_t$  is transmitted load

$\psi$  is helix angle

$\phi$  is pressure angle

$\gamma$  is pitch angle for the gear of interest

Like the axial force, the radial force is different for each load face. A positive sign (separating force) indicates the direction of force is away from the mate. A negative sign (attracting force) indicates the direction of force is towards the mate.

$$W_r = \frac{W_t}{\cos \psi} (\tan \phi \cos \gamma - \sin \psi \sin \gamma) \quad \text{concave load face}$$

$$W_r = \frac{W_t}{\cos \psi} (\tan \phi \cos \gamma + \sin \psi \sin \gamma) \quad \text{convex load face}$$

#### Equation 48

where

$W_r$  is the axial force or thrust load

$W_t$  is transmitted load

$\psi$  is helix angle

$\phi$  is pressure angle

$\gamma$  is the pitch angle for the gear of interest

Force analysis for the bevel gear sizing tool is in Table 38 of APPENDIX C:  
BEVEL GEAR RATING CALCULATIONS.

## Contact Stress

The rating formula for bevel gear bending stress is:

$$s_c = C_p \sqrt{\frac{2T_p}{Fd^2I} K_o K_v K_m C_s C_{xc}}$$

**Equation 49**

where

- $s_c$  is calculated contact stress
- $C_p$  is elastic coefficient
- $C_s$  is size factor
- $T_p$  is operating pinion torque (lb in)
- $K_o$  is overload factor
- $K_v$  is dynamic factor
- $F$  is net face width
- $d$  is pinion outer pitch diameter
- $K_m$  is load distribution factor
- $C_{xc}$  is crowning factor
- $I$  is pitting resistance

Much of the rating calculations for bevel gears follow the rating procedure for spur or helical gears (see page 73).  $C_p$  is derived from Equation 33.  $K_o$  is from Table 6.  $K_v$  is from Figure 22. The factors  $C_s$ ,  $K_m$ ,  $C_{xc}$ , and  $I$  as they apply to aerospace gears are listed below.

## Size Factor, $C_s$

The size factor for pitting resistance accounts for nonuniformity of material and is a function of face width:

$$C_s = 0.125F + 0.4375$$

**Equation 50**

where

$$\begin{aligned} 0.5 \leq F \leq 4.5 \\ \text{for } F > 4.5, C_s = 1.0 \end{aligned}$$

**Load Distribution Factor,  $K_m$**

The load distribution factor accounts for non-uniform loads across along the line of contact. The factor is expressed in Equation 51.  $K_{mb}$  is:

- 1.00 for both members straddle mounted
- 1.10 for one member straddle mounted
- 1.25 for neither member straddle mounted.

$$K_m = K_{mb} + 0.0036F^2$$

**Equation 51**

where

$K_{mb}$  is load distribution modifier  
F is net face width

**Crowning Factor,  $C_{xc}$**

The crowning factor compensates for variation in the crowning during manufacturing.  $C_{xc}$  is 1.50 for properly crowned teeth and 2.0 for larger non-crowned teeth. A value of 1.50 has been used in the bevel gear calculations.

**Geometry Factor,  $I$**

The geometry factor for pitting resistance is:

$$I = \frac{s\rho_o \cos\psi \cos\phi}{FdC_i m_{NI}} \frac{P_d}{P_m}$$

**Equation 52**

Geometry factor calculations for the bevel gear model are included in Table 42: Bevel Gear Pitting Resistance Geometry Factor of APPENDIX C: BEVEL GEAR RATING CALCULATIONS. The geometry factor,  $I$ , is found by assuming a critical loading point over the tooth line. The true critical point and  $I$  occur as the minimum from Figure 31.

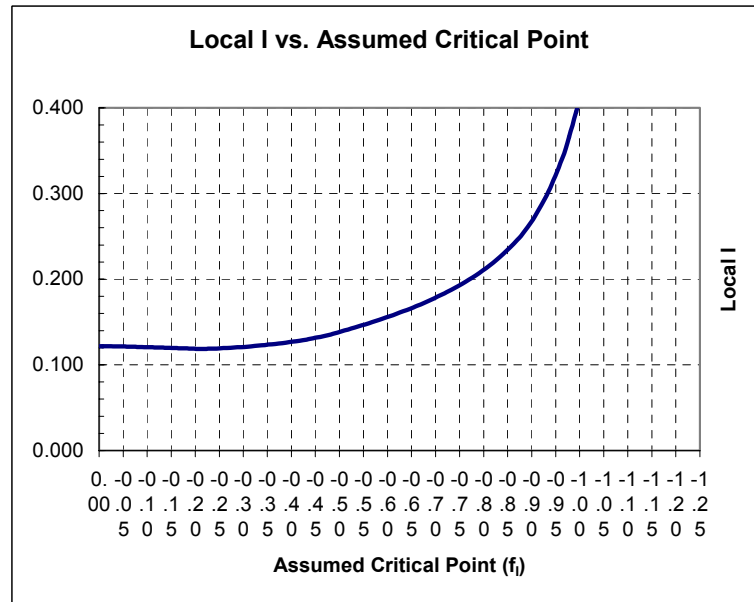


**Figure 31: Finding the Bevel Gear Geometry Factor,  $I$**

### Allowable Contact Stress

The relationship between contact stress and allowable contact stress is expressed in Equation 53.  $C_L$  is found from Figure 23.  $S_H$  has the same considerations as for spur and helical gears. Unity is used for  $S_H$  during preliminary analysis.

$$s_c \leq \frac{s_{ac} C_L C_H}{S_H K_T C_R}$$

### Equation 53

where

$s_{ac}$  is allowable contact stress

$C_L$  is stress cycle factor

$S_H$  is contact safety factor

$C_H$  is hardness ratio

$K_T$  is temperature factor

$C_R$  is reliability factor

### Temperature Factor, $K_T$

For gear blank temperatures at or below 250° F,  $K_T$  is 1.0. For operations above 250° F,  $K_T$  is:

$$K_T = \frac{460 + T_T}{710}$$

### Equation 54

where

$T_T$  is the peak operating gear blank temperature

### Reliability Factors, $C_R$

The reliability factor is approximated in the same way as spur and helical gears but  $v$  is 0.156.<sup>71</sup> For bevel gears, Table 11 shows the factor for different requirements. An aerospace value of 1.09 has been applied to the bevel gear model. For this table,  $C_R$  is the square root of  $K_R$ .

---

<sup>71</sup> American Gear manufacturers Association, *AGMA 911-A94, Information Sheet-Design Guidelines for Aerospace Gearing* (Alexandria: AGMA, 1994), 43.

**Table 11: Bevel Gear Reliability Factors**

Desired Rate of Failure	Probability	C <sub>R</sub>	K <sub>R</sub>
Fewer than one failure in 10,000	0.9999	1.22	1.50
Fewer than one failure in 1,000	0.999	1.12	1.25
Aerospace Design (3σ)	0.99875	1.09	1.20
Fewer than one failure in 100	0.99	1.00	1.00
Fewer than one failure in 10	0.9	0.92	0.85
Fewer than one failure in 2	0.5	0.84	0.70

## Bending Stress

The formula for bending stress in a bevel gear is:

$$s_t = \frac{2T_p}{Fd} \frac{P_d K_o K_v}{1} \frac{K_s K_m}{K_x J}$$

### Equation 55

where

$s_t$  is calculated bending stress

$K_o$  is overload factor

$K_v$  is dynamic factor

$P_d$  is outer transverse diametral pitch

$K_s$  is size factor

$K_m$  is load distribution factor

$K_x$  is tooth lengthwise curvature factor

$J$  is bending strength factor

$K_o$  is found as in spur and helical gears using Table 6.  $K_v$  is from Figure 22.  $K_m$  is the same value as in pitting resistance (Equation 51).

### **Size Factor, $K_s$**

Instead of being a function of face width like pitting resistance, the size factor for bending stress is a function of outer transverse pitch. For  $16 \geq P_d \geq 0.5$ , the range of aerospace gearing, the size factor is:

$$K_s = 0.4867 + \frac{0.2133}{P_d}$$

**Equation 56**

### **Lengthwise Curvature Factor, $K_x$**

The lengthwise curvature factor is a function of spiral angle and tooth curvature. Table 38 and Table 39 of APPENDIX C: BEVEL GEAR RATING CALCULATIONS contain the relevant geometry and calculations for the factor.

### **Bending Strength Geometry Factor, $J$**

Calculations for the bending strength geometry factor for bevel gears is complex and beyond the needs of a preliminary design. Often charts are used for faster reference of  $J$  in preliminary design. To permit automated estimations, the geometry factor charts are calculated from least squares regressions for the following values:

Straight bevel gears for	$\psi = 0^\circ, \phi = 20 - 25^\circ, \Sigma = 90^\circ$
Spiral bevel gears for	$\psi = 35^\circ, \phi = 20^\circ, \Sigma = 60 - 90^\circ$
	$\psi = 15 - 35^\circ, \phi = 20^\circ, \Sigma = 90^\circ$



## Allowable Bending Stress

The relationship between bending stress and allowable bending stress is expressed in Equation 57.  $K_L$  is found with Figure 27.  $K_T$  estimated with Equation 54. The bevel gear calculations employ an aerospace reliability of 0.99875 ( $3\sigma$ ) which yields a  $K_R$  value of 1.20 (Table 11). The bending safety factor has the same considerations as spur and helical gears and is assumed to be unity for preliminary design.

$$s_t \leq \frac{s_{at} K_L}{S_F K_T K_R}$$

### Equation 57

where

$s_{at}$  is allowable bending stress

$S_F$  is bending safety factor

$K_L$  is stress cycle factor

$K_T$  is temperature factor

$K_R$  is reliability factor

## Bevel Gear Materials

Helicopter gearing demands the high strength, hardened steels that carburized, case hardened alloy steels provide (refer to Spur and Helical Gear Materials on page 66); however, for most helicopter drives, bevel gears are not used at the last few stages of the drive as the thrust loading becomes excessive. Operating earlier in the drive train, bevel gears tend to have higher speeds (rpm) and lower torque values.

Steels listed in Table 12 are suggested steels for bevel gears with tested strengths and properties.<sup>72</sup> All steels are recommended for accessory drives but only Grade 3, carburized and case hardened steels are strong enough for heavy lift main drive applications.

---

<sup>72</sup> ANSI/AGMA 2003-B97, Rating the Pitting Resistance and Bending Strength of Generated Straight Bevel, Zerol Bevel and Spiral Bevel Gear Teeth. (AGMA: Alexandria), 1997, p. 24.

**Table 12: Spur-Helical Gear Steels**

<b>Description</b>	<b>Units</b>	<b>Steel TH (Grade 2)</b>	<b>Steel C-H (Grade 1)</b>	<b>Steel C-H (Grade 2)</b>	<b>Steel C-H (Grade 3)</b>	<b>Nitr alloy 135M (Grade 2)</b>
<b>AMS Spec</b>		AGMA Class 5				
<b>Heat Treatment</b>		TH	C-H	C-H	C-H	Nitrided
<b>Main drive Application</b>					X	
<b>Accessory application</b>		X	X	X	X	X
<b>Case Hardness</b>	<b>HRC</b>	43	59.5	61	61	60
<b>Core Hardness</b>	<b>HRC</b>		21	25	30	
<b>Brinell Hardness</b>	<b>BH</b>	400	610	632	632	614
<b>Allowable Contact Stress</b>	<b>psi</b>	175,000	200,000	225,000	250,000	145,000
<b>Allowable Bending Stress</b>	<b>psi</b>	25,180	30,000	35,000	40,000	24,000
<b>Poisson's Ratio</b>		0.300	0.300	0.300	0.300	0.291
<b>Modulus of Elasticity</b>		30E6	30E6	30E6	30E6	30E6
<b>Density (weight)</b>	<b>lb/in3</b>	0.282	0.282	0.282	0.282	0.280

*C-H is Case Hardened. TH-N is Through Harden and Nitride.*

## **Scuffing Hazard**

Bevel gear scuffing hazard is not easily calculated and usually found through testing. The bevel gear rating model, due to these reasons, omits scuffing hazard assessment for bevel gears.

# SHAFTING

## **Simplified Shafting Model**

Transmission shafting experiences three-dimensional loads in the x, y, and z-directions; undergoing a combination of bending loads, torsional loads, and axial tension or compression loads. The Preliminary Design Handbook for Helicopter Engineering suggest that even though “a complete analysis normally would not be performed during the preliminary design phase, the principal static and dynamic loads should be analyzed sufficiently to insure structural integrity with the selected size, weight, and performance of the drive.”<sup>73</sup> Capturing gear shaft loading, to include aerodynamic loads, can quickly become one of the “most complex loading conditions of the drive system.”<sup>74</sup> To estimate the loads and moments on shafts in the preliminary design phase, a simplified loading model for the y and z-directions is created (the x-direction contains the axial loads and does not impact shear or bending moments). Figure 32 shows a loading diagram in the y-direction.

---

<sup>73</sup> Headquarters, U.S. Army Material Command, AMC Pamphlet 706-201 Engineering Design Handbook: Helicopter Engineering (Part One: Preliminary Design) (Alexandria: GPO, 1974), 4-70.

<sup>74</sup> Headquarters, U.S. Army Material Command, AMC Pamphlet 706-201 Engineering Design Handbook: Helicopter Engineering (Part One: Preliminary Design) (Alexandria: GPO, 1974), 4-74.

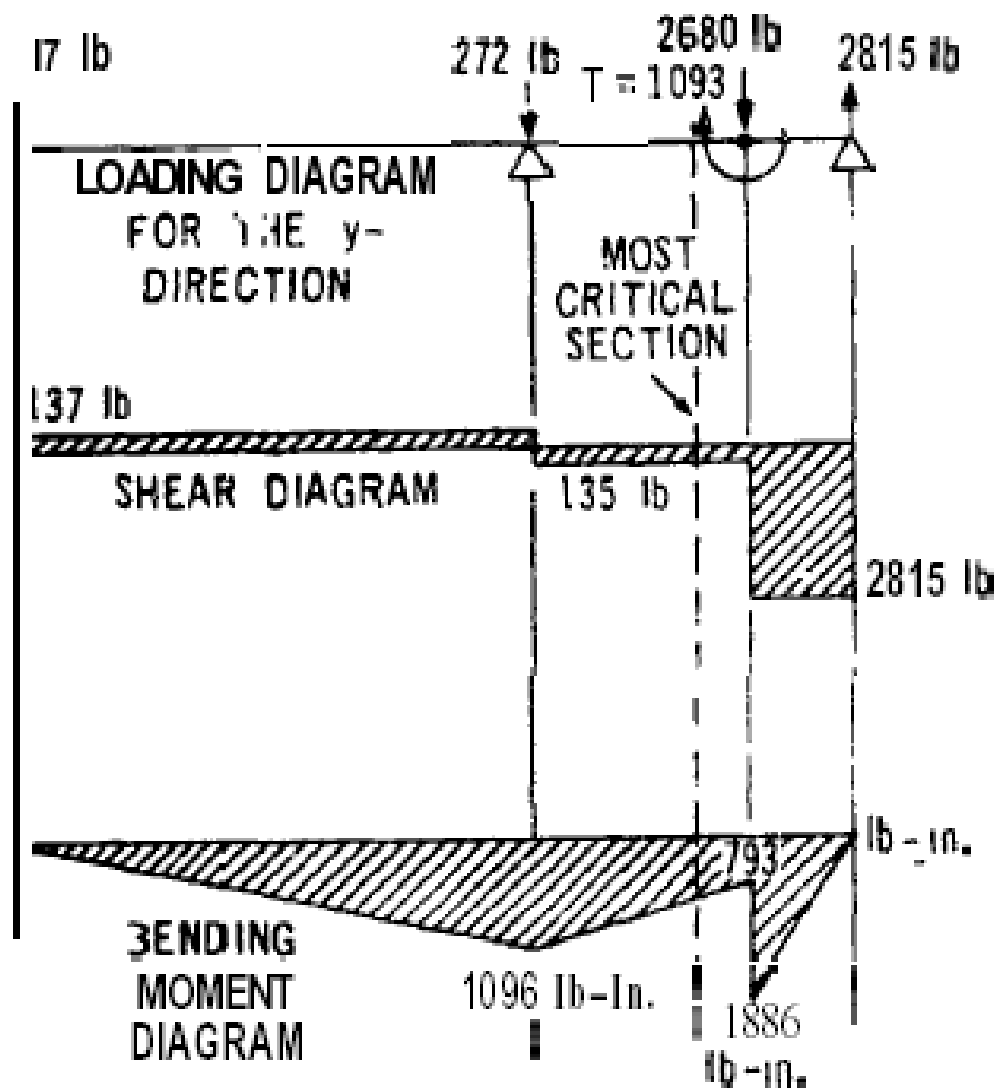


Figure 32: Loading Diagram for y-Direction<sup>75</sup>

<sup>75</sup> Headquarters, U.S. Army Material Command, AMC Pamphlet 706-201 Engineering Design Handbook: Helicopter Engineering (Part One: Preliminary Design). (Alexandria: GPO, 1974), 4-75.

The sample of the shafting tool shown in APPENDIX C: SHAFT DESIGN CALCULATIONS contains a simple bearing-gear (or loading)-bearing arrangement similar to Figure 33. The example shown in the figure has no moment about the z-axis and a significant moment (-275,000 in lb) moment about the y-axis. Other configurations are possible: the example shown in Figure 32 contains a bearing-gear-gear-bearing arrangement (BGGB). Within the shafting model, the user may select any of the following arrangements:

1. BGB
2. BGBG
3. GBGB
4. GBBG
5. BGGB

where

B is support bearing

G is splined gear or any applied load or torsion

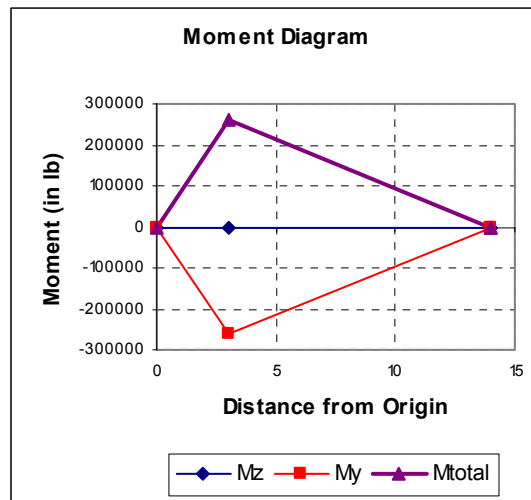


**Figure 33: Sample Shaft Moment Diagram**

## **Margin of Safety**

Total moment on the shaft does not have a steady direction with respect to the shaft because the shaft is rotating. This loading is “of a vibratory nature”<sup>76</sup> and requires an interaction equation to account for vibratory bending stress, axial tension stress, and torsion shear stress. The Preliminary Design Handbook for Helicopter Engineering suggest a margin of safety based upon the maximum shear theory of failure:<sup>77</sup>

$$MS = \frac{1}{\sqrt{\left(\frac{f_b}{F_{en}} + \frac{f_a}{F_{ty}}\right)^2 + 4\left(\frac{f_s}{F_{sy}}\right)^2}}$$

**Equation 58**

where

MS is margin of safety

$f_a$  is axial tension stress, psi

$f_b$  is vibratory bending stress, psi

$f_s$  is torsional shear stress, psi

$F_{en}$  is endurance limit stress, psi

$F_{sy}$  is shear yield stress, psi

$F_{ty}$  is tensile yield stress, psi

The maximum shear theory accounts for the fact that shaft failures normally occur from fatigue loading.<sup>78</sup> To save weight, transmission shafting is usually hollow with as high of a diameter to thickness ratio as possible.<sup>79</sup> The shafting tool in APPENDIX C: SHAFT DESIGN CALCULATIONS iterates the Margin of Safety by varying the shafts

---

<sup>76</sup> Headquarters, U.S. Army Material Command, AMC Pamphlet 706-201 Engineering Design Handbook: Helicopter Engineering (Part One: Preliminary Design) (Alexandria: GPO, 1974), 7-3.

<sup>77</sup> Headquarters, U.S. Army Material Command, AMC Pamphlet 706-201 Engineering Design Handbook: Helicopter Engineering (Part One: Preliminary Design) (Alexandria: GPO, 1974), 7-3.

<sup>78</sup> Headquarters, U.S. Army Material Command, AMC Pamphlet 706-201 Engineering Design Handbook: Helicopter Engineering (Part One: Preliminary Design) (Alexandria: GPO, 1974), 4-75.

<sup>79</sup> Headquarters, U.S. Army Material Command, AMC Pamphlet 706-201 Engineering Design Handbook: Helicopter Engineering (Part One: Preliminary Design). (Alexandria: GPO, 1974), 7-2.



diameter and thickness. The output recommends the lightest shaft that meets the user specified minimum Margin of Safety.

## Vibratory Bending Stress

From the maximum shear theory, the alternating bending stress is:

$$f_b = \frac{Mc}{I}$$

**Equation 59<sup>80</sup>**

where

M is the total bending moment

c is the radius where stress is calculated

I is the moment of inertia for a hollow shaft

$$I = \frac{\pi(D^4 - d^4)}{64}$$

The maximum bending stress will occur at the outer diameter where product of the moment and a stress concentration factor,  $K_b$ , are greatest:

$$f_{b \max} = \frac{32K_b M_{\max} D}{\pi(D^4 - d^4)}$$

**Equation 60**

---

<sup>80</sup> Peter Lynwander, Gear Drive Systems Design and Application (New York: Marcel Dekker, 1983), 137.

According to Mischke, the endurance limit or fatigue limit of steels maybe approximated as:

$$F_{en} = \begin{cases} 0.504 S_{ut} & S_{ut} < 200 \text{ kpsi} \\ 100 \text{ kpsi} & S_{ut} > 200 \text{ kpsi} \end{cases}$$

**Equation 61<sup>81</sup>**

where

$S_{ut}$  is the ultimate tensile strength

### **Axial Tension Stress**

On helicopter shafting, axial tension or compression stress is the axial loading from helical or bevel gears and also from aerodynamic loads (thrust) on the main rotor or tail rotor drive shafts. Axial stress is the force to area ratio and is expressed as:

$$f_a = \frac{F}{A} = \frac{4F}{\pi(D^2 - d^2)}$$

**Equation 62**

where

$f_a$  is axial stress

A is cross sectional area

F is the axial load

D is the outer shaft diameter

d is the inner shaft diameter (d = 0 for a solid shaft; D – d = thickness)

---

<sup>81</sup> Joseph Shigley and Charles Mischke, Mechanical Engineering Design, 5<sup>th</sup> ed (New York: McGraw-Hill, 1989), 278.

The tensile yield stress,  $F_{ty}$ , is also referred to as the yield strength and is an easily referenced material property.

### **Torsional shear stress**

Engine drive and tail rotor drive shafting primarily carry torsional loads.<sup>82</sup> For the simple model, the torsional shear stress is assumed steady and equal to:

$$f_s = \frac{Tr}{J}$$

**Equation 63<sup>83</sup>**

where

$f_s$  is torsional shear stress

$T$  is torque

$r$  is radial distance of the desired stress point

$J$  is the polar moment of inertia

$$J = \frac{\pi(D^4 - d^4)}{32}$$

The maximum shear stress will occur along the outside diameter at the greatest value of the product of the stress concentration factor  $K_s$ , and the local moment:

$$f_{s \max} = \frac{16TK_s D}{\pi(D^4 - d^4)}$$

**Equation 64**

---

<sup>82</sup> Headquarters, U.S. Army Material Command, AMC Pamphlet 706-201 Engineering Design Handbook: Helicopter Engineering (Part One: Preliminary Design) (Alexandria: GPO, 1974), 7-3.

<sup>83</sup> Peter Lynwander, Gear Drive Systems Design and Application (New York: Marcel Dekker, 1983), 138.

Most often, the critical area on a shaft occurs at a sharp narrowing of the shaft diameter. This increased stress is captured with a stress concentration factor,  $K_s$ .

For the maximum-shear stress theory, the endurance limit stress is one-half the yield strength.<sup>84</sup>

$$F_{sy} = 0.5F_{ty}$$

### **Equation 65**

## **Critical Speeds**

One of the greatest challenges to shaft design is the divergence phenomenon nicknamed named “critical speeds.” As shaft speed increase, residual unbalances create large centrifugal forces. The centrifugal forces bend the rotating shaft and are balanced by the elastic forces in the shaft. This balance is likened to a skipped rope.<sup>85</sup> As the shaft increases past this critical speed, the bent mass moves to the centerline until the shaft rotates about its axis.

Operation below the critical speed is called a subcritical condition while operation above the critical speed is termed supercritical. For safe operation, subcritical shafts must not operate within 30% of the critical speed. Supercritical shafts must not operate within 10% of the critical speed.<sup>86</sup> Drive shafts connecting gearboxes and engines

---

<sup>84</sup> Joseph Shigley and Charles Mischke, Mechanical Engineering Design, 5<sup>th</sup> ed (New York: McGraw-Hill, 1989), 250.

<sup>85</sup> Headquarters, U.S. Army Material Command, AMC Pamphlet 706-201 Engineering Design Handbook: Helicopter Engineering (Part One: Preliminary Design) (Alexandria: GPO, 1974), 7-62.

<sup>86</sup> Headquarters, U.S. Army Material Command, AMC Pamphlet 706-201 Engineering Design Handbook: Helicopter Engineering (Part One: Preliminary Design) (Alexandria: GPO, 1974), 7-69.

usually operate below or between critical speeds.<sup>87</sup> If a shaft is designed to run above the critical speed, damping is required during run-up as the shaft passes through the avoid range.

## Nonuniform Shafts

Nonuniform shafts are defined as having a nonuniform rigidity or concentrated masses such as splined gears. A variation on Rayleigh's method as outlined in the Preliminary Design Handbook for Helicopter Engineering derives the natural frequency by comparing kinetic energy with potential energy.<sup>88</sup> This is done by dividing the shaft into concentrated mass of  $m_i$  connected by massless, stiff shaft elements (Figure 34). The shaft deflection from a bending moment maybe calculated by numerically integrating:

$$y = \int \int \frac{M}{EI} dx dx$$

### Equation 66

where

y is shaft deflection (in)  
M is bending moment  
E is modulus of elasticity  
I is moment of inertia

---

<sup>87</sup> Headquarters, U.S. Army Material Command, AMC Pamphlet 706-201 Engineering Design Handbook: Helicopter Engineering (Part One: Preliminary Design) (Alexandria: GPO, 1974), 7-3.

<sup>88</sup> Headquarters, U.S. Army Material Command, AMC Pamphlet 706-201 Engineering Design Handbook: Helicopter Engineering (Part One: Preliminary Design) (Alexandria: GPO, 1974), 7-63.

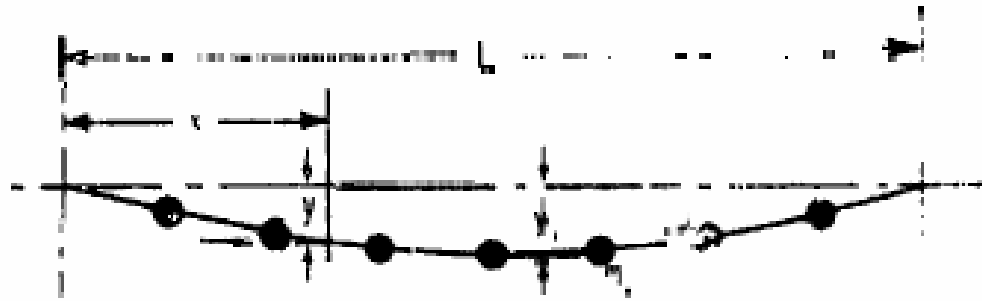


**Figure 34: Mathematical Model of Nonuniform Shaft**<sup>89</sup>

As an example, Equation 66 is numerically integrated with Simpson's Rule in Table 47. Figure 35 shows the shaft bending and moment for the shaft example in Table 47.

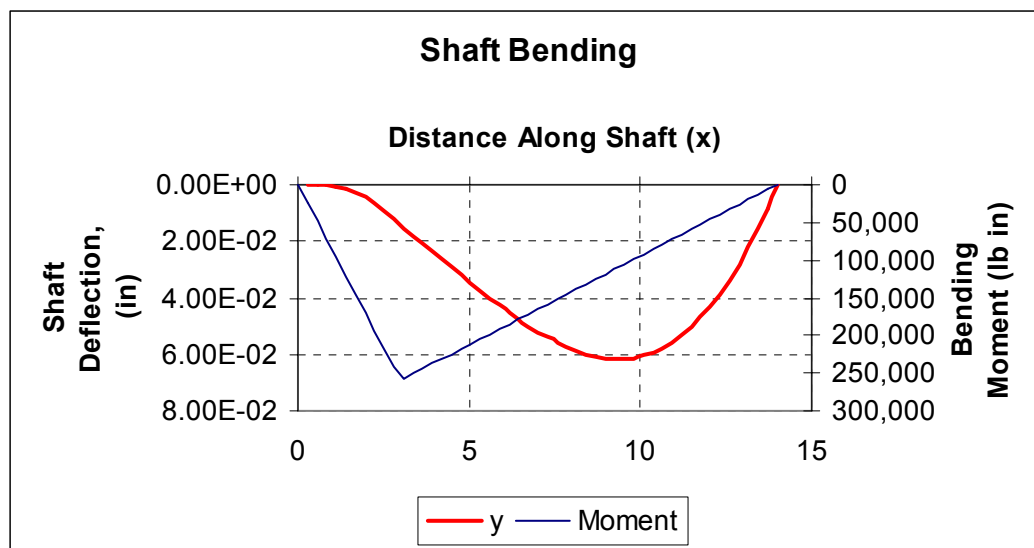


**Figure 35: Nonuniform Shaft Bending**

<sup>89</sup> Headquarters, U.S. Army Material Command. AMC Pamphlet 706-201 Engineering Design Handbook: Helicopter Engineering (Part One: Preliminary Design) (GPO: Alexandria, Virginia), August 1974, p. 7-64.

With the deflection known, the kinetic energy is:

$$T = \frac{\omega^2}{2} \sum_{i=1}^p \frac{w_i}{g} y_i^2$$

**Equation 67**

where

T is kinetic energy (in lb)

$\omega$  is shaft frequency

$w_i$  are lumped weights

$g$  is 386.4 in/sec<sup>2</sup>

$y_i$  is element deflection

The potential energy is:

$$V = \frac{1}{2} \sum_{i=1}^p w_i y_i$$

**Equation 68**

where

V is potential energy (in lb)

$w_i$  are lumped weights

$y_i$  is element deflection

The natural frequency is found by equating potential energy to kinetic energy.

Expressing the natural frequency as a critical speed in rpm yields:

$$N_c = \frac{60}{2\pi} \sqrt{g \frac{\sum_{i=1}^p w_i y_i}{\sum_{i=1}^p w_i y_i^2}}$$

**Equation 69**

where

$N_c$  is critical speed (rpm)

## Uniform Shafts

For shafts with uniform mass distribution and with no moment restraint on the bearings, there will be no bending moment. This is common in the tail rotor drive shaft connecting the main transmission to the tail rotor gearbox. This type of shaft maybe modeled as a beam with length L where bearings support the ends. The critical speed for a uniform shaft is a “function of the mean radius of the tube and the length between supports.”<sup>90</sup> The critical speed,  $N_c$ , is expressed in rpm as:

$$N_c = \frac{30\pi^3}{2\pi L^2} \sqrt{\frac{4gE\pi(D^4 - d^4)}{64\pi\rho(D^2 - d^2)}}$$

**Equation 70**

where

L is shaft length  
g is 386.4 in/sec<sup>2</sup>  
E is modulus of elasticity  
ρ is density (weight)  
D is outside diameter  
d is inside diameter

## **Shaft Materials**

Lightweight metals such as aluminum alloys and titanium are preferred for shafts in helicopter drives systems. Great strength can be gained from high diameter to thickness ratios that permits the use of weight saving aluminum alloys. The Boeing HLH

---

<sup>90</sup> Headquarters, U.S. Army Material Command. AMC Pamphlet 706-201 Engineering Design Handbook: Helicopter Engineering (Part One: Preliminary Design) (GPO: Alexandria, Virginia), August 1974, p. 7-63.



employed aluminum alloy for most shafting except in the main rotor drive shaft. There, the stronger titanium was added to withstand high aerodynamic loads. The shafting model has several aluminum alloys, steel 4340 and the same titanium found in the HLH for user selection (Table 49). All designs presented in this thesis use Aluminum Alloy T7075 and Titanium Forging 6 A1-4V. Table 13 has representative samples from the material database.

**Table 13: Shaft Material Properties**

<b>Property</b>	<b>Units</b>	<b>Aluminum Alloy T7075</b>	<b>Steel AISI 4340</b>	<b>Titanium Forging (6 A1-4V)</b>
Ultimate tensile strength	psi	86,000	250,000	135,821
Yield tensile strength	psi	78,600	230,000	122,642
Shear yield stress	psi	39,300	115,000	61,321
Endurance strength	psi	20,000	100,000	20,000
Endurance limit	psi	14,280	71,400	14,280
Surface factor		1.00	1.00	1.00
Size factor		0.70	0.70	0.70
Load factor		1.00	1.00	1.00
Temperature factor		1.02	1.02	1.02
Miscellaneous effects		1.00	1.00	1.00
Total endurance factor		0.71	0.71	0.71
Density (weight)	lb/in <sup>3</sup>	0.098	0.283	0.161
Modulus of Elasticity		10.3E6	30.0E6	15.5E6

Endurance strength has been derated in accordance with Shigley and Mischke<sup>91</sup> to account for outside factors on the material strength (Equation 71). Values for each

---

<sup>91</sup> Joseph Shigley and Charles Mischke, Mechanical Engineering Design, 5<sup>th</sup> ed (New York: McGraw-Hill, 1989), 283.

modifying factor are in Table 13. Total endurance factor k, is estimated as 0.71.

$$k = k_a k_b k_c k_d k_e$$

**Equation 71**

## GEARBOX COOLING

Although gear efficiency is high, at the power levels of the JHL sizeable amounts of heat must be dissipated by the lubrications system. Mesh efficiencies maybe taken as:<sup>92</sup>

1. 99.5% per spur mesh
2. 99.5% per helical mesh
3. 99.5% per bevel mesh
4. 99.25% per planetary set

Power loss from a gear mesh is a function of the efficiency,  $\eta$ , and applied power, HP:

$$HP_{loss} = (1 - \eta)HP$$

### Equation 72

Assuming any power loss is converted into heat by the meshing gears, the oil temperature rise across the gearbox is:

$$\Delta T = \frac{Q}{MC_p}$$

### Equation 73

where

$\Delta T$  is temperature rise (°F)

---

<sup>92</sup> Headquarters, U.S. Army Material Command. AMC Pamphlet 706-201 Engineering Design Handbook: Helicopter Engineering (Part One: Preliminary Design) (GPO: Alexandria, Virginia), August 1974, p. 7-6 to 7-12.

M is oil flow (lb/min)

Q is heat generated (Btu/min) where  $Q = HP (42.4)$

Cp specific heat of oil  $\approx 0.5$  Btu/lb-°F

For example, in the sample spur gear calculations of Table 32 and summarized below, total oil flow required to maintain a  $\Delta T$  of 30° F is 5.32 gallons.

**Table 14: Sample Cooler Design**

Value	General Rule	Aerospace Limit
HP	2,600 hp	
$\eta$	99.5%	
HP <sub>loss</sub>	13.3 hp	
Q	563.9 Btu/min	
M	39.9 lb/min or 5.3 gal/min	25.1 lb/min or 3.3 gal/min
T <sub>oilin</sub>	125° F	125° F
$\Delta T$	30 ° F	45° F
T <sub>oilout</sub>	155° F	170° F
T <sub>oilavg</sub>	140° F	147.5° F

Aerospace designs normally operate up to a maximum  $\Delta T$  of 45° F.<sup>93</sup> The calculations used in the lubrication and cooling model utilize a  $\Delta T$  of 45°F to determine oil flow required. A typical helicopter main gearbox lubrication system is shown in Figure 36.

---

<sup>93</sup> Darle Dudley, Handbook of Practical Gear Design (Lancaster: Technomic, 1994), 3.129.

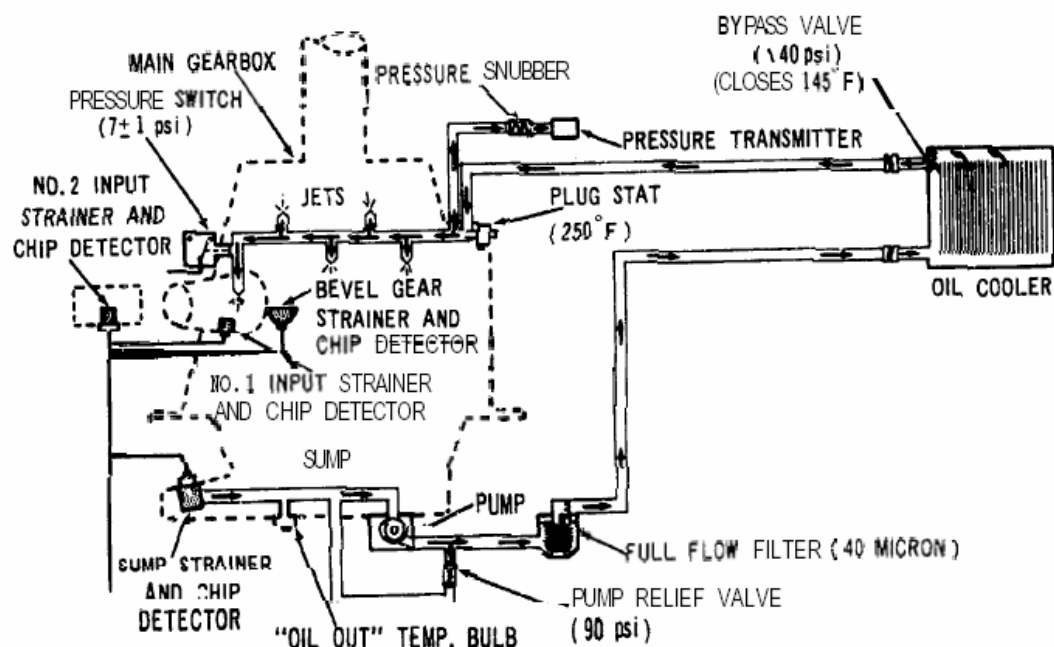


**Figure 36: Typical Main Gearbox Lubrication System<sup>94</sup>**

<sup>94</sup> Headquarters, U.S. Army Material Command. AMC Pamphlet 706-201 Engineering Design Handbook: Helicopter Engineering (Part One: Preliminary Design) (GPO: Alexandria, Virginia), August 1974, p. 7-4.

## TRADITIONAL PLANETARY MODEL

The traditional planetary drive system model consists of a 2-stage planetary main gear box where the sun gear of the first stage is the input and the carrier of the second stage is the output and transfers torque to the main rotor shaft. The main gearbox is similar to the Boeing prototype HLH's forward or aft transmissions. The tandem rotor HLH transmission had a 2-stage planetary gearset driving both the forward and aft rotors. A sketch of the HLH's transmission layout is shown in Figure 37 and the 2-stage planetary aft transmission is shown in Figure 38.

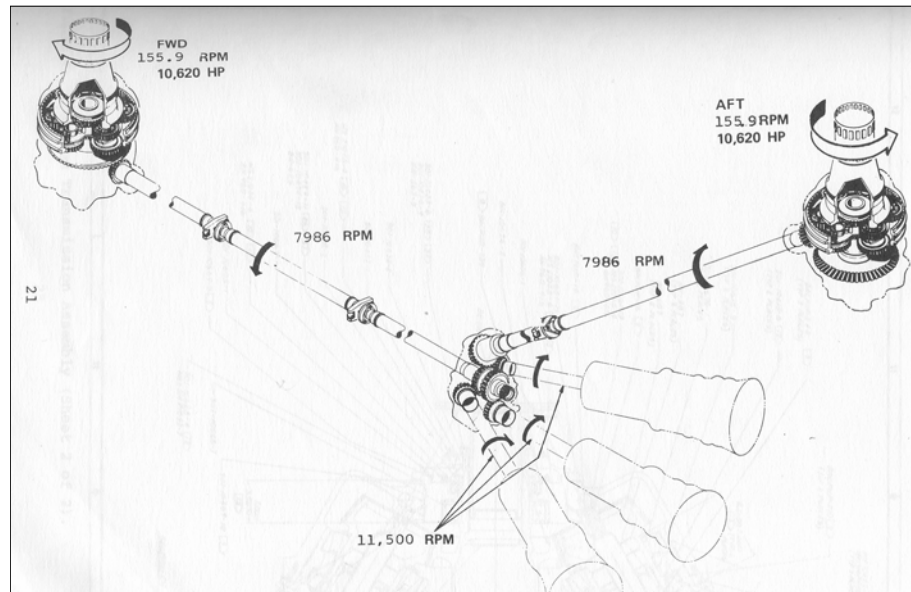


**Figure 37: HLH Drive System Arrangement<sup>95</sup>**

---

<sup>95</sup> Mack, J.C., USAAMRDL-TR-77-38: HLH Drive System (Boeing Vertol: Philadelphia, 1977), p. 21.

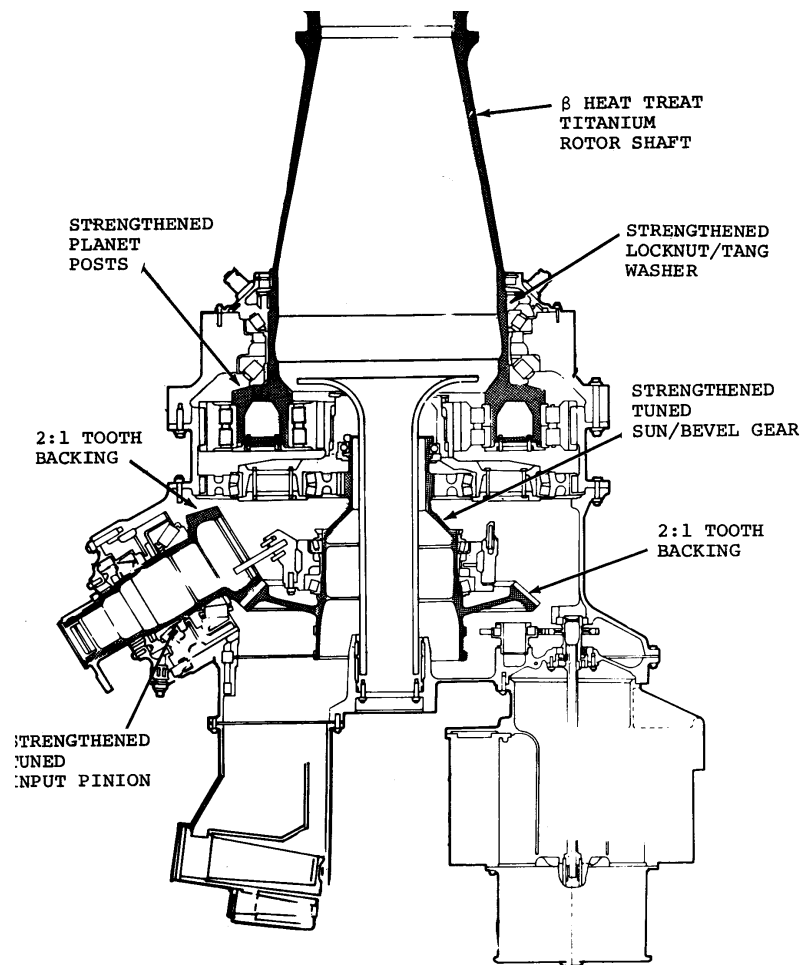
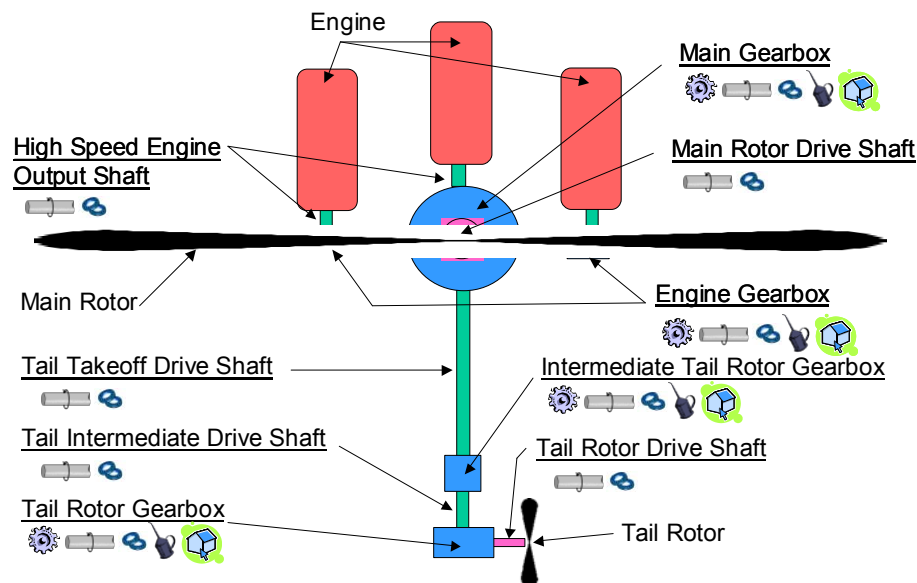


Figure 38: HLH Aft Transmission<sup>96</sup>

<sup>96</sup> Mack, J.C., USAAMRDL-TR-77-38: HLH Drive System (Boeing Vertol: Philadelphia, 1977).219.

## **Drive Arrangement**

The Supplemental Information defines the JHL baseline aircraft with 3 scaleable turbine engines, a single main rotor and traditional anti-torque tail rotor (Figure 4 and Figure 5). While the Boeing HLH was a tandem helicopter, the aft and front 2-stage planetary main gearbox was used as the model for the JHL planetary gearbox. Figure 39 shows the planetary drive system that fits within the requirements of the JHL Supplement.<sup>97</sup> Although there are many possible configurations that satisfy the JHL Supplement's requirements, this arrangement follows a traditional layout for helicopters.



**Figure 39: Drive System Components**

<sup>97</sup> Aviation Applied Technology Directorate, "Joint Heavy Lift Supplemental Package" (Fort Eustis: AATD, November 4, 2004).



### **Engine Input Gearbox**

Each turbine engine undergoes an initial reduction ratio at the Engine Input Gearbox. Inside the gearbox is a freewheeling unit to allow autorotation. The left and right Engine Input Gearbox have a pair of bevel gears to change the direction of the drive 90°. The bevel gear also mates with an accessory bevel gear to power the left or right accessory set. The center engine has a helical idler and helical gear to power the accessory set.

### **Bevel Crown**

The bevel crown resides below the 2-stage planetary set and receives the power input from the Engine Gearbox Output Shaft. Three bevel pinions drive the Crown Bevel gear which drives the 1<sup>st</sup> stage sun gear.

### **Oil Cooler Gearbox**

A tail takeoff bevel pinion mates with the crown gear and links an oil cooler located directly aft of the main gearbox. The oil cooler gearbox distributes power to the main oil cooler, an auxiliary accessory module, and the tail take off shaft.

### **Intermediate Tail Rotor Gearbox**

The tail takeoff shaft has 12 equally spaced 45” segments linked down the tail boom of the aircraft. A bevel gear set conducts a 60° direction change to power the intermediate tail rotor shaft. The shaft connects to the tail rotor gearbox at the top of the vertical tail.

## Tail Rotor Gearbox

The Tail Rotor Gearbox conducts a final speed reduction and a 90° direction change to drive the Tail Rotor Drive Shaft.

## Planetary Main Gearbox

The planetary gearbox overall ratio is considered an independent variable; however, the individual reduction ratio of each planetary stage is minimized for weight according to Willis' "Lightest-weight gears" procedure for compound drives.<sup>98</sup> Figure 40 shows the weight minimization for a 2-stage planetary gearset.

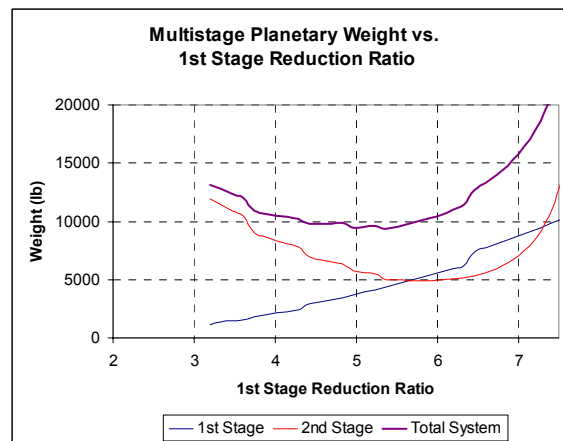


**Figure 40: Example Optimized 2-Stage Planetary Gearbox**

---

<sup>98</sup> R.J. Willis, "New Equations and Chart Pick Off Lightest-weight Gears," *Product Engineering* v. 34, n.s. 2 (January 21, 1963): 65.

For a given overall reduction ratio, the procedure assumes a first stage gear ratio. The corresponding second stage ratio is the quotient of the overall ratio to the 1<sup>st</sup> stage ratio.

$$m_{G2} = M_G/m_{G1}$$

**Equation 74**

The total rotor volume is computed for each assumed first stage reduction ratio. The procedure iterates until the minimum total rotor volume (and weight) is found. The iteration is complicated by the fact that the number of planets is a function of a planetary gear's reduction ratio. As the stage reduction ratio increase, the number of allowable whole planets decreases. This function is not continuous but a step since it is impossible to have a fraction of a planet installed. The discrete function is what gives rise to the step-like nature of the curves. These calculations are found in Table 54: Planetary Drive Minimum Weight Solution.

### **Planetary Drive Modeling**

To capture the behavior of the planetary drive, the weight estimation and shafting elements were entered into Model Center 6.0. Model Center's planetary drive model consisted of a weight estimation spreadsheet (Table 50) and individual shaft sizing spreadsheets (refer to SHAFTING for shaft discussion and APPENDIX C: SHAFT DESIGN CALCULATIONS for sample calculations). Shafting spreadsheets were added to include the engine output shaft, main rotor drive shaft, tail takeoff shaft, intermediate

tail rotor shaft, and tail rotor drive shaft. Figure 41 shows the planetary drive model in Model Center:

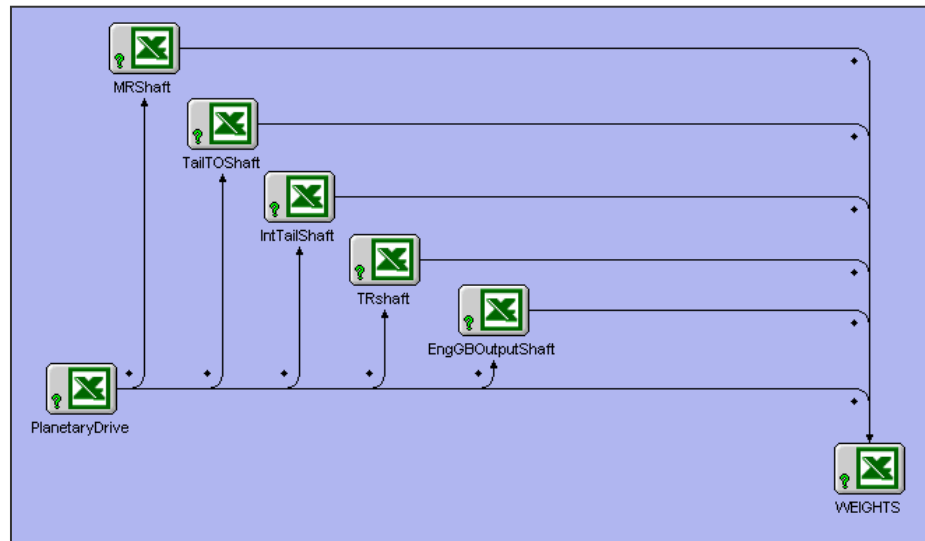


**Figure 41: Planetary Drive in Model Center**

The weight estimation spreadsheet calculated all speed, torque, power, and power losses for each gear and shaft of the drive system. This spreadsheet also provided a total gearbox weight based on the solid rotor volume method, and total drive system weight estimations based on the Boeing-Vertol and RTL weight equations. Since the solid rotor volume method only estimates gearbox weight, shafting linking gearboxes needed inclusion. To accomplish this, individual spreadsheets were added into Model Center for all external shafts connecting the drive's gearboxes. A final spreadsheet called "WEIGHTS" summed all gearbox, shaft, and drive system weights to allow easy comparison of estimates.

### **Weight Estimation Results**

Weight equations results for the baseline JHL from the solid rotor volume method plus individual shafting calculations, Boeing-Vertol, and RTL yielded a minimum weight results shown in Table 15. The optimal baseline design was determined through a variable metric method optimization in Model Center. The drive system design methodology compares very favorably to the Boeing-Vertol and RTL predictions.

**Table 15: Planetary Drive Weight Estimate Results**

<b>Component</b>	<b>Shafting Plus Solid Volume Rotor</b>	<b>Predicted from RSE</b>	<b>Boeing- Vertol</b>	<b>RTL</b>
Total Gearbox Weight (lb)	13,729			15,835
Total Shafting Weight (lb)	1,474			785
Main Rotor Drive Weight (lb)			12,024	
Tail Rotor Drive Weight (lb)			1,338	
Total Drive System Weight (lb)	15,203	15,262	13,361	16,620

The key parameters for the weight optimized baseline aircraft is shown below.

**Table 16: Planetary Baseline Design Summary**

<b>Parameter</b>	<b>Value</b>	<b>Parameter</b>	<b>Value</b>
Overall Reduction Ratio	130.43	MR Power (hp)	22,247
Engine Input Gearbox Reduction Ratio	2.68	Tail Rotor Power (hp)	1989
Crown Bevel Reduction Ratio	4.86	Accessory Power (hp)	120
1 <sup>st</sup> Stage Planetary Reduction Ratio	3.74	Main Rotor Speed (rpm)	115
2d Stage Planetary Reduction Ratio	2.67	Tail rotor Speed (rpm)	476.3
Overall Planetary Reduction Ratio	10	Main Gearbox Weight (lb)	13,729
Short Shaft Bevel Takeoff Reduction Ratio	0.51	Shaft Weight (lb)	1,474
Intermediate Tail Rotor GB Reduction	1.59	Drive System Weight (lb)	15,203
Tail Rotor Gearbox Reduction Ratio	2.98	Efficiency	97.18%

## SPLIT TORQUE MODEL

A split-torque drive offers great weight savings potential. Litvin (2000) sums up the benefit of the split torque model best by commenting:

“Gear volume is proportional to the square of gear diameter, while torque-carrying capacity of gearing is proportional to lower order determinants of gear diameter (depending on whether bending or compressive stress evaluations are being used). Therefore, if torque is reduced by approximately one-half (based on the actual percentage of torque split between gears) for a load carrying gear, the weight of the gear can be reduced by more than one-half, due to the square relationship of weight to gear diameter.”<sup>99</sup>

The Mi-26 houses a highly successful, operational split-torque helicopter transmission that is close to the JHL needs. The 105,000 lb Mi-26 is about 35,000 lb lighter than the JHL Baseline. The Mi-26 main gearbox served as the initially layout for the JHL torque-split drive. Below is a picture of the Mi-26 main gearbox.

---

<sup>99</sup> F.L. Litvin et al, NASA/CR-2000-209909 Handbook on Face Gear Drives With a Spur Involute Pinion (NASA, March 2000), 47.



**Figure 42: Mi-26 Main Gearbox<sup>100</sup>**

### **Drive Arrangement**

With a dual engine configuration, the Mi-26 transmission splits the torque evenly three times for a total torque split of  $8 (2^3)$  per engine. The engine input shafts extend through the main gearbox housing power two bevel gears for the main drive and one set of bevel gears to the tail rotor shaft. The total gearbox reduction ratio is 62.52.

---

<sup>100</sup> Figure extracted from Reductor website: <http://www.reductor-pm.ru/eng/allpr.html>, September 14, 2005.



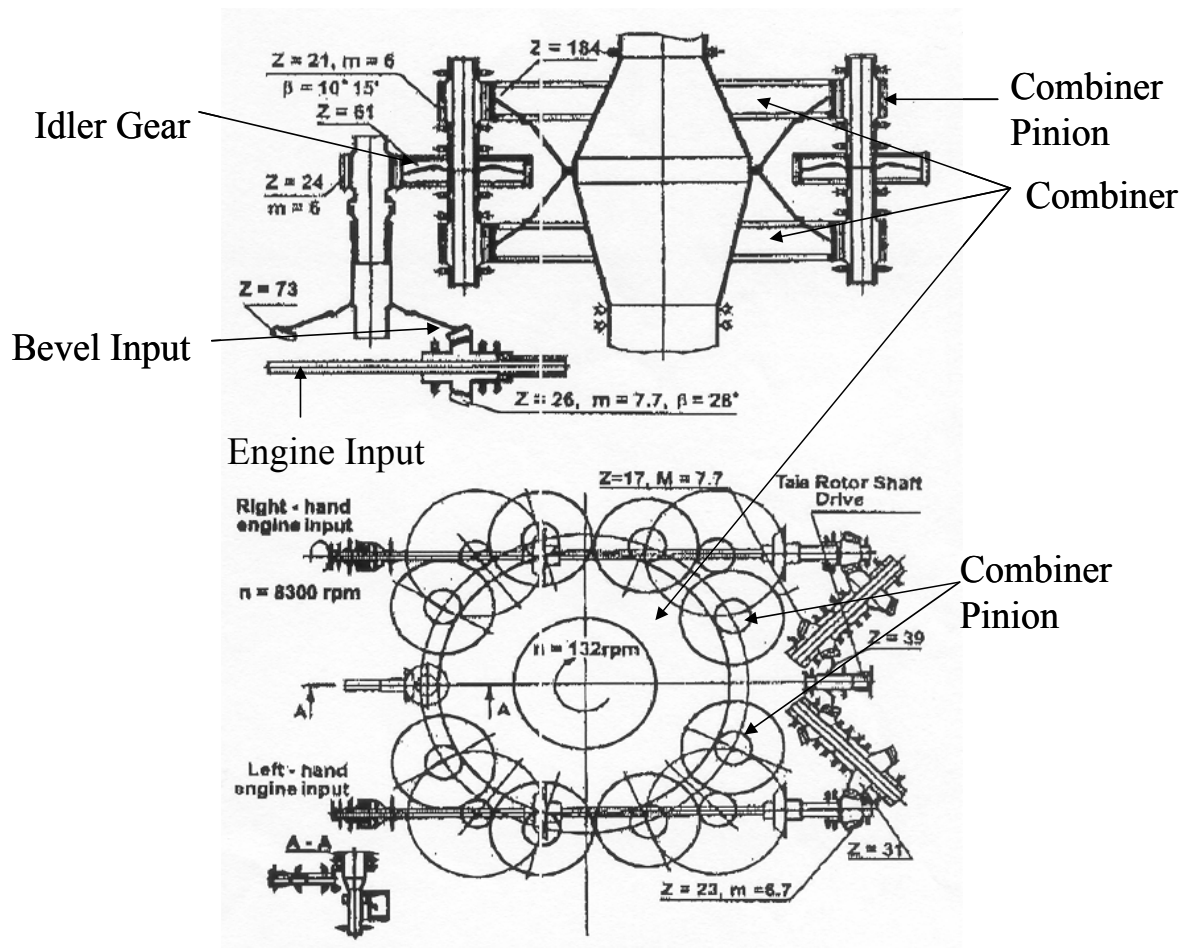


Figure 43: Mi-26 Main Gearbox Arrangement<sup>101</sup>

<sup>101</sup> Marat N. Tishchenko, "Mil Design Bureau Heavy-Lift Helicopters" (as presented at local chapters of the AHS in June 1996), 142.

The split-torque drive study in this thesis follows the same layout and torque splits as the Mi-26; however, the baseline JHL's overall reduction ratio is 130. This figure is almost twice that of the Mi-26's ratio and presents a new challenge in design. Additionally, the JHL has a third engine which means the combiner receives input from 24 combiner pinions as opposed to the Mi-26's 16 pinions. Finally, the tail rotor must also have a bevel takeoff from each combiner to permit power from all three engines.

### **Torque Split Drive Modeling**

The model employed in Model Center for the torque split drive is similar to the planetary drive model. Shafting spreadsheets capture shaft weight for the main rotor drive shaft, tail shaft, intermediate tail rotor shaft, and tail rotor drive shaft. Speed, torque, and power were calculated for the split torque drive much the same way the planetary drive spreadsheet functioned. All calculations are shown in APPENDIX E: SPLIT TORQUE DRIVE CALCULATIONS.

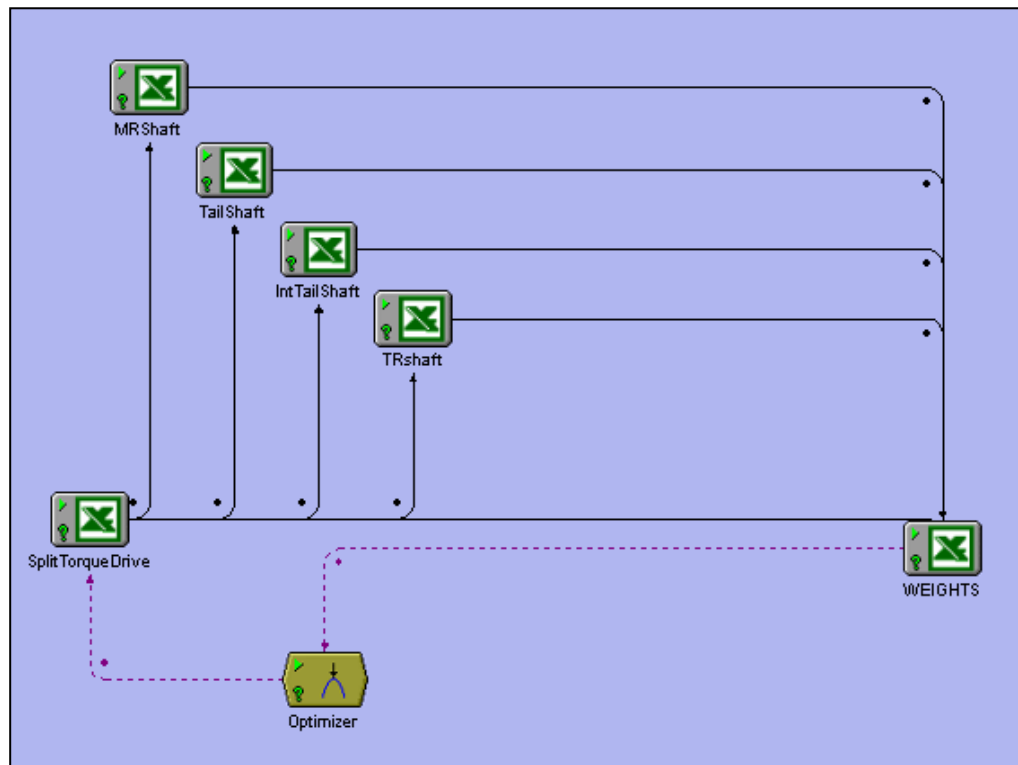


**Figure 44: Split Torque in Model Center**

### **Weight Estimation Results**

To achieve the higher reduction ratio required by the baseline JHL, slightly higher gear ratios at each stage are required. Especially important is the final stage between the combiner pinion and combiner. In the last stage, the Mi-26 has a reduction ratio of 8.76:1. In the JHL, the last stage has a reduction ratio of 11-13:1. The last stage reduction ratio results in a larger combiner gear, increasing the total size of the main gear box. A reduction ratio close to 12:1 places the main gearbox at the space limits for the

current structure. A reduction ratio just over 13:1 causes the pitchline velocity of the spur combiner to exceed the general spur gear limit of 4,000 feet per minute.<sup>102</sup>

As shown by Figure 45, the success of the split torque drive as configured depends greatly on the final stage reduction ratio.

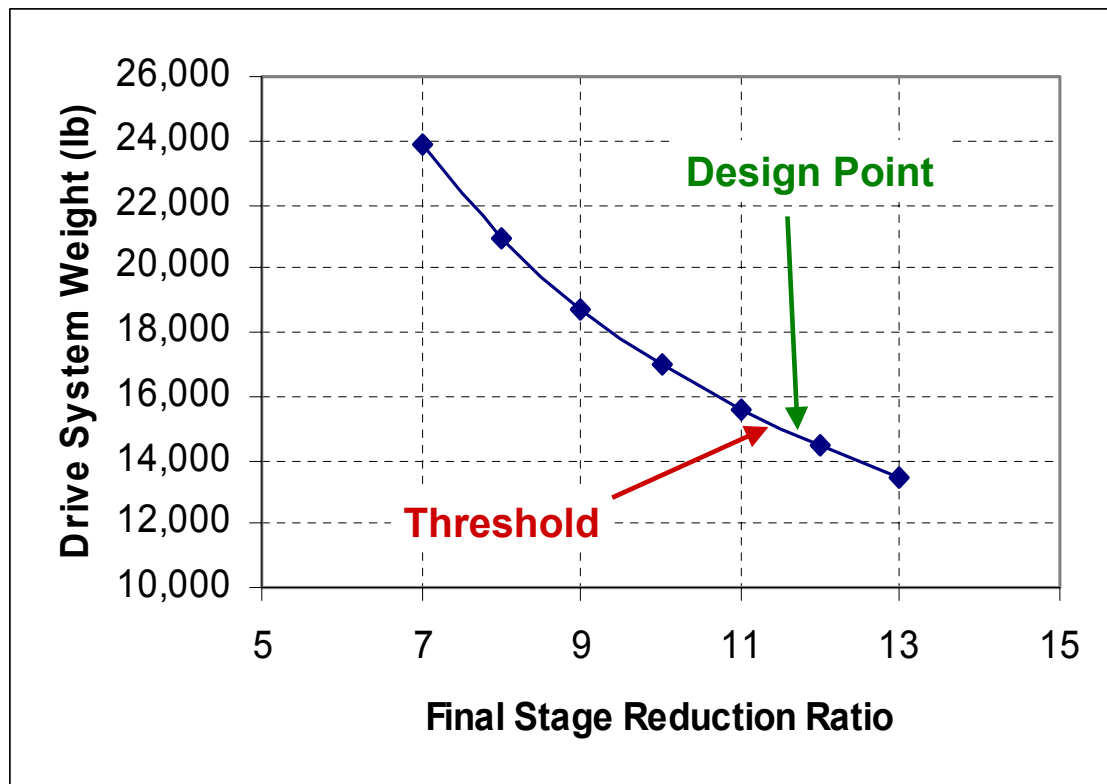


**Figure 45: Drive System Weight vs. Final Reduction Ratio**

From the graph, the threshold point where the split torque drive becomes lighter than the 15,200 lb planetary drive occurs at a reduction ratio of 11.2:1. The size of the combining gear imposes a limit of 11.7:1 on the reduction ratio. This limit becomes the design point for the final reduction ratio and the main gearbox.

---

<sup>102</sup> Darle Dudley, Handbook of Practical Gear Design (Lancaster: Technomic, 1994), 1.27.

At 11.7:1, the total system weight is 14,749.6 pounds. Boeing-Vertol and RTL's weight equations are a little higher than the solid rotor volume and shafting estimate. In both the planetary and split torque drive systems, the model's shafting weight is almost double the RTL's estimate.

**Table 17: Split Torque Drive Weight Estimate Results**

<b>Component</b>	<b>Shafting Plus Solid Rotor Volume</b>	<b>Predicted from RSE</b>	<b>Boeing- Vertol</b>	<b>RTL</b>
Total Gearbox Weight (lb)	13,325			14,274
Total Shafting Weight (lb)	1,425			835
Main Rotor Drive Weight (lb)			15,619	
Tail Rotor Drive Weight (lb)			914	
Total Drive System Weight (lb)	14,750	14,478	16,534	15,109

The key parameters for the weight optimized baseline aircraft is shown below.

**Table 18: Split Torque Baseline Design Summary**

<b>Parameter</b>	<b>Value</b>	<b>Parameter</b>	<b>Value</b>
Overall Reduction Ratio	130.43	MR Power (hp)	22,247
Input Bevel Reduction Ratio	3.39	Tail Rotor Power (hp)	1989
Idler Reduction Ratio	3.29	Accessory Power (hp)	120
Combiner Reduction Ratio	11.7	Main Rotor Speed (rpm)	115
Tail Takeoff Reduction Ratio	0.64	Tail rotor Speed (rpm)	476.3
Intermediate Tail Rotor Gearbox Reduction Ratio	2.19	Main Gearbox Weight (lb)	13,325
Tail Rotor Gearbox Reduction Ratio	2.00	Shaft Weight (lb)	1,425
		Drive System Weight (lb)	14,750
		Efficiency	97.90%

# RESPONSE SURFACE METHODOLOGY

## Overview

Response Surface Methodology (RSM) is a technique to build and optimize empirical models. Through multivariate least squares regression, RSM approximates output response to input parameters with a polynomial empirical equation. This multivariate equation is known as the Response Surface Equation (RSE). To intelligently obtain the regression data, a Design of Experiments (DoE) is created. A properly designed DoE with RSM can capture the underlying factors which influence a response. Using a polynomial equation as an RSE permits rapid, efficient prediction of a much more complex, time consuming calculation.

Initially, a Taylor series, second order approximation form is used for the RSE.<sup>103</sup>

$$R = b_0 + \sum_{i=1}^k b_i x_i + \sum_{i=1}^k b_i x_i^2 + \sum_{i=1}^{k-1} \sum_{j=i+1}^k b_{i,j} x_i x_j + \varepsilon$$

**Equation 75**

where

- R is the dependent parameter (response of interest)
- $b_i$  are regression coefficient for the first order terms
- $b_{ii}$  are coefficients for the pure quadratic terms
- $b_{ij}$  are the coefficients for the cross-product terms
- $x_{ij}$  are the independent variables
- $\varepsilon$  is the associated error for neglecting higher order effects

---

<sup>103</sup> Michelle R. Kirby, “An Overview of Response Surface Methodology” as presented in AE6373 lecture (Atlanta: Georgia Institute of Technology, August 25, 2004), 7.

Design of Experiments are “a series of tests in which purposeful changes are made to input variables so that one may observe and identify the reasons for change in an output response.”<sup>104</sup> The DoE varies input parameters in an intelligent pattern to capture the response of the system over the entire design space.

To model the drive system responses, an initial DoE casts a wide net around many independent variables in order to obtain data that identifies the most influential factors. This is called a screening test. A Pareto Chart is a convenient method to graphically communicate the percent of response variability, in the given ranges, attributed to a single input parameter. Generally, 20% of the input variables are responsible for 80% of the system variability. The purpose of the screening test is to identify the most important factors influencing the response.

Once the most important independent variables are identified, a second DoE is established that contains only those selected important input parameters. This DoE typically has more independent variable levels and iterations to yield higher fidelity to the final model. The regression data is again fit to the second order linear model and the final RSE is calculated.

### **Planetary Drive RSM**

The planetary drive has 12 independent variables for weight estimation. These variables are:

1. Main rotor power

---

<sup>104</sup> Michelle R. Kirby, “An Overview of Response Surface Methodology” as presented in AE6373 lecture (Atlanta: Georgia Institute of Technology, August 25, 2004), 8.



2. Main rotor rpm
3. Planetary reduction ratio
4. Tail rotor rpm
5. Engine input gearbox reduction ratio
6. Tail rotor gearbox reduction ratio
7. Engine rpm
8. Intermediate tail rotor reduction ratio
9. Accessory rpm
10. Accessory power
11. Oil cooler power
12. Tail rotor power required

A DoE with a fractional (half) factorial (2,048 runs) on the twelve variables permitted screening of six variables (for cumulative 95%) as shown by the Pareto chart; however, tail rotor power required was kept to allow for future regression of shaft weight.

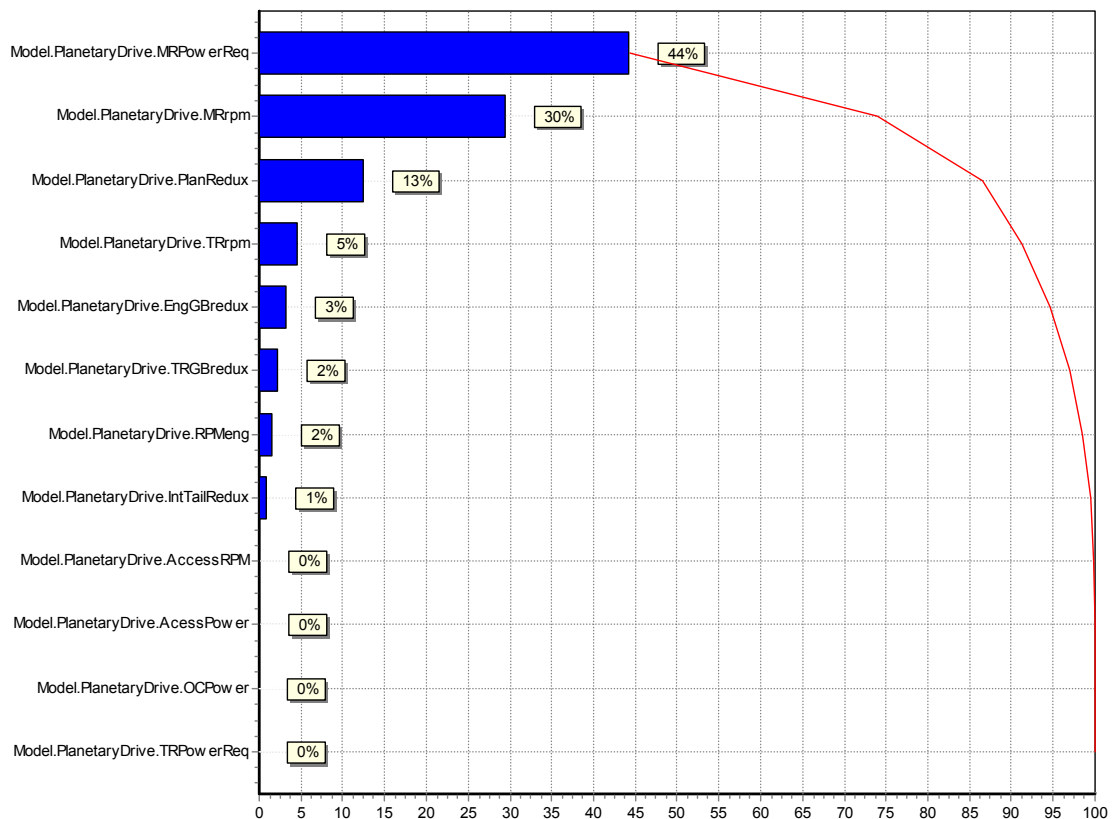


**Figure 46: Planetary Drive Screening Test Pareto Chart**

For the remaining seven variables, a 3-level full factorial DoE (2,187 runs) captured the data for the RSE model. The RSE formulation from JMP is shown in APPENDIX F: MODEL FIT FOR PLANETARY DRIVE. An optimization within Model Center of the baseline JHL showed the following input variables for the RSE:

**Table 19: Baseline Planetary Drive RSE Input Variables**

RSE Input Variables	Units	Type	Value
Intermediate Tail Rotor GB Reduction		Optimized	1.593
MR Power Required	hp	Baseline	22,247
Main Rotor rpm	rpm	Baseline	115
Overall Planetary Reduction Ratio		Optimized	10
Tail Rotor Gearbox Reduction Ratio		Optimized	2.984
Tail rotor rpm	rpm	Optimized	476.3
Tail rotor power	hp	Baseline	1,989
Baseline Drive System Weight	lbs		15,203
RSE Prediction	lbs		15,262

The fitted RSE for the planetary drive demonstrates excellent promise as a weight estimation model. The optimized baseline drive system weight within Model Center was 15,203 pounds while the RSE predicted 15,262 pounds. This residual of 59 pounds is a -0.4% model percent error, which is only a slight deviation from the weight prediction. The RSE has an  $R^2$  of 99.9% and an  $R^2$  Adjusted of 99.9%--both well above the recommend 90%. The Actual by Predicted plot (Figure 47) is excellent with vary little deviation from the perfect fit line. The Residual by Predicted plot (Figure 47) shows a good normal distribution about the mean and no discernable pattern—all good

indications. The total span of error (about 600 lbs) over the minimum predicted (about 10,000 lbs) is close to 6%--an acceptable, but not ideal, level for this model fit.

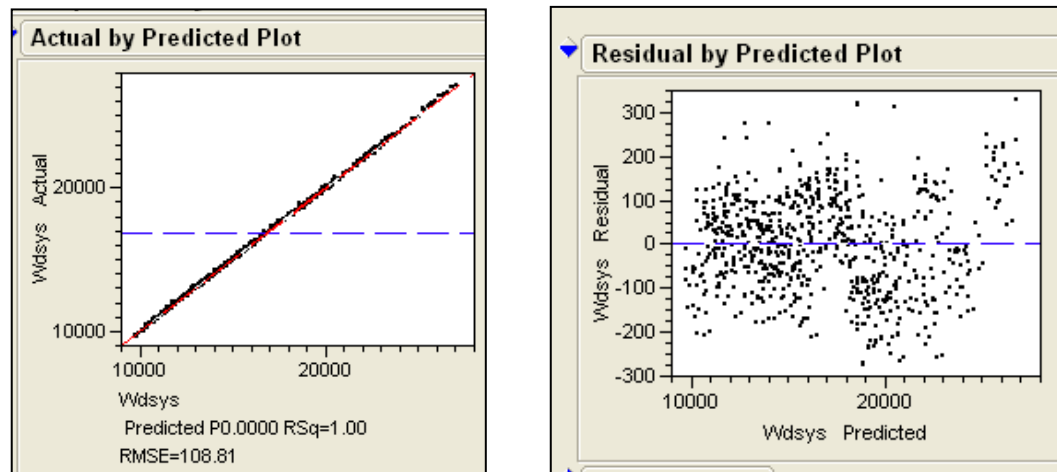


**Figure 47: Planetary Drive RSE Model Fit**

### **Split Torque Drive RSM**

The split torque drive has lower variety of shafts and gears than the planetary drive. For the split torque drive nine independent variables were present in the calculation of weight:

1. Combiner reduction ratio
2. Main rotor HP
3. Main rotor RPM
4. Tail rotor HP
5. Idler reduction ratio
6. Engine RPM
7. Tail rotor gearbox reduction ratio
8. Tail rotor RPM
9. Intermediate tail rotor reduction ratio

The screening test consisted of a 2-level full factorial with 512 runs ( $2^9$ ). As shown by the Pareto Chart, the intermediate tail rotor reduction ratio and tail rotor reduction ratio accounted for little influence on the weight response. Of the nine variables, these two were eliminated from consideration.

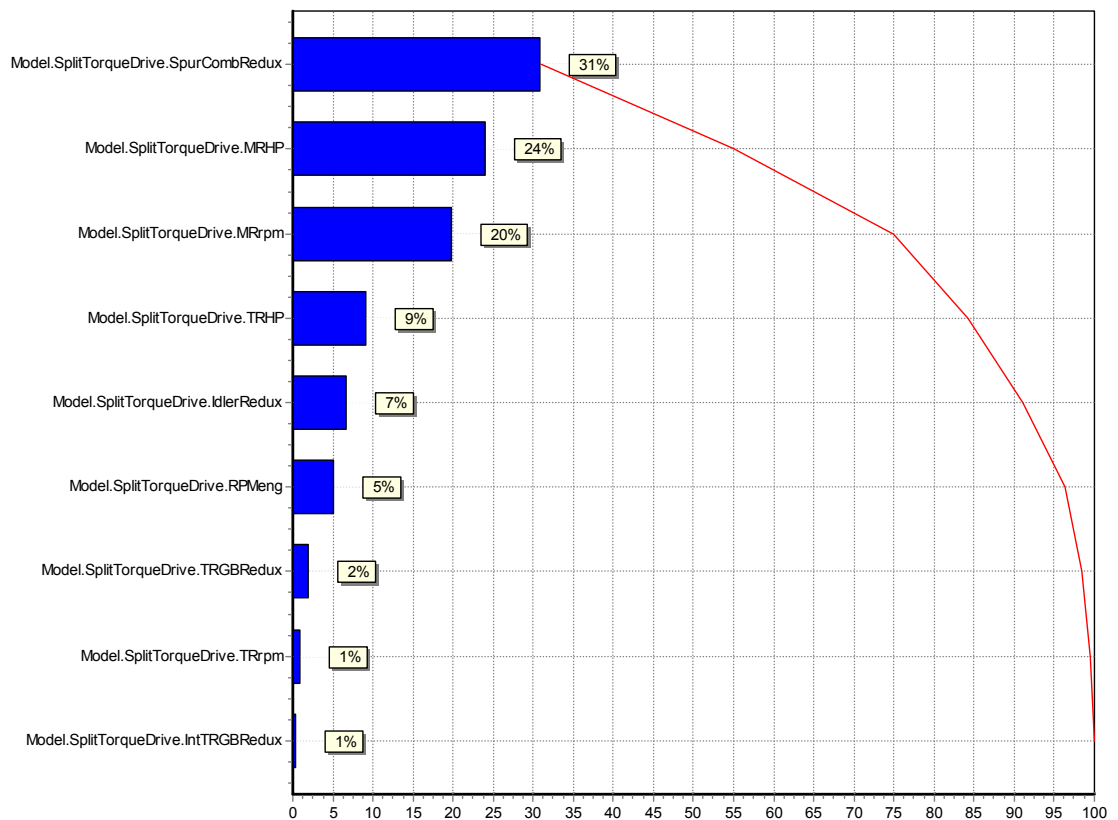


**Figure 48: Split Torque Screening Test Pareto Chart**

The second DoE consisted of a 3-level, full factorial with 2,187 ( $3^7$ ) runs. From this data, a response surface was generated using JMP (see APPENDIX G: MODEL FIT FOR SPLIT TORQUE DRIVE for regression analysis data). Of the 2,187 data sets, 49 or

2.2% did not converge properly for weight estimation and were removed as outliers from the regression data.

**Table 20: Split Torque RSE Baseline Inputs**

<b>RSE Input Variables</b>	<b>Units</b>	<b>Type</b>	<b>Value</b>
Main rotor speed	rpm	Baseline	115
Main rotor power	hp	Baseline	22,274
Tail rotor power	hp	Baseline	1,989
Engine speed	rpm	Baseline	15,000
Combiner reduction ratio		Optimized	11.7
Idler reduction ratio		Optimized	3.29
Tail rotor gearbox reduction ratio		Optimized	2.19
Baseline Drive System Weight	lbs		14,750
RSE Prediction	lbs		14,478

The initial model fit for the split torque drive was not as successful as the fit for the planetary drive. Although the initial RSE had an  $R^2$  of 99.6% and an  $R^2$  Adjusted of 99.6%, the Actual by Predicted and Residual by Predicted plots (Figure 49) proved unacceptable. The Actual by Predicted plot showed decent adherence to the perfect fit until about 30,000 lbs; however, the model over predicts at weights above 30,000 lbs. This is confirmed by the Residual by Predicted plot's undesirable S-curve trend. The RSE fit had to be improved for the model to acceptable and serve as a useful tool.

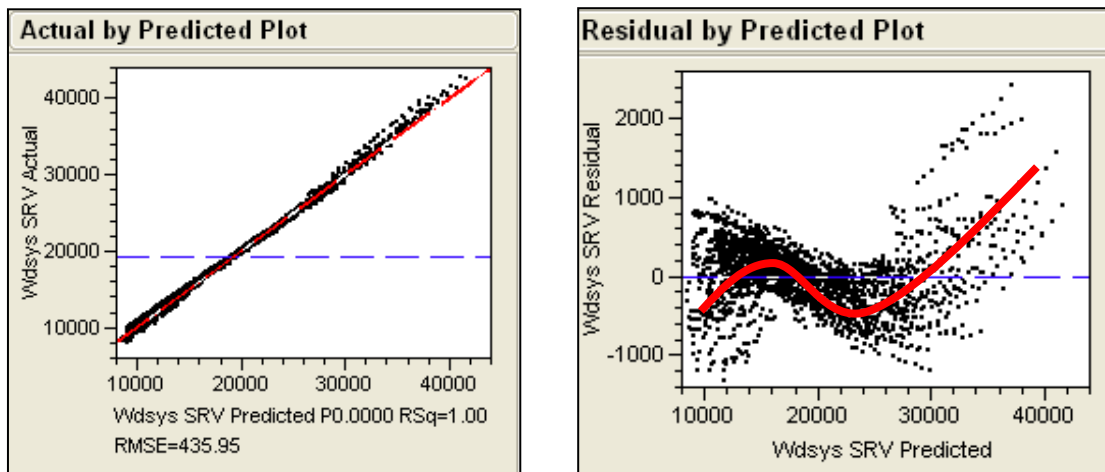


**Figure 49: Initial Split Torque RSE Model Fit**

To improve the model fit, several techniques were attempted. Results are shown in Table 21. The final model fit output from JMP is listed in APPENDIX G: MODEL FIT FOR SPLIT TORQUE DRIVE.

**Table 21: Split Torque Model Fit Comparison**

Type of Model Fit	Weight (lbs)	Model Percent Error
Optimized Baseline from Model Center	14,750	
Initial RSE	14,122	4.3%
Bias (x3) RSE	14,133	4.2%
3/2 Power Transformation RSE	13,710	7.1%
Square Root Transformation RSE	14,384	2.5%
Cube Root Transformation RSE	14,478	1.8%

The first technique applied was to bias the fit towards the baseline by adding three data points of the baseline input and response to the DoE data table. Although the biasing did improve the baseline residual, the impact was so minor as to not warrant further application. The second technique consisted of checking different transformations on the response. Drive system weight was transformed by 3/2 power (R

$= W_{\text{dsys}}^{3/2}$ ), square root ( $R = W_{\text{dsys}}^{1/2}$ ), and cube root ( $R = W_{\text{dsys}}^{1/3}$ ) and then fitted against the 2d order polynomial RSE. The 3/2 power transformation exacerbated the model fit's flaws while transforming in the  $1/2$  power direction improved the model in the correct direction (Table 21). Extending to a cube root transformation showed even better results and served as the final model fit. Higher root transformation did reduce the baseline residual; however, the reduction is minimal and higher root transformations experience a condition of diminishing improvement.

The final RSE fit for the split torque drive exhibited good potential as a weight estimation model. The optimized baseline drive system weight within Model Center was 14,750 pounds and the RSE predicted 14,478 pounds. This 272 pound residual is a 1.8% model percent error. The RSE possesses an  $R^2$  of 99.9% and an  $R^2$  Adjusted of 99.9%--both well above the recommended 90%. The Actual by Predicted plot (Figure 50) is acceptable with improved adherence to the perfect fit line at extremes. The Residual by Predicted plot (Figure 50), showed adequate normal distribution and little discernable pattern. The total span of error (about  $0.7 \text{ lbs}^{1/3}$ ) over the minimal predicted ( $20 \text{ lbs}^{1/3}$ ) is approximately 3.5%--a good value for this model.

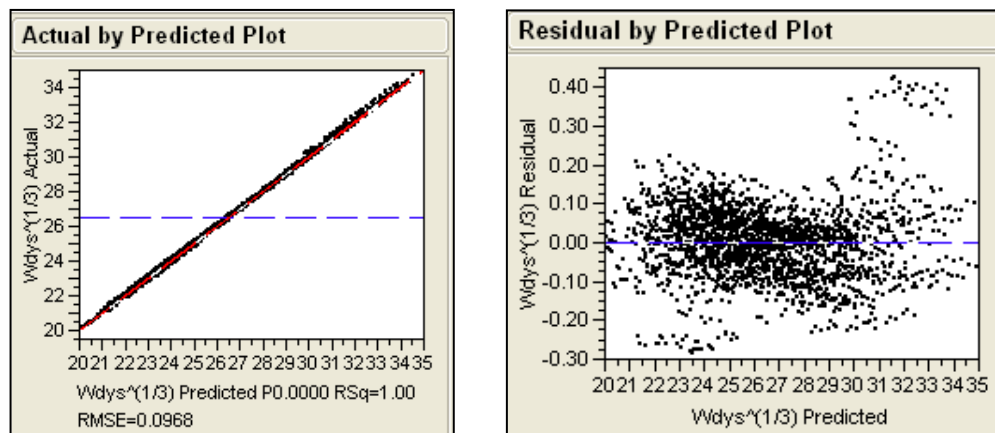


**Figure 50: Split Torque Final RSE Model Fit**

## CONCLUSIONS

A drive system design methodology was presented that permitted integration of detailed component design and allowed higher fidelity and better weight estimates. The methodology is an open architecture allowing the designer to insert and remove component tools as necessary. Component tools for gearing, shafting, and gearbox are included as examples.

A spreadsheet component tool to size spur, helical, or bevel gears for bending and compressive stress as well as scuffing resistance revealed several important conclusions about heavy lift drive gearing. Due to high torque values in the main gearbox, the scuffing hazard proved the most difficult design criteria to meet. VASCO X2M steel with MIL-L-23699 provides the best resistance to scuffing for these high torque gears. Bending strength sized planetary gears due to the reduction in strength from reverse loading. Aerospace gears throughout the drive train operate at very high pitchline velocities requiring high precision, ground gears to reduce dynamic loading and create smooth meshing. Due to the critical nature of helicopter gearing, high reliabilities of a minimum  $3\sigma$  at a long 2,500 to 5,000 hour life are required. Despite high efficiency gearing, the massive amounts of transmitted power produce a sizeable amount of lost power transformed into heat. In addition to increasing the gear blank temperature and higher scuffing hazards, these high heat quantities require large amounts of force-fed oil flow to properly cool gearing.



A shafting model is also included as a component tool and integrated into the solid rotor volume weight estimate model. Due to the vibratory nature of the bending moments, an interaction equation is required to calculate a total margin of safety for the combined bending, shear, and torsional stresses experienced by a rotating shaft. From this interaction equation, it was shown that helicopter drive shafts tend to have high diameter to thickness ratios in order to withstand the high torsional stress while maintaining light weight. Throughout the drive system, hollow aluminum alloy shafts were preferred because of great weight savings; however, for shafts with high applied loads such as the main rotor and tail rotor drive shafts, heavier titanium had better resistance to bending and shear stresses. For uniform shafting, the critical speed is simply a function of shaft radius and length. For nonuniform shafting with mass concentrations or bending moments, the critical speed is calculated using a variation of Rayleigh's method. From the variation, the natural frequency is found by comparing the shaft's kinetic energy to its potential energy. For the heavy lift helicopter, shafts linking gearboxes are uniform and typically operate at subcritical speeds while gear shafts and drive shafts are nonuniform and may operate at supercritical or subcritical speeds.

The methodology demonstrated good potential to serve as a system weight predictor. Methodology weight estimates (combined solid rotor volume method and shaft weight estimations) for both a planetary and split torque drive system were within

approximately 10% of the Boeing-Vertol and RTL weight equation estimates (Table 22).

**Table 22: Total Drive System Weight Method Summary**

Weight Method	Planetary Drive Weight (lb)	Split Torque Weight (lb)
Optimized Baseline	15,203	14,750
RSE Prediction	15,262	14,478
Boeing-Vertol Estimate	13,361	16,534
RTL Estimate	16,620	15,109

This weight estimation method was successfully applied to a traditional multi-stage planetary drive and to a split torque drive similar to the Mi-26's main gearbox. For the planetary main gearbox, low planetary reduction ratios are preferred because of increased load sharing gained from more planets. The ideal main gearbox reduction ratio is a function of each stages reduction ratio. The shown split torque drive included three torque splits for a final stage total of eights paths per engine. Splitting the torque showed great weight savings potential over the traditional, 2-stage planetary drive system if high reduction ratios (above 12:1) can be achieved in the final stage. This requirement for a high final reduction ratio means the split torque design shown is an excellent candidate to benefit from high ratio face gears.

Approximating the more complicated model created in Model Center by Response Surface Methodology produced good results. The planetary model's initial RSE was an excellent fit with a model percent error less than 1%; however, the split torque regression required a cube root transformation to yield a workable model with a model percent error less than 2%. With correct model fitting, Response Surface Methodology demonstrated the ability to serve as a simplified response predictor for a more complicated, high component integrated drive system model.

## FUTURE WORK

The addition of detailed, user friendly tools for bearings, freewheeling units, rotorbrakes, splines, housing, structural support, and aerodynamic loads on drives shafts is needed to fully capture the drive system behavior and find a feasible, optimized solution.

In addition to the RSM, the drive modeling must be examined from a probabilistic point of view. Placing distributions on assumptions and key factors will capture the uncertainty associated with a design. The impact and overall probability of success may then be judged through the application of Monte Carlo simulations.

Lastly, the face gear holds potential to save weight in split-torque designs and are “optimal for large reduction ratio applications” that occur in helicopter drive trains.<sup>105</sup> Testing of prototype face gears for a split-torque helicopter transmission by Handschuh, Lewicki, and Bossler (1992),<sup>106</sup> and the recent success of the 5,100 HP RDS-21 Demonstrator Gearbox (2004),<sup>107</sup> have confirmed the weight saving benefits. Handschuh, Lewicki, and Bossler indicated that face gears can have “an improved weight advantage compared to spiral bevel gears at [reduction] ratios higher than approximately 3.5:1.” Face gear technology is a major facet of the RDS-21 and future drive systems.

---

<sup>105</sup> Yuriy Gmirya, et al, “Design and Analysis of 5100 HP RDS-21 Demonstrator Gearbox” 60<sup>th</sup> Annual Forum Proceedings, vol 2, (Alexandria: AHS International, 2004), 1224.

<sup>106</sup> Handschuh, R., D. Lewicki, and R. Bossler, NASA TR 92-C-008 Experimental Testing of Prototype Face Gears for Helicopter Transmissions prepared for “Gearbox Configurations of the 90’s” sponsored by the Institute of Mechanical Engineers Solihull, West Midlands, United Kingdom, October 28, 1992.

<sup>107</sup> Yuriy Gmirya, et al, “Design and Analysis of 5100 HP RDS-21 Demonstrator Gearbox” 60<sup>th</sup> Annual Forum Proceedings, vol 2, (Alexandria: AHS International, 2004),

Development of a standardized, analytical estimate of gear stresses becomes the key to integrating face gear technology into the future drive system design methodology.

**APPENDIX A: JHL SUPPLEMENTAL PACKAGE**

**EXTRACTS**

**Table 23: JHL Baseline Aircraft Data**

Design	Baseline	E1	E2	E2A	E4	E5	E6	E7
Design Payload, ton	20	16	26	26	20	20	20	20
Design Radius, nm	250	250	250	250	400	500	250	250
High / Hot, 1000 ft / deg F	4k/95	4k/95	4k/95	4k/95	4k/95	4k/95	6k/95	4k/95
Shipboard Operations	Capable	Capable	Capable	Capable	Capable	Capable	Capable	Compatible
<b>Summary</b>								
Design Cruise Speed, kt	171.7	170.3	173.4	xxx.x	173.1	174.1	175	xxx.x
Design Gross Weight, lb	138,868	114,035	177,392	xxx,xxx	172,197	206,501	148,606	xxx,xxx
Disk Loading, psf	12.3	12.3	12.3	xx.x	12.3	12.3	12.3	xx.x
Download %GW	4.06%	4.66%	3.44%	x.xx%	3.51%	3.11%	3.87%	x.xx%
Max Alternate Gross Wt, lb	173,556	142,529	221,759	xxx,xxx	215,184	258,036	185,754	xxx,xxx
Number Engines	3	3	3	3	3	3	3	3
Engine Size, shp	10,985	9,114	13,912	xx,xxx	13,495	16,066	13,113	xx,xxx
Drive Rating (TO rpm), shp	25,964	21,420	33,011	xx,xxx	30,642	35,469	27,567	xx,xxx
Fuel Tank Capacity (JP-8), lb	50,015	40,899	63,823	xx,xxx	65,557	81,131	51,552	xx,xxx
Unit Flyaway Cost, FY05 \$M	120.38	98.80	154.94	xxx.xx	149.32	179.76	139.92	xxx.xx
<b>Primary Thruster</b>								
Number Primary Thrusters	1	1	1	1	1	1	1	1
Number Blades per Rotor	6	6	6	6	6	6	6	6
Hover Tip Speed, fps	725	725	725	725	725	725	725	725
Diameter, ft	120	108.6	135.5	xxx.x	133.5	146.2	124	xxx.x
Rotor Hub Separation, ft	-	-	-	-	-	-	-	-
Effective Disk Area, sq ft	11,310	9,263	14,420	xx,xxx	13,998	16,787	12,076	xx,xxx
<b>Dimensions</b>								
Operating Footprint, sq ft	17,904	14,683	22,832	xx,xxx	22,161	26,565	19,121	xx,xxx
Operating Length, ft	149.2	135.2	168.5	xxx.x	166	181.7	154.2	xxx.x
Operating Width, ft	120	108.6	135.5	xxx.x	133.5	146.2	124	xxx.x
Stowed Footprint, sq ft	3,744	x,xxx	x,xxx	x,xxx	x,xxx	x,xxx	x,xxx	x,xxx
Stowed Length, ft	90.88	xxx.x	xxx.x	xxx.x	xxx.x	xxx.x	xxx.x	xxx.x
Stowed Width, ft	41.2	xxx.x	xxx.x	xxx.x	xxx.x	xxx.x	xxx.x	xxx.x
Stowed Height, ft	25.19	xx.x	xx.x	xx.x	xx.x	xx.x	xx.x	xx.x
Cargo Box Volume, cu ft	5,080	5,080	5,080	x,xxx	5,080	5,080	5,080	5,080
Cargo Box Length, ft	50	50	50	xx.x	50	50	50	50
Cargo Box Width, ft	11.1	11.1	11.1	xx.x	11.1	11.1	11.1	11.1
Cargo Box Height, ft	9.2	9.2	9.2	xx.x	9.2	9.2	9.2	9.2
<b>Weight Summary</b>								
Weight Empty, lb	76,739	63,074	98,454	xx,xxx	94,500	113,207	84,961	xx,xxx
Scar Weight, lb	x,xxx	x,xxx	x,xxx	x,xxx	x,xxx	x,xxx	x,xxx	x,xxx
Operating Weight, lb	78,829	65,124	100,584	xx,xxx	96,590	115,297	87,051	xx,xxx
Struc Design GW (SDGW), lb	138,845	114,024	177,407	xxx,xxx	172,148	206,429	148,603	xx,xxx
Maximum Payload Wt, lb	65,000	52,000	84,500	xx,xxx	65,000	65,000	65,000	65,000
Max VTOL Gross Wt, lb	xxx,xxx	xxx,xxx	xxx,xxx	xxx,xxx	xxx,xxx	xxx,xxx	xxx,xxx	xxx,xxx
<b>Program Cost (FY05 \$)</b>								
JHL Fleet Size	400	400	400	400	400	400	400	400
Development (RDT&E), \$B	x,xxx	x,xxx	x,xxx	x,xxx	x,xxx	x,xxx	x,xxx	x,xxx
Procurement, \$B	xx,xxx	xx,xxx	xx,xxx	xx,xxx	xx,xxx	xx,xxx	xx,xxx	xx,xxx
O&S (30 years), \$B	xx,xxx	xx,xxx	xx,xxx	xx,xxx	xx,xxx	xx,xxx	xx,xxx	xx,xxx
<b>Unit Cost (FY05 \$)</b>								
Flyaway, \$M	120.38	98.80	154.94	xxx.xx	149.32	179.76	139.92	xxx.xx
Flyaway / (Wt Empty), \$/lb	1,569	1,566	1,574	x,xxx	1,580	1,588	1,647	x,xxx
O&S (150 FH/yr), \$/FH	x,xxx	x,xxx	x,xxx	x,xxx	x,xxx	x,xxx	x,xxx	x,xxx
O&S (600 FH/yr), \$/FH	x,xxx	x,xxx	x,xxx	x,xxx	x,xxx	x,xxx	x,xxx	x,xxx

**Table 24: Example JHL Substantiation**

<b>Design</b>	<b>Baseline</b>	<b>E1</b>	<b>E2</b>	<b>E2A</b>	<b>E3</b>	<b>E4</b>	<b>E5</b>	<b>E6</b>	<b>E7</b>
Design Payload, ton	20	16	26	26	20	20	20	20	20
Design Radius, nm	250	250	250	250	210	400	500	250	250
High / Hot, 1000 ft / deg F	4k/95	4k/95	4k/95	4k/95	4k/95	4k/95	4k/95	6k/95	4k/95
Shipboard Operations	Capable	Capable	Capable	Capable	Capable	Capable	Capable	Capable	Compatible
<b>Areas</b>									
Wetted (total), sq ft	5,723	5,428	6,151	x,xxx	5,640	6,093	6,460	5,864	x,xxx
Drag Area (cruise mode), sq ft	108.7	95.2	129.3	xxx.x	104.8	126.5	144.7	114.1	xxx.x
Drag Area (hover mode), sq ft	108.7	95.2	129.3	xxx.x	104.8	126.5	144.7	114.1	xxx.x
<b>Group Weights</b>									
Wing Group, lb	0	0	0	0	0	0	0	0	0
Rotor Group, lb	19,250	14,802	26,640	xx,xxx	17,961	25,594	32,591	22,321	xx,xxx
Empennage Group, lb	2,250	1,750	3,073	x,xxx	2,122	2,879	3,563	2,441	x,xxx
Fuselage Group, lb	13,836	11,886	16,728	xx,xxx	13,297	16,339	18,816	14,580	xx,xxx
Alighting Gear Group, lb	3,627	2,979	4,635	x,xxx	3,446	4,497	5,393	3,882	x,xxx
Nacelle Group, lb	1,211	1,000	1,544	x,xxx	1,153	1,497	1,791	1,453	x,xxx
Air Induction Group, lb	247	199	323	x,xxx	234	312	381	302	x,xxx
Total Structure, lb	40,421	32,615	52,943	xx,xxx	38,213	51,118	62,535	44,979	xx,xxx
Propulsion Group, lb	20,092	16,468	25,755	xx,xxx	19,137	24,692	29,426	21,999	xx,xxx
Flight Controls Group, lb	3,995	3,280	5,134	x,xxx	3,799	4,979	5,995	4,925	x,xxx
Auxiliary Power Group, lb	300	275	350	x,xxx	300	300	300	300	x,xxx
Instruments Group, lb	135	135	135	x,xxx	135	135	135	135	x,xxx
Hydraulic Group, lb	963	839	1,133	x,xxx	937	1,089	1,210	1,091	x,xxx
Pneumatic Group, lb	0	0	0	x,xxx	0	1	2	3	x,xxx
Electrical Group, lb	820	754	886	x,xxx	820	820	820	820	x,xxx
Avionics Group, lb	1,150	1,150	1,150	x,xxx	1,150	1,150	1,150	1,150	x,xxx
Armament Group, lb	145	145	145	x,xxx	145	145	145	145	x,xxx
Furnishings & Equip., lb	950	910	990	x,xxx	950	950	950	950	x,xxx
Environmental Control, lb	750	750	750	x,xxx	750	750	750	750	x,xxx
Anti-Icing Group, lb	1,631	1,338	2,087	x,xxx	1,549	2,025	2,430	1,885	x,xxx
Load & Handling Group, lb	1,275	1,040	1,710	x,xxx	1,275	1,275	1,275	1,275	x,xxx
Contingency, lb	4,112	3,375	5,286	x,xxx	3,914	5,073	6,087	4,558	x,xxx
Total Weight Empty, lb	76,739	63,074	98,454	xx,xxx	73,074	94,501	113,210	84,965	xx,xxx

**Table 25: JHL Baseline Tabulated Data**

Heavy Lift Helicopter (JHL-JH-20T) Tabulated Data			
Main Rotor		Wetted Areas	
Diameter	120.00 ft	Fuselage	3,409.20 ft <sup>2</sup>
Chord	4.24 ft	Sponson	1,455.60 ft <sup>2</sup>
Twist	-12.00 deg	Nacelles	310.50 ft <sup>2</sup>
Blades	6	Pylon	491.10
Tail Rotor		Landing Gear	
Diameter	29.07 ft	Main Gear Track	20.05 ft
Chord	2.85 ft	Main Gear Tread	16.67 ft
Blades	5	Wheelbase	38.33 ft
Horizontal Tail		Cargo Compartment	
Planform Area	212.21 ft <sup>2</sup>	Length	50.00 ft
Span	32.57 ft	Width	11.08 ft
Chord	6.51 ft	Height	9.17 ft
Aspect Ratio	5.00 ND	Floor Area	554.00 ft <sup>2</sup>
Taper Ratio	1.00 ND	Ramp Opening Width	11.08 ft
Sweep Angle	0.00 deg	Ramp Opening Height	9.17 ft
Dihedral Angle	0.00 deg		
Incidence Angle	1.00 deg		
Thickness to Chord Ratio	0.12 ND		
Vertical Tail			
Planform Area	168.72 ft <sup>2</sup>		
Span	18.69 ft		
Chord	7.60 ft		
Aspect Ratio	2.07 ND		
Taper Ratio	0.75 ND		
Sweep Angle	35.00 deg		
Dihedral Angle	0.00 deg		
Incidence Angle	1.50 deg		
Thickness to Chord Ratio	0.12 ND		

Sample: A004 Aircraft Drawings and Dimensions 6.b.



**Table 26: JHL Baseline Power vs. Airspeed Data 0 to 110 knots**

<b>Hi/Hot (4k/95 F) at DGW; Power vs Airspeed Data - Helicopter Example</b>							
<b>Gross Weight, lb</b>	<b>138,867</b>						
<b>Airspeed, kt</b>	<b>0</b>	<b>20</b>	<b>40</b>	<b>60</b>	<b>80</b>	<b>100</b>	<b>110</b>
Power Required, shp	22,247	20,402	16,369	13,050	11,291	10,746	10,840
Primary Thruster, shp	19,346	17,871	14,516	11,677	10,128	9,643	9,734
Induced, shp	17,309	15,770	12,295	9,287	7,351	6,152	5,786
Profile, shp	2,037	2,054	2,101	2,201	2,346	2,525	2,632
Parasite, shp	-	48	120	190	431	966	1,316
Control + Prop, shp	1,989	1,631	1,018	625	474	433	434
Drive Sys Loss, shp	792	779	716	628	569	549	552
Accessory Loss, shp	120	120	120	120	120	120	120
Power Available							
AEO Engine (MRP), shp	23,413	23,426	23,465	23,535	23,631	23,753	23,824
OEI Engine (MRP), shp	15,609	15,618	15,643	15,690	15,754	15,836	15,883
AEO Engine (MCP), shp	17,381	17,393	17,428	17,487	17,569	17,675	17,737
OEI Engine (MCP), shp	11,587	11,595	11,619	11,658	11,713	11,783	11,825
Drive System Rating, shp	25,964	25,964	25,964	25,964	25,964	25,964	25,964
Fuel Consumption							
SFC, lbf/hp-hr	0.349	0.356	0.374	0.398	0.416	0.422	0.420
Spec Range, nm/lb	0	0.0028	0.0065	0.0116	0.0171	0.0221	0.0242
Main Rotor							
Tip Speed, ft/sec	725	725	725	725	725	725	725
Thrust, lb	144,500	144,146	142,596	142,516	142,915	142,226	141,937
TPP AoA (+ backward), deg	-3.58	-0.31	-0.39	-0.41	-0.7	-1.27	-1.57
CT/Sigma (TW)	0.10057	0.10032	0.09924	0.09919	0.09946	0.09899	0.09878
Lift							
Primary Thruster, lb	144,492	144,144	142,593	142,512	142,905	142,192	141,883
Wing, lb	0	0	0	0	0	0	0
Propulsion							
Primary Thruster, lb	-1,482	785	978	1,030	1,754	3,147	3,898
Aux Thruster, lb	0	0	0	0	0	0	0
Conversion States - N/A for Single Main Helicopter							
<b>Data for Points on Pwr Required Curves</b>	<b>V-be (kts)</b>	<b>V-br (kts)</b>	<b>90% MCP</b>				
Airspeed, kts	121.5	167.0	171.7				
Power Req, shp	11,212	15,637	16,435				

**Table 27: JHL Baseline Power vs. Airspeed Data 120 knots or more**

<b>Hi/Hot (4k/95 F) at DGW; Power vs Airs</b>							
<b>Gross Weight, lb</b>							
							V-mcp
Airspeed, kt	120	130	150	160	170	180	182
Power Required, shp	11,150	11,663	13,297	14,546	16,132	17,979	18,380
Primary Thruster, shp	10,022	10,499	12,022	13,189	14,676	16,412	16,789
Induced, shp	5,542	5,406	5,434	5,596	5,815	6,016	6,054
Profile, shp	2,750	2,880	3,180	3,464	3,921	4,547	4,690
Parasite, shp	1,730	2,212	3,407	4,129	4,940	5,849	6,045
Control + Prop, shp	444	462	520	566	626	701	718
Drive Sys Loss, shp	564	582	636	671	710	747	753
Accessory Loss, shp	120	120	120	120	120	120	120
Power Available							
AEO Engine (MRP), shp	23,901	23,988	24,181	24,288	24,405	24,525	24,549
OEI Engine (MRP), shp	15,934	15,992	16,121	16,192	16,270	16,350	16,366
AEO Engine (MCP), shp	17,806	17,880	18,048	18,141	18,241	18,347	18,369
OEI Engine (MCP), shp	11,871	11,920	12,032	12,094	12,161	12,231	12,246
Drive System Rating, shp	25,964	25,964	25,964	25,964	25,964	25,964	25,964
Fuel Consumption							
SFC, lbf/hp-hr	0.415	0.409	0.391	0.381	0.369	0.359	0.357
Spec Range, nm/lb	0.0259	0.0273	0.0288	0.0289	0.0285	0.0279	0.0277
Main Rotor							
Tip Speed, ft/sec	725	725	725	725	725	725	725
Thrust, lb	141,704	141,524	141,338	141,337	141,399	141,528	141,563
TPP AoA (+ backward), deg	-1.9	-2.25	-3	-3.41	-3.84	-4.29	-4.39
CT/Sigma (TW)	0.09862	0.0985	0.09837	0.09837	0.09841	0.0985	0.09852
Lift							
Primary Thruster, lb	141,627	141,416	141,144	141,086	141,081	141,131	141,148
Wing, lb	0	0	0	0	0	0	0
Propulsion							
Primary Thruster, lb	4,697	5,545	7,402	8,409	9,470	10,588	10,824
Aux Thruster, lb	0	0	0	0	0	0	0
Conversion States - N/A for Single Main Helicopte							
<b>Data for Points on Pwr Required Curves</b>							
Airspeed, kts							
Power Req, shp							

## **APPENDIX B: SPUR-HELICAL GEAR RATING CALCULATIONS**

Spur-Helical Gear Summary

Table 28: Spur-Helical Gear Summary

**SPUR-HELICAL RATING SUMMARY**

<u>MDLCTR</u>	<u>SYMBOL</u>	<u>DESCRIPTION</u>	<u>UNITS</u>	<u>PINION</u>	<u>MESH</u>	<u>GEAR</u>	
	J	Pitting Resistance Geometry Factor		0.0920		0.0920	AGMA Stress
	J	Bending Strength Geometry Factor		0.4591		0.4796	AGMA Stress
SH_swt_P, SH_swt_G	swt	Working bending stress number	psi	38,242.4	1.095	38,568.7	AGMA Stress
SH_st_P, SH_st_G	st	Bending tensile stress	psi	34,909.3		33,168.4	AGMA Stress
SH_swc_P, SH_swc_G	swc	Working contact stress number	psi	169,054.5	1.111	171,281.2	AGMA Stress
SH_sc_P, SH_sc_G	sc	Contact stress	psi	152,170.9		151,609.4	AGMA Stress
<b>DESIGN BALANCE</b>							
					0.986	1.029	
SH_R_P, SH_R_G	R	Standard (reference) pitch radius	in	5.4167		7.6389	AGMA Stress
SH_Fe	Fe	Effective face width		3.5000	3.5000	3.5000	AGMA Stress
SH_W_P, SH_W_G	W	Estimated Weight	lb	102.7		204.2	211.2 AGMA Stress

SH_Tmember_P, SH_Tmember_G	Tmember	Torque (per member)	in lb	240,527.2		339,205.0	AGMA Stress
SH_T_P, SH_T_G	T, TQ, Q	Torque (per mesh)	in lb				
SH_PLV	vt, V, PLV	Pitch Line Velocity	ft/min	60,131.8		84,801.3	AGMA Stress
SH_Wt	Wt	Tangential load (transmitted)	lb		7,907.2		AGMA Stress
SH_Wr	Wr	Radial load	lb		11,101.3		AGMA Stress
SH_Wa	Wa	Axial load (thrust)	lb		4,040.5		AGMA Stress
SH_mg	mg	Gear ratio			0.0		AGMA Stress
					1.4103		

Table 28: Spur-Helical (continued)

[illegible]

## User Inputs and Selections

**Table 29: Spur-Helical User Inputs and Selections**

### USER INPUTS & SELECTIONS

SH_NP, SH_NG	n, N	Number of Teeth	39	1.41	55	AGMA Stress
SH_GT_P, SH_GT_G	Gear Type		1	1	1	AGMA Stress
SH_K	K	Weight coefficient		0.25		AGMA Stress
SH_nc	nc	Carrier Speed (Planetary Only)		0		AGMA Stress
SH_n_P	n	Speed	2788		1,976.9	AGMA Stress
SH_Nplanets	Nplanets	Number of planets		4		AGMA Stress
SH_Hpsys	HPsys	Total horsepower for system		10.640.0		AGMA Stress
SH_phin	$\phi_v$	Pressure angle (standard normal)		20		AGMA Stress
SH_psi	$\psi$	Helix angle		0.3630		AGMA Stress
SH_Pnd	Pnd	Normal diametrical pitch		0.0000		AGMA Stress
SH_F_P, SH_F_G	F	Desired face width	3.5	3.6		AGMA Stress
	Fe	Effective face width	3.5000	3.5000	3.5	AGMA Stress
	acoeff	Addendum coefficient	1	3.5000	3.5000	AGMA Stress
	bcoeff	Dedendum coefficient	1.2500		1	AGMA Stress
	rfcoeff	Fillet radius coefficient		0.4	1.2500	AGMA Stress
SH_rfcoeff SH_Bcoeff	Bcoeff	Total backlash coefficient		0.0480		AGMA Stress
SH_Q	Q	Gear Quality Rating	12		12	AGMA Stress
	Cmc	Lead correction factor	0.8		0.8	AGMA Stress
	Ce	Mesh alignment correction factor				AGMA Stress
	Cma	Mesh alignment factor	1		1	AGMA Stress
SH_Kbs	Ka=Ko	Application/overload factor	0.1148		0.1148	AGMA Stress
	Kbs	Calibration factor for bending stress		1.25		AGMA Stress
				1.00		AGMA Stress
SH_Kcs	Kcs	Calibration factor for contact stress		1.00		AGMA Stress

Table 29: Spur-Helical User Inputs and Selections (continued)

[illegible]

## AGMA Stress Equations

**Table 30: Spur-Helical AGMA Stress Equations**

### AGMA STRESS SUMMARY

SYMBOL	DESCRIPTION	UNITS	PINION	MESH	GEAR
I	Pitting Resistance Geometry Factor		0.0920		0.0920
J	Bending Strength Geometry Factor		0.4591		0.4796
S <sub>wt</sub>	Working bending stress number	psi	38,242.4	1.095	38,568.7
S <sub>t</sub>	Bending tensile stress	psi	34,909.3		33,168.4
S <sub>wc</sub>	Working contact stress number	psi	169,054.5	1.111	171,281.2
S <sub>c</sub>	Contact stress	psi	152,170.9		151,609.4
R	Standard (reference) pitch radius	in	5.4167		7.6389
t <sub>cmax</sub>	Maximum contact temperature	°F		371.306	
	Scuffing Risk			LOW	
S <sub>B</sub>	Safety Factor (Scoring)			1.39	
	Estimated Weight		102.7		204.2
			Input	Input-Output	Output
			1	Mesh	2

### INPUT PARAMETERS

		PINION	MESH	GEAR
n, N	Number of Teeth	39	1.41	55
Gear Type		1	1	1
K	Weight coefficient		0.25	
n <sub>c</sub>	Carrier Speed (Planetary Only)		0	
n	Speed	2788		1,976.9
N <sub>planets</sub>	Number of planets		4	

### FORCE ANALYSIS

		PINION	MESH	GEAR
HP, P, H	Horsepower (per mesh)	2,660.0		2,660.0
T, TQ, Q	Torque	5,011.0		7,066.8
		60,131.8		84,801.3
v <sub>t</sub> , V, PLV	Pitch Line Velocity		7,907.2	
			94,886.6	
W <sub>t</sub>	Tangential load (transmitted)		11,101.3	
W <sub>r</sub>	Radial load		4,040.5	
W <sub>a</sub>	Axial load (thrust)		0.0	
W	Total force		11,813.7	



Table 30: Spur-Helical AGMA Stress Equations (continued)

GEAR GEOMETRY			PINION	MESH	GEAR
$P, P_d$	Diametrical pitch (transverse)	teeth/in		3.6000	
$P_{design}$	Recommended diametrical pitch for Hertz stress			5.4152	
$\phi_n$	Pressure angle (standard normal)	degrees		20	
		radians		0.3491	
$\phi, \phi_t$	Standard traverse pressure angle	degrees		20.0000	
		radians		0.3491	
$\psi$	Helix angle	degrees		0	
		radians		0.0000	
$P_{nd}$	Normal diametrical pitch	teeth/in		3.6	1.103377919
$F_{design}$	Recommended spur face width for Hertz stress	in		7.2020	
$F$	Desired face width	in	3.5		3.5
$F_e$	Effective face width	Manual (Face)	3.5000	3.5000	3.5000
$m_G$	Gear ratio			1.4103	
$R$	Standard (reference) pitch radius	in	5.4167		7.6389
$d, d_p$	Operating pitch diameter of pinion	in		10.8333	
$R_b$	Base radius	in	5.0900		7.1782
$C_r$	Operating center distance	in		13.0556	
$\phi_r$	Operating transverse pressure angle	degrees		20.0000	
		radians		0.3491	
$p_b$	Transverse base pitch	in/tooth		0.8200	
$p_N$	Normal base pitch	in/tooth		0.8200	
$\psi_b$	Base helix angle	degrees		0.0000	
		radians		0.0000	
$x1, x2$	Addendum modification		0		0
$a_{coeff}$	Addendum coefficient		1		1
$a$	Addendum	in	0.2778		0.2778
$b_{coeff}$	Dedendum coefficient		1.2500		1.2500
$b$	Dedendum	in	0.3472		0.3472
$c$	Clearance	in	0.0694		0.0694
$r_{coeff}$	Fillet radius coefficient			0.4	
$r_f$	Fillet radius	in		0.1431	
$Bl_{coeff}$	Total backlash coefficient			0.0480	
$BL_{total}$	Total backlash	in		0.0133	
$R_o$	Outside radius	in	5.6944		7.9167
$C_6$		in		4.465262982	
$C_1$		in		1.126558456	
$C_3$		in		1.85260911	
$C_4$	HPSTC	in		1.946594966	
$C_5$		in		2.553151047	
$C_2$	LPSTC	in		1.733114537	
$Z$	Length of line of contact	in		1.42659259	
$m_p$	Transverse contact ratio			1.7397	
$p_x$	Axial pitch			999,999.9999	
$m_F$	Axial contact ratio			0	
$n_r$	fractional part of $m_p$			0.7397	
$n_a$	fractional part of $m_F$			0	
$L_{min}$	Minimum length of lines of contact	in		3.5000	
$m_N$	Load sharing ratio			1.0000	
$\psi_r$	Operating helix angle	degrees		0	
		radians		0.0000	
$\phi_{nr}$	Operating normal pressure angle	degrees		20	
		radians		0.3491	

Table 30: Spur-Helical AGMA Stress Equations (continued)

## BENDING STRESS

			PINION	MESH	GEAR
$S_t$	Bending tensile stress	psi	34,909.3		33,168.4
$t_{r\_min}$	Minimum rim thickness below tooth root	in	0.7500		0.7500
$h_t$	Whole depth	in	0.6250		0.6250
$m_B$	Backup ratio		1.2000		1.2000
$K_B$	Rim thickness factor		1		1
Q	Gear Quality Rating		12		12
$Q_v$	Transmission Quality Rating			12	
B				0	
A				106	
$v_t$	Pitch line velocity	fps		7,907.2	
$v_{tmax}$	Maximum pitch line velocity	fps		13,225.0	
$K_v$	Dynamic factor			1.0000	
$K_s$	Size factor		1		1
$C_{mc}$	Lead correction factor	Properly modified leads	0.8		0.8
$F/(10d)$			0.0500		0.0500
$C_{pf}$	Pinion proportion factor		0.0386		0.0292
$C_{pm}$	Pinion proportion modifier		1.1		1.1
Ce	Mesh alignment correction factor	Gearing adjusted at assembly	1		1
A	Mesh alignment empirical constant		0.0675		0.0675
B	Mesh alignment empirical constant		0.0128		0.0128
C	Mesh alignment empirical constant		-0.0000926		-0.0000926
$C_{ma}$	Mesh alignment factor	Precision enclosed	0.1112		0.1112
$C_{mf}$	Face load distribution factor		1.1229		1.1146
$C_{mt}$	Transverse load distribution factor		1		1
$K_m$	Load distribution factor		1.1229		1.1146
$K_a=K_o$	Application/overload factor			1.25	
$K_{bs}$	Calibration factor for bending stress			1.00	

## CONTACT STRESS

			PINION	MESH	GEAR
$s_c$	Contact stress	psi	152,170.9		151,609.4
$C_p$	Elastic coefficient	psi <sup>1/2</sup>		2,276.7	
$C_a=C_o$	Application/overload factor			1.25	
$C_v$	Dynamic factor			1.0000	
$C_s$	Size factor		1		1
d, $d_p$	Operating pitch diameter of pinion	in		10.8333	
$F_e$	Effective face width of narrowest member in			3.5000	
$C_m$	Load distribution factor		1.1229		1.1146
$C_f$	Surface condition factor		1		1
I	Pitting Resistance Geometry Factor			0.0920	
$K_{cs}$	Calibration factor for contact stress			1.00	

Table 30: Spur-Helical AGMA Stress Equations (continued)

### PITTING RESISTANCE GEOMETRY FACTOR, I

			PINION	MESH	GEAR
$d, d_p$	Operating pitch diameter of pinion	in		10.8333	
$R_{m1}$	Mean radius of pinion	in		5.4167	
$\rho_1$	Radius of curvature for pinion			1.7331	
$\rho_2$	Radius of curvature for gear			2.7321	
$\rho_{m1}$	Radius of curv. at mean radius of pinion			1.8526	
$\rho_{m2}$	Radius of curv. at mean radius of gear			2.6127	
$C_\psi$	Helical overlap factor			1.0000	
I	Pitting Resistance Geometry Factor			0.0920	

### BENDING STRENGTH GEOMETRY FACTOR, J

			PINION	MESH	GEAR
$\psi$	Helix angle	degrees	0		0
$N_G$	Gear tooth count		39		55
$N_{mate}$	Mate tooth count		55		39
$J_{helixregext}$	J for helical, external gears		0.5351		0.5071
	J for spur (external or internal)		0.4591		0.4796
	J for helical, internal gears (est)		0.5951		0.5671
J	Bending Strength Geometry Factor		0.4591		0.4796

### BENDING STRESS

			PINION	MESH	GEAR
$s_t$	Bending tensile stress	psi	34,909.3		33,168.4
$t_{r\_min}$	Minimum rim thickness below tooth root	in	0.7500		0.7500
$h_t$	Whole depth	in	0.6250		0.6250
$m_B$	Backup ratio		1.2000		1.2000
$K_B$	Rim thickness factor		1		1
Q	Gear Quality Rating		12		12
$Q_v$	Transmission Quality Rating			12	
B				0	
A				106	
$v_t$	Pitch line velocity	fps		7,907.2	
$v_{tmax}$	Maximum pitch line velocity	fps		13,225.0	
$K_v$	Dynamic factor			1.0000	
$K_s$	Size factor		1		1
$C_{mc}$	Lead correction factor	Properly modified leads	0.8		0.8
$F/(10d)$			0.0500		0.0500
$C_{pf}$	Pinion proportion factor		0.0386		0.0292
$C_{pm}$	Pinion proportion modifier		1.1		1.1
Ce	Mesh alignment correction factor	Gearing adjusted at assembly	1		1
A	Mesh alignment empirical constant		0.0675		0.0675
B	Mesh alignment empirical constant		0.0128		0.0128
C	Mesh alignment empirical constant		-0.0000926		-0.0000926
$C_{ma}$	Mesh alignment factor	Precision enclosed	0.1112		0.1112
$C_{mf}$	Face load distribution factor		1.1229		1.1146
$C_{mt}$	Transverse load distribution factor		1		1
$K_m$	Load distribution factor		1.1229		1.1146
$K_a=K_o$	Application/overload factor			1.25	
$K_{bs}$	Calibration factor for bending stress			1.00	

Table 30: Spur-Helical AGMA Stress Equations (continued)

### CONTACT STRESS

			PINION	MESH	GEAR
$s_c$	Contact stress	psi	152,170.9		151,609.4
$C_p$	Elastic coefficient	psi <sup>1/2</sup>		2,276.7	
$C_a=C_o$	Application/overload factor			1.25	
$C_v$	Dynamic factor			1.0000	
$C_s$	Size factor		1		1
$d, d_p$	Operating pitch diameter of pinion	in		10.8333	
$F_e$	Effective face width of narrowest member in			3.5000	
$C_m$	Load distribution factor		1.1229		1.1146
$C_f$	Surface condition factor		1		1
$I$	Pitting Resistance Geometry Factor			0.0920	
$K_{cs}$	Calibration factor for contact stress			1.00	

### ALLOWABLE BENDING STRESS

			PINION	MESH	GEAR
$s_{wt}$	Working bending stress number	psi	38,242.4		38,568.7
$s_{at}$	Allowable bending stress	psi	51,990.1		51,990.1
Rev	Reverse loading factor		1.00		1.00
$K_T$	Temperature factor for bending strength		1.00		1.00
$L$	Life	hrs	3,500.0		3,500.0
$n$	Speed	rpm	2,788.0		1,976.9
$q$	Number of contacts per revolution		4		4
$N$	Number of stress cycles		2.342E+09		1.661E+09
$Y_N$	Stress cycle factors		0.8809		0.8885
$s_{at}Y_N$	Localized yielding limit	psi	45,800.6		46,191.3
$H_B$	Brinell hardness number		647		647
$s_{ay}$	Allowable yield strength number		279,202.5		279,202.5
	Reliability Requirement		Fewer than one in 800 (Aerospace 3 s.d.)		
$K_R$	Reliability factor			1.20	
	Manual entry for standard deviations			3.0000	
	Number of standard deviations			3.0000	
	Desired reliability			0.9987	
	Coefficient of variation (bending)			0.1560	
$FS_B$	Factor of Safety for Bending		1.00		1.00
$K_{ba}$	Bending Calibration Factor			1.00	

### ALLOWABLE CONTACT STRESS

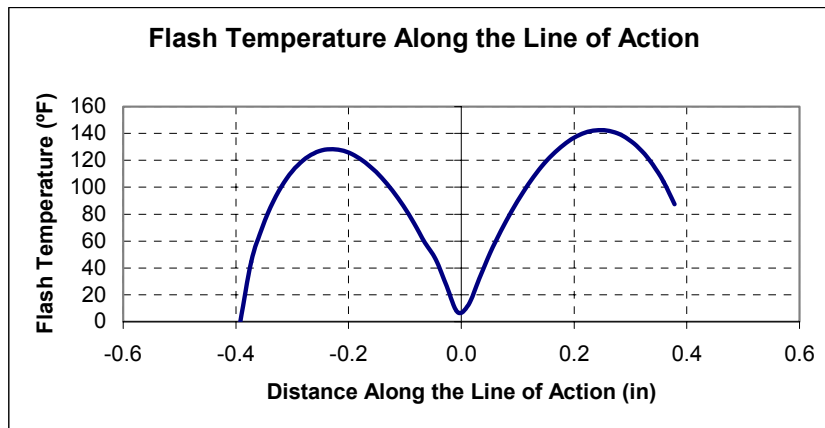
			PINION	MESH	GEAR
$s_{wc}$	Working contact stress number	psi	169,054.5		171,281.2
$s_{ac}$	Allowable contact stress number	psi	250,144.9		250,144.9
$Z_N$	Stress cycle factor for pitting resistance		0.8094		0.8201
$H_B$	Brinell hardness number		647		647
$H_{BP}/H_{BG}$	Pinion to gear hardness ratio			1	
$A$				0.000000	
$C_H$	Hardness ratio factor for pitting resistance		1.0000		1.0000
$C_T$	Temperature factor		1.00		1.00
$C_R$	Reliability factor		1.20		1.20
$FS_C$	Factor of Safety for Contact		1.00		1.00
$K_{ca}$	Pitting Calibration Factor			1.000	

## Scuffing (Scoring) Summary

**Table 31: Spur-Helical Gear Scuffing**

### A. SCORING SUMMARY

<u>SYMBOL</u>	<u>DESCRIPTION</u>	<u>UNITS</u>	<u>PINION</u>	<u>MESH</u>	<u>GEAR</u>
$t_{flmax}$	Maximum flash temperature	°F		142.53	
$t_{oil}$	Oil temperature	°F		144.1333333	
$t_M$	Bulk temperature	°F		228.7766041	
$t_{cmax}$	Maximum contact temperature	°F		371.31	
	Type of Lubricant		VASCO MIL-L-23699		
$\mu_{ts}$	Mean scuffing temperature	°F		459	
$\sigma_{ts}$	Standard temperature deviation	°F		31	
	Probability of scoring hazard			0.23%	
	Scuffing Risk			LOW	
	Safety Factor			1.3860	



### FLASH TEMPERATURE INDEX (DUDLEY/AMCP)

$n, N$	Number of teeth		39		55
$\rho_1, \rho_2$	Transverse radii of curvature at general contact point	in	2.3035		2.1618
		degrees		20.0000	
$\phi, \phi_t$	Standard traverse pressure angle	radians		0.3491	
$P_d$	Diametrical pitch (transverse)	teeth/in		3.6	
$Z_t$	Geometry constant			0.004597605	
$W_{te}$	Effective tangential load	lb		12465.19157	

Table 31: Spur-Helical Gear Scuffing (continued)

$F_e$	Effective face width	in	3.5
$s$	Mean surface finish	rms	18
$n_p$	Speed of pinion	rpm	2788
$t_b$	Gear body temperature	°F	158.2666667
$t_{flash}$	Flash temperature	°F	93.94686554
$t_f$	Flash temperature index	°F	252.2135
	Low Risk of Scoring (Dudley)		300
	High Risk of Scoring (Dudley)		350
	Risk of Scoring (Dudley)		LOW

### A.3.1 BASIC GEAR GEOMETRY

			PINION	MESH	GEAR
$A_p, A_g$	Type of gear (internal=-1)		1	1	1
$n, N$	Number of Teeth		39		55
$m_g$	Gear ratio			1.4103	
$R$	Standard (reference) pitch radius	in	5.4167		7.6389
$C_r$	Operating center distance	in		13.0556	
$R_r$	Operating pitch radius		5.4167		7.6389
		degrees		20.0000	
$\phi, \phi_t$	Standard traverse pressure angle	radians		0.3491	
$R_{b1}, R_{b2}$	Base radii	in	5.0900		7.1782
		degrees		20.0000	
$\phi_r$	Operating transverse pressure angle	radians		0.3491	
$p_b$	Transverse base pitch	in/tooth		0.8200	
$p_N$	Normal base pitch	in/tooth		0.8200	
$p_x$	Axial pitch			999999.9999	
		degrees		0.0000	
$\psi_b$	Base helix angle	radians		0.0000	
		degrees		0.0000	
$\psi_r$	Operating helix angle	radians		0.0000	
		degrees		20.0000	
$\phi_{nr}$	Operating normal pressure angle	radians		0.3491	
$R_{o1}, R_{o2}$	Outside radius	in	5.6944		7.9167
		degrees	26.6384		24.9439
$\phi_{o1}, \phi_{o2}$	Tip pressure angles	radians	0.4649		0.4354

Table 31: Spur-Helical Gear Scuffing (continued)

### A.3.2 DISTANCE ALONG THE LINE OF ACTION

$C_6$		in	4.4653
$C_1$	SAP	in	1.1266
$C_3$	Operating pitch point	in	1.8526
$C_4$	HPSTC	in	1.9466
$C_5$	EAP	in	2.5532
$C_2$	LPSTC	in	1.7331
$Z$	Length of line of contact	in	1.4266

### A.3.3 PARAMETER ALONG THE LINE OF ACTION

$n, N$	Number of Teeth	39	55
$\Gamma_A$	Linear coordinate in the transverse plane on the line of action (SAP)	-0.3919	
$\Gamma_B$	Linear coordinate in the transverse plane on the line of action (LPSTC)	-0.0645	
$\Gamma_D$	Linear coordinate in the transverse plane on the line of action (HPSTC)	0.0507	
$\Gamma_E$	Linear coordinate in the transverse plane on the line of action (EAP)	0.3781	

### A.3.4 CONTACT RATIOS

$m_p$	Transverse contact ratio	1.7397
$m_F$	Axial contact ratio	0.0000
$n_r$	fractional part of $m_p$	0.7397
$n_a$	fractional part of $m_F$	0.0000
$L_{\min}$	Minimum length of lines of contact	in 3.5000

### A.3.5 ROLL ANGLES

$\varepsilon_1$	Roll angle at $C_1$	degrees	12.6811
		radians	0.2213
$\varepsilon_2$	Roll angle at $C_2$	degrees	19.5089
		radians	0.3405
$\varepsilon_3$	Roll angle at $C_3$	degrees	20.8540
		radians	0.3640
$\varepsilon_4$	Roll angle at $C_4$	degrees	21.9119
		radians	0.3824
$\varepsilon_5$	Roll angle at $C_5$	degrees	28.7396
		radians	0.5016

Table 31: Spur-Helical Gear Scuffing (continued)

### A.3.6 PROFILE OF RADII OF CURVATURE

$\varepsilon$	Roll angle	degrees	25.9294	
		radians	0.4526	
$\Gamma_i$	Parameter on line of action		0.2434	for max flash
$\rho_1, \rho_2$	Transverse radii of curvature at general contact point	in	2.3035	2.1618
$\rho_r$	Transverse relative radius of curvature	in	1.1152	
$\rho_{rc}$	Normal relative radius of curvature	in	1.0840	
	Equivalent radius of a cylinder that represents the gear pair curvatures in contact along the line of action	in	1.1152	

### A.4 GEAR TOOTH VELOCITIES AND LOADS

$n_P, n_G$	Speed of member	rpm	2,788.0	1,976.9
$\omega_1, \omega_2$	Rotational (angular) velocity	rad/s	292.0	207.0
$v_{tr}$	Operating pitchline velocity	fpm	7,907.2	
$v_{r1}, v_{r2}$	Rolling velocities	in/s	672.5260	447.5401
$v_s$	Sliding velocity	in/s	225.0	
$v_e$	Entraining velocity	in/s	1,120.1	
$P$	Power	hp	2,660.0	
$(W_{tr})_{nom}$	Nominal tangential load	lb	11,101.3	
$K_s=K_o$	Application/overload factor		1.25	
$K_v$	Dynamic factor		1.00	
$K_m$	Load distribution factor		1.12	
$C_D$	Combined derating factor		1.40	
$W_{tr}$	Actual tangential load	lb	15,581.5	
$W_{Nr}$	Normal operating load	lb	16,581.5	
$w_{tr}$	Transverse unit load	lb	4,451.9	
$w_{Nr}$	Normal unit load	lb	4,737.6	

### A.5 LOAD SHARING FACTOR

$\varepsilon$	Roll angle	degrees	25.9294	
		radians	0.4526	
$X_{tr}$	Load sharing factor (unmodified tooth profiles)		0.4705	
$X_{tr}$	Load sharing factor (modified tooth profiles pinion driving)		0.4957	
$X_{tr}$	Load sharing factor (modified tooth profiles gear driving)		0.3528	
$X_{tr}$	Load sharing factor (designed for smooth meshing)		0.6995	
$X_{tr}$	Type of tooth profile modification		Modified (pinion drives)	
$X_{tr}$	Load sharing factor		0.4957	



Table 31: Spur-Helical Gear Scuffing (continued)

## A.6 HERTZIAN CONTACT BAND

$X_r$	Load sharing factor			0.4957	
$w_{Nr}$	Normal unit load	lb		4,737.6	
	Equivalent radius of a cylinder that represents the gear pair curvatures in contact along the line of action	in		1.1152	
$\rho_n$					
$\nu_1, \nu_2$	Poisson's ratio		0.300		0.300
$E_1, E_2$	Modulus of elasticity	psi	29.64E+6		29.64E+6
$E_r$	Reduced modulus of elasticity	psi		32.57E+6	
$b_H$	Semi-width of rectangular band	in		0.0143	

### A.7.3.1 MEAN COEFFICIENT OF FRICTION

$\sigma_1, \sigma_2$	Surface finish	rms	13	13
S	Average surface roughness	rms		13
	Check on surface roughness			1.3514
$\mu_m$	Mean coeff of friction (approx)			0.0811

### A.7.4 THERMAL ELASTIC FACTOR

$X_M$	Thermal elastic factor (martensitic steels)	$^{\circ}\text{F lbs}^{-0.75} \text{s}^{0.5} \text{in}^{0.5}$	1.7500
-------	---	---	--------

### A.7.5 GEOMETRY FACTOR

$X_G$	Scoring Geometry Factor		0.1482
-------	-------------------------	--	--------

### A.7.2 FLASH TEMPERATURE EQUATION

$t_{fmax}$	Maximum flash temperature	$^{\circ}\text{F}$	142.5297
------------	---------------------------	--------------------	----------

## *Lubrication Analysis*

**Table 32: Spur-Helical Lubrication Analysis**

### **LUBRICATION ANALYSIS**

<u>SYMBOL</u>	<u>DESCRIPTION</u>	<u>UNITS</u>	<u>PINION</u>	<u>MESH</u>	<u>GEAR</u>
HP	Power	hp	2,660.0		2,646.7
$\eta_{\text{mesh}}$	efficiency			99.5%	
$P_{\text{loss}}$	Power dissipated	hp		13.3	
Q	heat generated	Btu/min		563.92	
$C_p$	Specific heat of oil	Btu/lb-°F		0.5	
	Oil flow design		Recommended (30°)		
		lb/min		39.9	
M	Oil flow	gal		5.32	
		lb/min		114	
$M_{\text{manual}}$	Oil flow	gal		15.2	
		lb/min		25.1	
$M_{\text{min}}$	Minimum oil flow ( $\Delta T = +45^\circ\text{F}$ )	gal		3.3	
		lb/min		37.6	
$M_{\text{rec}}$	Recommended oil flow	gal		5.0	
		gpm/hp		0.002	
	Rule of thumb	gpm		5.3200	
$\Delta T$	Temperature rise	°F		28.3	
$t_{\text{in}}$	Incoming oil temperature	°F		130	
$t_{\text{out}}$	Outgoing oil temperature	°F		158.3	
$t_{\text{oil}}$	Oil temperature (average)	°F		144.1	

### Material Properties

### Table 33: Spur-Helical Gear Properties

GEAR MATERIALS

DESCRIPTION	UNITS	VASCO X2M	VASCO X2M	GEAR	AISI 9310	Aero (Table 15) & Aero Carb (Table 1)			AISI 4340
						VASCO X2M	Y	ROWEAR 5	CBS600
AMS Spec		N/A	N/A			6265/6260	N/A	6308	6255
Heat treatment		C-H	C-H			C-H	C-H	C-H	C-H
Main drive application		X	X			X	X	X	TH-N
Accessory application						X			X
High temperature application		X	X				X	X	
Case hardness (HRC)	HRC	62	62			61	62	62	60
Core hardness (HRC)	HRC	40	40			37	40	40	38
Surface hardness (HR15N)	HR15N								
Minimum Brinell hardness	HB	647	647			632	647	647	617
Allowable contact stress number	psi	250,145	250,145			244,897	250,145	250,145	239,736
Allowable bending stres number	psi	51,990	51,990			52,102	51,990	51,990	52,149
Poisson's ratio		0.300	0.300			0.292	0.300	0.292	0.296
Young's moduli of elasticity	psi	29.64E+6	29.64E+6			29.00E+6	29.64E+6	30.00E+6	29.30E+6
Density	lb/in <sup>3</sup>	0.280	0.280			0.283	0.280	0.282	0.282
		2	2			1	2	3	4

Table 33: Spur-Helical Gear Properties (continue)

SCORING AND LUBRICANTS

Mean Standard Deviation	VASCO MIL-L- 23699				Carb Steel MIL-L-7808				Carb Steel MIL-L-6081				Carb Steel MIL-L-23699				VASCO MIL-L-23699			
	459	31	4		366	56.6	1		264	74.4	2		391	58.65	3		459	31	4	

## Bending Stress Geometry Factor

Table 34: Spur-Gear Bending Strength Geometry Factor for Pinion

<b>J</b>	<b>0.4591</b>
----------	---------------

### A.1 INPUTS

SYMBOL	VALUE	DESCRIPTION	UNITS
P	3.6	diametrical pitch	teeth/in
p	0.872665	circular pitch	teeth/in circum
A <sub>G</sub>	1	gear	
A <sub>M</sub>	1	mate	
phi	20	pressure angle	degree
	0.349066		radians
N <sub>G</sub>	39	number of teeth in gear	
N <sub>mate</sub>	55	number of teeth in mate	
b design	1.25	design dedendum of gear	
b	0.347222	dedendum of gear	in
a design	1	design addendum gear	
a <sub>mate</sub>	0.277778	addendum of mate	in
t <sub>p</sub>	0.429666	circular tooth thickness of gear	in
r <sub>f</sub>	0.143137	fillet radius of gear	in
t <sub>pmate</sub>	0.429666	circular tooth thickness of mate	in
BL <sub>total</sub>	0.013333	total backlash	in

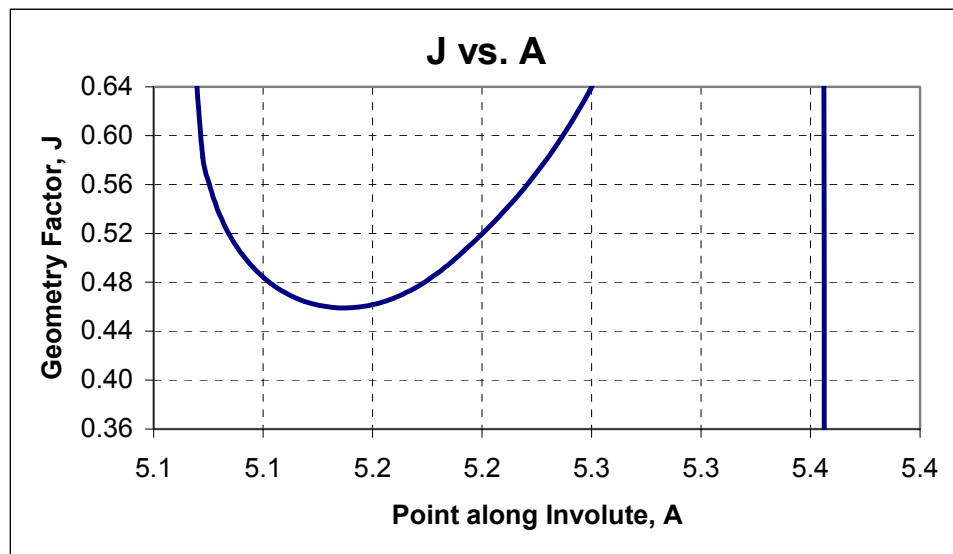


Table 34: Spur-Gear Bending Strength Geometry Factor for Pi (continued)

## A.2 GEOMETRY FACTOR CALCULATION

R	5.416667	pitch radius of gear	in	
R <sub>r</sub>	5.069444	root radius of gear	in	
R <sub>b</sub>	5.090002	base circle radius of gear	in	
R <sub>mate</sub>	7.638889	pitch radius of mate	in	
R <sub>omate</sub>	7.916667	outside radius of mate	in	
R <sub>bmate</sub>	7.178208	base circle radius of mate	in	
P <sub>b</sub>	0.820037	base pitch	in	
C	13.05556	center distance	in	
$\phi_h$	20.92861	pressure angle at highest point of single tooth contact on involute	degrees	A.1
	0.365273		radians	A.1
t <sub>b</sub> '	0.55548	tooth thickness on base circle	in	A.2
$\phi_n$	18.78552	angle which the normal force makes with a line perpendicular to the tooth centerline	degrees	A.3
	0.327869	at highest point of single tooth contact radius on tooth centerline to point of application of worst load	radians	A.3
R <sub>x</sub>	5.376399	radius to tangency point of fillet and gear	in	A.4
A <sub>1</sub>	5.183607	tooth profile	in	A.6 & A.7
T <sub>1</sub>	10.90505	pressure angle at the intersection of the fillet and involute	degrees	A.6 & A.7
	0.190329		radians	
$\alpha'$	0.02832			A.8
x'	0.146779	x coordinate of fillet-involute inflection	in	
y'	5.181529	y coordinate of fillet-involute inflection	in	
delta	0.218649			
aa	0.00705	x coordinate of fillet radius center	in	A.9
bb	5.212576	y coordinate of fillet radius center	in	A.8
A	<b>5.137657</b>			
$\alpha$	0.024921			A.12 or A.13
h	0.246691			A.14
t	0.571353			A.15
			LOW	5.06944444
J	0.127526		R <sub>r</sub>	5.06944444
X	0.330823		A <sub>1</sub>	5.18360708
K <sub>t</sub>	1.976036		R <sub>x</sub>	5.37639889
H	0.180044		HI	5.18360708
L	0.149972			
M	0.450028			

Table 35: Spur Gear Bending Strength Geometry Factor for Gear

<b>J</b>	<b>0.4796</b>
----------	---------------

## A.1 INPUTS

<u>SYMBOL</u>	<u>VALUE</u>	<u>DESCRIPTION</u>	<u>UNITS</u>
P	3.6	diametrical pitch	teeth/in
p	0.872665	circular pitch	teeth/in circum
A <sub>G</sub>	1	gear	
A <sub>M</sub>	1	mate	
phi	20	pressure angle	degree
	0.349066		radians
N <sub>G</sub>	55	number of teeth in gear	
N <sub>mate</sub>	39	number of teeth in mate	
b design	1.25	design dedendum of gear	
b	0.347222	dedendum of gear	in
a design	1	design addendum gear	
a <sub>mate</sub>	0.277778	addendum of mate	in
t <sub>p</sub>	0.429666	circular tooth thickness of gear	in
r <sub>f</sub>	0.143137	fillet radius of gear	in
t <sub>pmate</sub>	0.429666	circular tooth thickness of mate	in
BL <sub>total</sub>	0.013333	total backlash	in

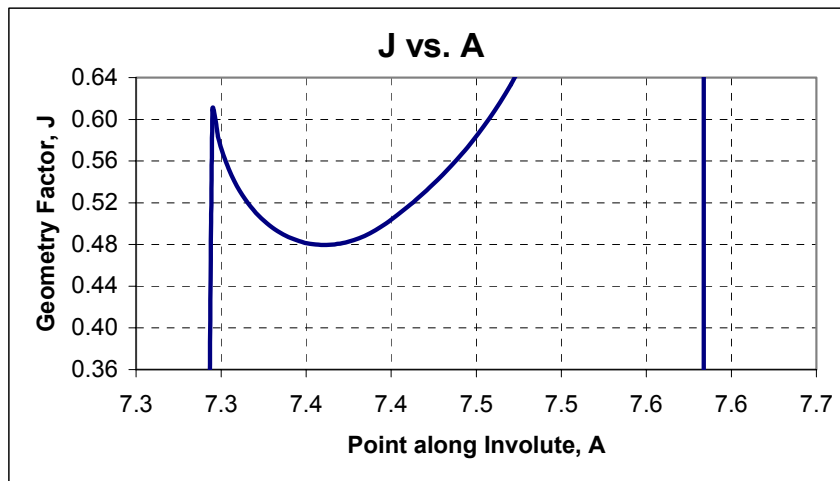


Table 35: Spur Gear Bending Strength Geometry Factor (continued)

## A.2 GEOMETRY FACTOR CALCULATION

R	7.638889	pitch radius of gear	in	
R <sub>r</sub>	7.291667	root radius of gear	in	
R <sub>b</sub>	7.178208	base circle radius of gear	in	
R <sub>mate</sub>	5.416667	pitch radius of mate	in	
R <sub>omate</sub>	5.694444	outside radius of mate	in	
R <sub>bmate</sub>	5.090002	base circle radius of mate	in	
P <sub>b</sub>	0.820037	base pitch	in	
C	13.05556	center distance	in	
$\phi_h$	20.83768	pressure angle at highest point of single tooth contact on involute	degrees	A.1
	0.363686		radians	A.1
t <sub>b</sub> '	0.617727	tooth thickness on base circle	in	A.2
$\phi_n$	19.34243	angle which the normal force makes with a line perpendicular to the tooth centerline at highest point of single tooth contact	degrees	A.3
	0.337589	radius on tooth centerline to point of application of worst load	radians	A.3
R <sub>x</sub>	7.607612	radius to tangency point of fillet and gear tooth profile	in	A.4
A <sub>1</sub>	7.398814	tooth profile	in	A.6 & A.7
T <sub>1</sub>	14.02655	pressure angle at the intersection of the fillet and involute	degrees	A.6 & A.7
$\alpha'$	0.24481		radians	
x'	0.019103	x coordinate of fillet-involute inflection	in	A.8
y'	0.141329	y coordinate of fillet-involute inflection	in	
delta	7.397464			
aa	0.263912	x coordinate of fillet radius center	in	A.9
bb	0.003148	y coordinate of fillet radius center	in	A.8
A	#NUM!			
$\alpha$	#NUM!			A.12 or A.13
h	#NUM!			A.14
t	#NUM!			A.15
J	#NUM!	LOW	#NUM!	
X	#NUM!	R <sub>r</sub>	7.29166667	
K <sub>t</sub>	#NUM!	A <sub>1</sub>	7.39881417	
H	0.180044	R <sub>x</sub>	7.60761221	
L	0.149972	HI	#NUM!	
M	0.450028			



## **APPENDIX C: BEVEL GEAR RATING CALCULATIONS**

## Bevel Gear Summary

**Table 36: Bevel Gear User Inputs and Selections**

### BEVEL RATING SUMMARY

MDLCTR	SYMBOL	DESCRIPTION	UNITS	PINION	MESH	GEAR	WORKSHEET
	I	Selected Material		VASCO X2M		VASCO X2M	AGMA Stress
	J	Geometry factor for pitting resistance			0.1187		AGMA Stress
		Geometry factor for bending strength		0.2697		0.2631	AGMA Stress
BV_swg_P, BV_swg_G	$s_{wc}$	Permissible contact stress number	psi	212,984.3		227,546.6	AGMA Stress
BV_sc	$s_c$	Contact stress number	psi		207,070.9		AGMA Stress
BV_Bend_P, BV_Bend_G				<b>1.03</b>		<b>1.10</b>	AGMA Stress
BV_swt_P, BV_swt_G	$s_{wt}$	Permissible bending stress number	psi	37,936.1		27,286.1	AGMA Stress
BV_st_P, BV_st_G	$s_t$	Bending stress number	psi	26,157.9		26,811.0	AGMA Stress
BV_Contact_P, BV_Contact_G				<b>1.45</b>		<b>1.02</b>	AGMA Stress
BV_d_P, BV_d_G d, D		Standard reference pitch diameter	in	6.291		18.874	AGMA Stress
BV_W_P, BV_W_G, BV_W_Mesh	W	Estimated weight	lb	39.6	395.8	356.2	AGMA Stress
		DESIGN BALANCE		<b>0.7092</b>		<b>1.0797</b>	AGMA Stress
BV_Hpmesh	$HP_{mesh}$	Load Face Power per tooth mesh		Concave		Convex	Forces
					8,659.0		
BV_T_P, BV_T_G	$T_P, T_G$	Torque	in lb	36,382.4		109,147.3	Forces
BV_PLV	$V_t$	Pitch line velocity	fpm		19,738.5		Forces
BV_Wt	$W_{tP}, W_{tG}$	Tangential force	lb		14,476.6		Forces
BV_Wx_P, BV_Wx_G	$W_x$	Axial force	lb	11,650.5		2,896.8	Forces
BV_Wr_P, BV_Wr_G	$W_r$	Radial force	lb	2,896.8		11,650.5	Forces
BV_mG	$m_G$	Gear ratio			3.0000		
BV_gamma, BV_tau	$\gamma, \Gamma$	Pitch angle	degrees radians	18.4349 0.3218		71.5651 1.2490	Bevel Geometry Bevel Geometry

## User Inputs and Selections

Table 36: Bevel Gear User Inputs and Selections (continued)

### USER INPUTS & SELECTIONS

MDLCTR	SYMBOL	DESCRIPTION	UNITS	PINION	MESH	GEAR	WORKSHEET
BV_Kw	K <sub>w</sub>	Weight factor for bevel gears			0.25		
BV_Life	L	Life	hrs	3,600		3,600	AGMA Stress
BV_numbercontacts	q	Number of contacts per revolution	contacts		1		AGMA Stress
BV_rms	f <sub>p</sub>	Pinion surface roughness	μin	23.0			AGMA Stress
BV_Tt_P, BV_Tt_G	T <sub>T</sub>	Peak operating gear blank temperature	° F	250.0000		250.0000	AGMA Stress
BV_FSc	S <sub>H</sub>	Contact factor of safety		1.00		1.00	AGMA Stress
BV_Kac	K <sub>ac</sub>	Calibration factor to allow contact			1.0000		AGMA Stress
		Reliability Requirement			Fewer than one in 800 (Aerospace 3 s.d.)		AGMA Stress
BV_Rev_P, BV_Rev_G	Rev	Reverse loading factor		1.00		0.70	AGMA Stress
BV_FSb	S <sub>F</sub>	Bending factor of safety		1.00		1.00	AGMA Stress
BV_Kac	K <sub>ab</sub>	Calibration factor to allow bending			1.0000		AGMA Stress
BV_Ko	K <sub>o</sub>	Overload factor			1.25		AGMA Stress
BV_Q	Q	Gear Quality Rating		12		12	AGMA Stress
		Amount of straddle mounting			One member straddle mounted		AGMA Stress
		Properly crowned teeth			Yes		AGMA Stress
		Hand of Spiral		Right		Left	Forces
		Rotation		Counterclockwise		Clockwise	
		Power flow		Driver		Driven	Forces
		Load Face		Concave		Convex	Forces
BV_n_P, BV_n_G	n <sub>P</sub> , n <sub>G</sub>	Speed	rpm	15,000.0		5,000.0	Forces
BV_HPsys	P <sub>P</sub> , P <sub>G</sub>	Power	hp	8,659.0		8,659.0	Forces
BV_Pd	P <sub>d</sub>	Diametrical pitch	teeth/in		2.8611		Bevel Geometry
BV_NP, BV_NG	n, N	Number of teeth		18		54	Bevel Geometry
BV_ShaftAngle	Σ	Shaft angle	degrees		90		Bevel Geometry
			radians		1.5707963		Bevel Geometry
BV_F	F	Face	in		4		Bevel Geometry
BV_psi	ψ	Spiral angle	degrees		35		Bevel Geometry
			radians		0.6108652		Bevel Geometry
BV_phi	φ	Standard pressure angle (normal)	degrees		20		Bevel Geometry
			radians		0.3490659		Bevel Geometry
BV_DesiredmG	φ, φ <sub>n</sub>	Desired m <sub>G</sub>			3	2.864864865	Bevel Geometry
		Depth type for tooth taper			Duplex		Bevel Geometry
					Recommended		Bevel Geometry
BV_rcmanual		Cutter radius (Manual)	in		4.5		Bevel Geometry
		Type of cutting process			Face milling		Bevel Geometry
		Gear Material		VASCO X2M		VASCO X2M	Material Material

## AGMA Stress Equations

Table 37: Bevel Gear AGMA Stress Equations

### AGMA STRESS ANALYSIS FOR BEVEL GEARS

#### SUMMARY

		UNITS	PINION	MESH	GEAR
	Selected Material		VASCO X2M		VASCO X2M
I	Geometry factor for pitting resistance			0.1187	
J	Geometry factor for bending strength		0.2697		0.2631
$S_{wc}$	Permissible contact stress number	psi	212,984.3		227,546.6
$S_c$	Contact stress number	psi		207,070.9	
			<b>1.03</b>		<b>1.10</b>
$S_{wt}$	Permissible bending stress number	psi	37,936.1		27,286.1
$S_t$	Bending stress number	psi	26,157.9		26,811.0
			<b>1.45</b>		<b>1.02</b>
d, D	Standard reference pitch diameter	in	6.2913		18.8739
	Estimated weight	lb	39.5803		356.2226
	DESIGN BALANCE		<b>0.7092</b>		<b>1.0797</b>

#### FORCE ANALYSIS

$n_P, n_G$	Speed	rpm	15,000.0		5,000.0
$P_P, P_G$	Power	hp	8,659.0		8,659.0
		ft lb	3,031.9		9,095.6
$T_P, T_G$	Torque	in lb	36,382.4		109,147.3
$d_m, D_m$	Mean pitch diameter	in	5.026		15.079
$V_t$	Pitch line velocity	fpm		19,738.5	
$W_{tP}, W_{tG}$	Tangential force	lb		14,476.6	
$W_x$	Axial force	lb	11,650.5		2,896.8
$W_r$	Radial force	lb	2,896.8		11,650.5
W	Total force	lb	16,729.0		15,190.8

#### GEAR GEOMETRY

n, N	Number of teeth		18		54
d, D	Pitch diameter	in	6.2913		18.8739
$P_d$	Diametrical pitch (outer transverse)	teeth/in		2.8611	
$r_c$	Cutter radius	in		6.4808	
$A_m$	Mean cone distance	in		7.9474	
		degrees		35	
$\psi$	Spiral angle	radians		0.61086524	
F	Face	in		4	

Table 37: Bevel Gear AGMA Stress Equations (continued)

## PERMISSIBLE CONTACT STRESS

$s_{wc}$	Permissible contact stress number	psi	212,984.3	227,546.6
$s_{ac}$	Allowable contact stress number	psi	250,144.9	250,144.9
$C_L$	Stress cycle factor		0.9318	0.9955
L	Life	hrs	3,600	3,600
n	Speed	rpm	15,000.0	5,000.0
q	Number of contacts per revolution	contacts		1
$N_L$	Number of stress cycles	cycles	3.240E+09	1.080E+09
$C_H$	Hardness ratio factor		1.0000	1.0000
$H_{BP}, H_{BG}$	Minimum Brinell hardness		647	647
$B_1$	Intermediate variable			0.0007
$f_P$	Pinion surface roughness	$\mu$ in	23.0	
$B_2$	Intermediate variable			0.0006
$K_T$	Temperature factor		1.0000	1.0000
$T_T$	Peak operating gear blank temperature	$^{\circ}$ F	250.0000	250.0000
	Required reliability		Fewer than one in 800 (Aerospace 3 s.d.)	
$C_R$	Reliability factor			1.09
$S_H$	Contact safety of factor		1.00	1.00
$C_f$	Pitting resistance derating factor		0.8514	0.9097
$K_{ac}$	Calibration factor to allow contact			1.0000

## PERMISSIBLE BENDING STRESS

$s_{wt}$	Permissible bending stress number	psi	37,936.1	27,286.1
$s_{at}$	Allowable bending stress number	psi	51,990.1	51,990.1
$K_L$	Stress cycle factor		0.8739	0.8979
L	Life	hrs	3,600	3,600
n	Speed	rpm	15,000.0	5,000.0
q	Number of contacts per revolution	contacts		1
$N_L$	Number of stress cycles	cycles	3.240E+09	1.080E+09
$K_T$	Temperature factor		1.0000	1.0000
$T_T$	Peak operating gear blank temperature	$^{\circ}$ F	250.0000	250.0000

Table 37: Bevel Gear AGMA Stress Equations (continued)

	Reliability Requirement	Fewer than one in 800 (Aerospace 3 s.d.)	
$K_R$	Reliability factor	1.20	
$n_{\text{manual}}$	Manual entry for standard deviations	0.0000	
$n$	Number of standard deviations	3.0000	
$R_{\text{el}}$	Desired reliability	0.9987	
$v$	Coefficient of variation (bending)	0.1560	
		0	0
$Rev$	Reverse loading factor	1.00	0.70
$S_F$	Bending safety of factor	1.00	1.00
$K_f$	Bending strength derating factor	0.7297	0.5248
$K_{ab}$	Calibration factor to allow bending	1.0000	

## CONTACT STRESS FORMULA

$s_c$	Calculated contact stress number	psi	207,070.9	
$C_p$	Elastic coefficient	$(\text{lb/in}^2)^{0.5}$	2,276.7	
$\mu_P, \mu_G$	Poisson's ratio		0.300	0.300
$E_P, E_G$	Young's moduli of elasticity	psi	29.6E+06	29.6E+06
$C_s$	Size factor for pitting resistance		0.9375	
$F$	Face width	in	4.0000	
$T_P$	Operating pinion torque	in lb	36,382.4	109,147.3
$K_o$	Overload factor		1.25	
$K_v$	Dynamic factor		1.0500	
$Q$	Gear Quality Rating		12	12
$Q_v$	Transmission Quality Rating		12	
$B$	Intermediate coefficient		0	
$A$	Intermediate coefficient		106	
$d, D$	Pitch diameter	in	6.2913	18.8739
$n$	Speed	rpm	15,000.0	5,000.0
$v_t$	Pitch line velocity (outside edge)	fps	24,724.8	
$v_{t\text{max}}$	Maximum pitch line velocity	fps	13,225.0	
$F$	Net face width	in	4.0000	
	Amount of straddle mounting		One member straddle mounted	
$K_m$	Load distribution factor		1.1576	
$K_{mb}$	Load distribution modifier		1.1000	
	Properly crowned teeth		Yes	
$C_{xc}$	Crowning factor		1.5000	
$I$	Pitting resistance geometry factor		0.1187	

Table 37: Bevel Gear AGMA Stress Equations (continued)

## BENDING STRESS FORMULA

$s_t$	Calculated bending stress number	psi	26,157.9	26,811.0
$K_o$	Overload factor			1.25
$K_v$	Dynamic factor			1.05
$P_d$	Diametrical pitch (outer transverse)	teeth/in		2.8611
$K_s$	Size factor			0.56
	Amount of straddle mounting		One member straddle mounted	
$K_m$	Load distribution factor			1.16
$K_x$	Tooth lengthwise curvature factor			1.0000
$r_c$	Cutter radius	in		6.4808
$A_m$	Mean cone distance	in		7.9474
		degrees		35
$\psi$	Spiral angle	radians		0.6109
$q$	Intermediate coefficient			-1.1557
$J$	Bending strength geometry factor		0.2697	0.2631
$T_P$	Operating pinion torque	in lb	36,382.4	109,147.3
$F$	Net face width	in		4.0000
$d, D$	Pitch diameter	in	6.2913	18.8739

## Force Analysis

Table 38: Bevel Gear Force Analysis

### BEVEL GEAR FORCE ANALYSIS

Pinion hand of spiral	Gear hand of spiral	Rotation of driver	Rotation of driven	Load face	
				Driver	Driven
Right	Left	Clockwise	Counterclockwise	Convex	Concave
		Counterclockwise	Clockwise	Concave	Convex
Left	Right	Clockwise	Counterclockwise	Concave	Convex
		Counterclockwise	Clockwise	Convex	Concave

			PINION	GEAR
Hand of Spiral			Right	Left
Rotation			Counterclockwise	Clockwise
Power flow			Driver	Driven
Load Face			Concave	Convex
$n, N$	Number of teeth	teeth	18	54
$n_P, n_G$	Speed	rpm	15,000.0	5,000.0
$P_{Psys}, P_{Gsys}$	Power for gear system	hp	8,659.0	8,659.0
$q$	Number of contacts per rev	contacts		1
$P_P, P_G$	Power per mesh	hp	8,659.0	8,659.0
		ft lb	3,031.9	9,095.6
$T_P, T_G$	Torque	in lb	36,382.4	109,147.3
$d_m, D_m$	Mean pitch diameter	in	5.026376	15.07913
$V_t$	Pitch line velocity	fpm		19,738.5
$W_{tP}, W_{tG}$	Tangential force	lb		14,476.6
	Axial force (concave)	lb	11,650.5	9,307.7
	Axial force (convex)	lb	-7,582.4	2,896.8
$W_x$	Axial force	lb	11,650.5	2,896.8
	Radial force (concave)	lb	2,896.8	-7,582.4
	Radial force (convex)	lb	9,307.7	11,650.5
$W_r$	Radial force	lb	2,896.8	11,650.5
$W$	Total force	lb	16,729.0	15,190.8



## Bevel Gear Geometry

Table 39: Bevel Gear Geometry

### BEVEL DESIGN INPUTS

			PINION	GEAR
$P_d$	Diametrical pitch	teeth/in		2.8611
$n, N$	Number of teeth		18	54
		degrees		90
$\Sigma$	Shaft angle	radians		1.570796
$F$	Face	in		4
		degrees		35
$\psi$	Spiral angle	radians		0.610865
		degrees		20
$\phi, \phi_n$	Standard pressure angle (normal)	radians		0.349066
	Desired $m_G$			3

### BEVEL GEAR DESIGN FORMULAS

$m_G$	Gear ratio			3
$d, D$	Pitch diameter	in	6.291287	18.87386
		degrees	18.43495	71.56505
$\gamma, \Gamma$	Pitch angle	radians	0.321751	1.249046
$A_o$	Outer cone distance	in	9.947397	
$A_m$	Mean cone distance	in	7.947397	
$k_1$	Depth factor		2	
$h$	Mean working depth	in	0.457485	
$k_2$	Clearance factor		0.125	
$c$	Clearance	in	0.057186	
$h_m$	Mean whole depth	in	0.514671	
$m_{90}$	Equivalent 90° ratio		3	
$c_1$	Mean addendum factor		0.242222	
$p_m$	Mean circular pitch	in/teeth	0.877268	
$a_P, a_G$	Mean addendum	in	0.346672	0.110813
$b_P, b_G$	Mean dedendum	in	0.167999	0.403858

Table 39: Bevel Gear Geometry (continued)

	Depth type for tooth taper		Duplex	
$\Sigma\delta_S$	Sum of dedendum angles (Standard)	degrees	4.120045	
		radians	0.071908	
$\Sigma\delta_U$	Sum of dedendum angles (Uniform)	degrees	0	
		radians	0	
$\Sigma\delta_D$	Sum of dedendum angles (Duplex)	degrees	3.14617	
		radians	0.054911	
$\Sigma\delta_T$	Sum of dedendum angles (TRL)	degrees	3.14617	
		radians	0.054911	
$\Sigma\delta$	Sum of dedendum angles	degrees	3.14617	
		radians	0.054911	
			Recommended	
$r_c$	Cutter radius (Manual)	in	4.5	
	Cutter radius (Uniform)	in	5.69805	
	Cutter radius (Duplex)	in	6.480841	
	Cutter radius	in	6.480841	
$d_{PS}, \delta_{GS}$	Dedendum angles (Standard)	degrees	1.210985	2.90906
		radians	0.021136	0.050773
$\delta_{PU}, \delta_{GU}$	Dedendum angles (Uniform)	degrees	0	0
		radians	0	0
$\delta_{PD}, \delta_{GD}$	Dedendum angles (Duplex)	degrees	0.762072	2.384098
		radians	0.013301	0.04161
$\delta_{PT}, \delta_{GT}$	Dedendum angles (TRL)	degrees	0.762072	2.384098
		radians	0.013301	0.04161
$\delta_P, \delta_G$	Dedendum angles	degrees	0.762072	2.384098
		radians	0.013301	0.04161
$\gamma_o, \Gamma_o$	Face angle	degrees	20.81905	72.32712
		radians	0.363361	1.262346
$\gamma_R, \Gamma_R$	Root angle	degrees	17.67288	69.18095
		radians	0.30845	1.207435
$a_{oP}, a_{oG}$	Outer addendum	in	0.429941	0.137416
$b_{oP}, b_{oG}$	Outer dedendum	in	0.194602	0.487126
$h_k$	Outer working depth	in	0.567357	
$h_t$	Outer whole depth	in	0.624542	
$d_o, D_o$	Outside diameter	in	7.107042	18.96077
$x_o, X_o$	Pitch cone apex to crown	in	9.300971	3.015279
$P_{dm}$	Mean diametrical pitch	teeth/in	3.581109	
$d_m, D_m$	Mean pitch diameter	in	5.026376	15.07913
$k_3$	Thickness factor		0.1136	
$t_n, T_n$	Mean normal circular thickness			
	theoretical without backlash		0.471139	0.247477
B	Outer normal backlash allowance		0.01	
	Type of cutting process		Face milling	
$\Psi_{omilling}$	Outer spiral angle (face milling)	degrees	47.37766	
		radians	0.826896	

Table 39: Bevel Gear Geometry (continued)

$N_c$	Number of crown gear teeth	teeth	56.921	
$N_s$	Number of blade groups	groups	5	
		degrees	5.062248	
$v$	Lead angle of cutter	radians	0.088353	
		degrees	60.06225	
$\lambda$	First auxiliary angle	radians	1.048284	
$S1$	Center distance: crown gear to cutl in		7.331682	
		degrees	14.9963	
$\eta_1$	Second auxiliary angle	radians	0.261735	
	Lengthwise tooth mean radius of			
$\rho$	curvature	in	6.164631	
$Q$	Intermediate variable		6.739663	
		degrees	40.62781	
$\eta_o$	Intermediate angle	radians	0.709089	
		degrees	47.75562	
$\psi_{ohobbing}$	Outer spiral angle (face hobbing)	radians	0.833493	
		degrees	47.37766	
$\psi_o$	Outer spiral angle	radians	0.826896	
$t_{nc}, T_{nc}$	Mean normal chordal thickness	in	0.466935	0.243952
$a_{cP}, a_{cG}$	Mean chordal addendum	in	0.357146	0.111134
$m_p$	Transverse contact ratio		1.190935	

## BEVEL UNDERCUT CHECK

$A_{iG}$	Inner cone distance		5.947397	
	Inner gear spiral angle (straight	degrees	0	
$\psi_{iGspiral}$	bevel)	radians	0	
	Inner gear spiral angle (face	degrees	23.95187	
$\psi_{iGmilling}$	milling)	radians	0.418039	
		degrees	57.29215	
$\eta_i$	Gear offset angle at inside	radians	0.999937	
		degrees	22.12453	
$\psi_{iGhobbing}$	Inner gear spiral angle (hobbing)	radians	0.386146	
		degrees	23.95187	
$\psi_{iG}$	Inner gear spiral angle	radians	0.418039	
		degrees	22.81897	
$\phi_{Ti}$	Inner transverse pressure angle	radians	0.398266	
$b_{iIP}$	Limit inner dedendum	in	0.298173	
$b_{iP}$	Inner dedendum	in	0.141396	

## Material Properties

**Table 40: Bevel Gear Material Selection**

### MATERIAL SELECTION

	AMS Spec	Steel TH (Grade 2)	Steel F/1H (Grade 1)	Steel F/1H (Grade 2)	Steel C-H (Grade 1)	Steel C-H (Grade 2)	Steel C-H (Grade 3)	Nitralloy 135M (Grade 2)
	Heat treatment	TH	F/1H	F/1H	C-H	C-H	C-H	Nitrided
	Main drive application	X	50	X	X	X	X	X
	Accessory application							
	High temperature application							
	Case hardness (HRC)	43	50	50	59.5	61	61	60
	Core hardness (HRC)			28	21	25	30	90
	Surface hardness (HR15N)			482	610	632	632	614
	Minimum Brinell hardness	400	482					
	Allowable contact stress							
H <sub>BP</sub> , H <sub>BG</sub>	number	175,000	175,000	190,000	200,000	225,000	250,000	145,000
S <sub>ac</sub>	Allowable bending stress number	25,180	12,500	13,500	30,000	35,000	40,000	24,000
sat	Poisson's ratio	0.300	0.300	0.300	0.300	0.300	0.300	0.291
μ <sub>P</sub> , μ <sub>G</sub>	Young's moduli of elasticity	30.00E+6	30.00E+6	30.00E+6	30.00E+6	30.00E+6	30.00E+6	30.00E+6
E <sub>P</sub> , E <sub>G</sub>	Density	0.282	0.282	0.282	0.282	0.282	0.282	0.280
ρ								

## Bending Strength Geometry Factor

Table 41: Bevel Gear Bending Strength Geometry Factor

### GEOMETRY FACTOR FOR BENDING STRENGTH (J)

		<b>J</b>	
		0.2697	0.2631
		0.1344	0.0931
		PINION	GEAR
$P_d$	Diametrical pitch	teeth/in	2.8611
$n, N$	Number of teeth	18	54
$\Sigma$	Shaft angle	degrees	90
$F$	Face	radians	1.5708
		in	4
$\psi$	Spiral angle	degrees	35
		radians	0.6109
$\phi, \phi_n$	Standard pressure angle (normal)	degrees	20
		radians	0.3491

### INPUT VARIABLES

#### C.1.3.1 INITIAL DATA

		PINION	GEAR
$A_o$	Outer cone distance	in	9.9474
$a_{oP}, a_{oG}$	Outer addendum	in	0.4299
$d, D$	Pitch diameter	in	6.2913
$n, N$	Number of teeth	18	54
$\gamma, \Gamma$	Pitch angle	degrees	18.4349
		radians	0.3218
$\gamma_o, \Gamma_o$	Face angle	degrees	20.8190
		radians	0.3634

#### C.2.4.1 INITIAL DATA

$b_{oP}, b_{oG}$	Outer dedendum	in	0.1946016	0.4871264 Table 9
$k_r$	Tool edge radii factor		0.3	0.3
$r_{TP}, r_{TG}$	Tool edge radii	in	0.1048548	0.1048548
	Mean backlash per tooth	in	0.0039947	0.0039947
	Mean normal circular thickness theoretical without backlash		0.4711387	0.2474771
$t_n, T_n$	Mean normal circular thickness with backlash	in	0.467144	0.2434824
		degrees	0.7620723	2.3840978
$\delta_P, \delta_G$	Dedendum angles	radians	0.0133007	0.0416104
$b_P, b_G$	Mean dedendum	in	0.1679987	0.4038577

Table 41: Bevel Gear Bending Strength Geometry Factor (continued)

### C.2.4.1 DETERMINATION OF POINT OF LOAD APPLICATION FOR MAX BENDING STRESS

$m_o$	Modified contact ratio		3.459168866	
$p_N$	Mean normal base pitch	in	0.6753	
$\eta$	Length of action within the contact ellipse	in	2.3011	
$f_J$	Assumed locations of critical point on tooth for bending stress	in	0	
$\eta_J$	Length of action within the contact ellipse for bending		2.301052827	
$Z_N$	Length of action in mean normal section	in	1.1335	
$\psi_b$	Mean base spiral angle	degrees	32.6146	
$k'$	Location constant	radians	0.5692	
	Load Face		0.1471	
		Concave		Convex
	Location of points of load application on path of action (straight bevel)		0.5668	
	Location of points of load application on path of action (concave)		0.7229	
	Location of points of load application on path of action (convex)		0.4106	
$p_{3P}, p_{3G}$	Location of points of load application on path of action	in	0.7229	0.4106
	Factors used for calcs (straight)		0.289765129	
	Factors used for calcs (concave)		0.205586789	
	Factors used for calcs (convex)		0.205586789	
$x_o''_P, x_o''_G$	Factors used for pinion/gear calcs		0.2055868	0.2055868
$r_N, R_N$	Mean normal pitch radius	in	3.9480	35.5318
$\Sigma R_N$	Sum of mean normal pitch radii	in	39.4798	
$r_{bN}, R_{bN}$	Mean normal base radius	in	3.7099	33.3890
$r_{oN}, R_{oN}$	Mean normal outside radius	in	4.2946	35.6426
$\phi_{LP}, \phi_{LG}$	Normal pressure angles at point of load application	degrees	27.0725	20.1630
		radians	0.4725	0.3519
$\theta_{hP}, \theta_{hG}$	Rotation angles used in bending strength calcs	degrees	2.0312	0.1745
		radians	0.0355	0.0030
$\phi_{hP}, \phi_{hG}$		degrees	25.0413	19.9885
		radians	0.4371	0.3489
$\Delta r_N, \Delta R_N$	Distance from pitch circle to point of load application on tooth centerline	in	0.1468	-0.0026
$r, R$	Mean transverse pitch radius	in	2.6491	23.8422
$A_m$	Mean cone distance	in	7.9474	
$r_t, R_t$	Mean transverse radius to point of load application	in	2.8645	24.4564

Table 41: Bevel Gear Bending Strength Geometry Factor (continued)

### C.2.4.5 TOOTH FILLET RADIUS AT ROOT CIRCLE

$r_{fP}, r_{fG}$	Fillet radius at root of tooth	in	0.1058	0.1073
------------------	--------------------------------	----	--------	--------

### C.2.4.6 TOOTH FORM FACTOR

$Y_P, Y_G$	Tooth form factors excluding stress concentration factors		0.587038	0.3530
$t_{NP}, t_{NG}$	One-half tooth thickness at critical section		0.2661	0.2345
$h_{NP}, h_{NG}$	Load heights from critical section		0.2716	0.3254

### C.2.4.7 STRESS CONCENTRATION AND STRESS CORRECTION FACTORS

H	Empirical exponent		0.1800	
L	Empirical exponent		0.1500	
M	Empirical exponent		0.4500	
$K_{fP}, K_{fG}$	Stress concentration and stress correction factors		1.9047	1.6504

### C.2.4.8 TOOTH FORM FACTOR

$Y_{KP}, Y_{KG}$	Tooth form factor		0.3082	0.2139
------------------	-------------------	--	--------	--------

### C.2.4.9 LOAD SHARING RATIO

$f_J$	Assumed locations of critical point on tooth for bending stress	in	0.000000	
$\eta_J$	Length of action within the contact ellipse for bending		1.133500	
$p_N$	Mean normal base pitch	in	0.675278	
	Term A (k=1)		0	
	Term A (k=2)		0	
	Term B (k=1)		0	
	Term B (k=2)		0	
$\eta_J^3$			1.4563	
$m_{NJ}$	Load sharing ratio		1.0000	

### C.2.4.10 INERTIA FACTOR

$C_i$	Inertia factor for pitting resistance		1	
$K_i$	Inertia factor for bending strength		1	

Table 41: Bevel Gear Bending Strength Geometry Factor (continued)

### C.2.4.11 EFFECTIVE FACE WIDTH

$F_K$	Projected length of instantaneous line of contact in the lengthwise direction of the tooth		1.397990168
$\Delta F'_{TP}, \Delta F'_{TG}$	Toe increment	1.8392089	1.8392089
$\Delta F'_{HP}, \Delta F'_{HG}$	Heel increment	1.3372586	1.3372586
$\Delta F_{TP}, \Delta F_{TG}$		1.8392089	1.8392089
$\Delta F_{HP}, \Delta F_{HG}$		1.3372586	1.3372586
$F_{eP}, F_{eG}$	Effective face width	2.0197304	2.125104

### C.2.4 FORMULA FOR GEOMETRY FACTOR J

$Y_{KP}, Y_{KG}$	Tooth form factor		0.3082	0.2139
$m_{NJ}$	Load sharing ratio		1.0000	
$K_i$	Inertia factor for bending strength		1	
$r_t, R_t$	Mean transverse radius to point of load application	in	2.8645	24.4564
$r, R$	Mean transverse pitch radius	in	2.6491	23.8422
$F_{eP}, F_{eG}$	Effective face width		2.0197304	2.125104
$F$	Face width			4
$P_d$	Diametrical pitch	teeth/in		2.8611
$P_m$	Mean transverse diametrical pitch	in <sup>-1</sup>		3.5811



Table 41: Bevel Gear Bending Strength Geometry Factor (continued)

## REGRESSION WORK

n, N	Number of teeth		18		54
		degrees		90	
$\Sigma$	Shaft angle	radians		1.5708	
		degrees		35	
$\psi$	Spiral angle	radians		0.6109	
		degrees		20	
$\phi, \phi_n$	Standard pressure angle (normal)	radians		0.3491	
		Nmate	Ngear	Nmate	Ngear
		54	18	18	54
Straight Bevel ( $\psi=0, \phi=20, \Sigma=90$ ) Nmate $\leq$ 50		0.2632		0.1939	
Straight Bevel ( $\psi=0, \phi=20, \Sigma=90$ ) 50<Nmate<60		0.2532		0.2110	
Straight Bevel ( $\psi=0, \phi=20, \Sigma=90$ ) Nmate>60		0.2382		0.2366	
Straight Bevel ( $\psi=0, \phi=20, \Sigma=90$ ) Selected		0.2532		0.1939	
Straight Bevel ( $\psi=0, \phi=25, \Sigma=90$ ) Nmate $\leq$ 50		0.2546		0.2174	
Straight Bevel ( $\psi=0, \phi=25, \Sigma=90$ ) 50<Nmate<60		0.2486		0.1280	
Straight Bevel ( $\psi=0, \phi=25, \Sigma=90$ ) Nmate>60		0.2397		0.2454	
Straight Bevel ( $\psi=0, \phi=25, \Sigma=90$ ) Selected		0.2486		0.2174	
Straight Bevel ( $\psi=0, \phi=20$ to 25, $\Sigma=90$ ) Selected		0.2532		0.1939	
			$\psi$		
			35		
Spiral Bevel ( $\psi=15,25,35, \phi=20, \Sigma=90$ )		0.2697		0.2631	
Straight/Spiral for $\Sigma=90$		0.2697		0.2631	
Spiral Bevel ( $\psi=35, \phi=20, \Sigma=60$ )		0.2824		0.2777	
Spiral Bevel ( $\psi=35, \phi=20, \Sigma=60-90$ )		0.2697		0.2631	
Spiral Bevel ( $\psi=35, \phi=20, \Sigma=90$ )		0.2697		0.2631	
Spiral Bevel ( $\psi=35, \phi=20, \Sigma=60-90$ ) Selected		0.2697		0.2631	
Selected J		0.2697		0.2631	

## Pitting Resistance Geometry Factor

Table 42: Bevel Gear Pitting Resistance Geometry Factor

### GEOMETRY FACTOR FOR PITTING RESISTANCE (I)

			I	0.1187
$P_d$	Diametrical pitch	teeth/in		2.8611
$n, N$	Number of teeth		18	54
		degrees		90
$\Sigma$	Shaft angle	radians		1.5708
$F$	Face	in		4
		degrees		35
$\psi$	Spiral angle	radians		0.6109
		degrees		20
$\phi, \phi_n$	Standard pressure angle (normal)	radians		0.3491
	$f_{\text{manual}}$			-0.208532912

### INITIAL DATA

			PINION	GEAR
$A_o$	Outer cone distance	in		9.947397484
$a_{oP}, a_{oG}$	Outer addendum	in	0.4299	0.1374
$d, D$	Pitch diameter	in	6.2913	18.8739
$n, N$	Number of teeth		18	54
		degrees	18.4349	71.5651
$\gamma, \Gamma$	Pitch angle	radians	0.3218	1.2490
		degrees	20.8190	72.3271
$\gamma_o, \Gamma_o$	Face angle	radians	0.3634	1.2623

### INITIAL FORMULAS

$A_m$	Mean cone distance	in		7.9474
		degrees	2.3841	0.7621
$\alpha_P, \alpha_G$	Addendum angle	radians	0.0416	0.0133
$a_P, a_G$	Mean addendum	in	0.3467	0.1108
$k'$	Location constant			0.1471
$P_m$	Mean transverse diametrical pitch	$\text{in}^{-1}$		3.5811
$p$	Outer transverse circular pitch	in		1.0980
$p_N$	Mean normal base pitch	in		0.6753
$p_n$	Mean normal circular pitch	in		0.7186
$p_2$	Auxiliary pitch	in		0.9518

Table 42: Bevel Gear Pitting Resistance Geometry Factor (continued)

$r, R$	Mean transverse pitch radius	in	2.6491	23.8422
$r_N, R_N$	Mean normal pitch radius	in	3.9480	35.5318
$r_{bN}, R_{bN}$	Mean normal base radius	in	3.7099	33.3890
$r_{oN}, R_{oN}$	Mean normal outside radius	in	4.2946	35.6426
$Z'_P, Z'_G$	Length of mean normal addendum	in	0.8132	0.3203
$Z_N$	Length of action in mean normal section	in		1.1335
$m_p$	Transverse contact ratio			1.1909
$K_Z$	Intermediate variable			0.5373
$m_F$	Face contact ratio			3.2477
$m_o$	Modified contact ratio			3.4592
$\psi_b$	Mean base spiral angle	degrees		32.6146
	Length of action within the contact	radians		0.5692
$\eta$	ellipse	in		2.3011
$\rho_P, \rho_G$	curvature at pitch circle	in	1.2770	11.4934

DETERMINATION OF PROFILE RADIUS OF CURVATURE AT CRITICAL POINT

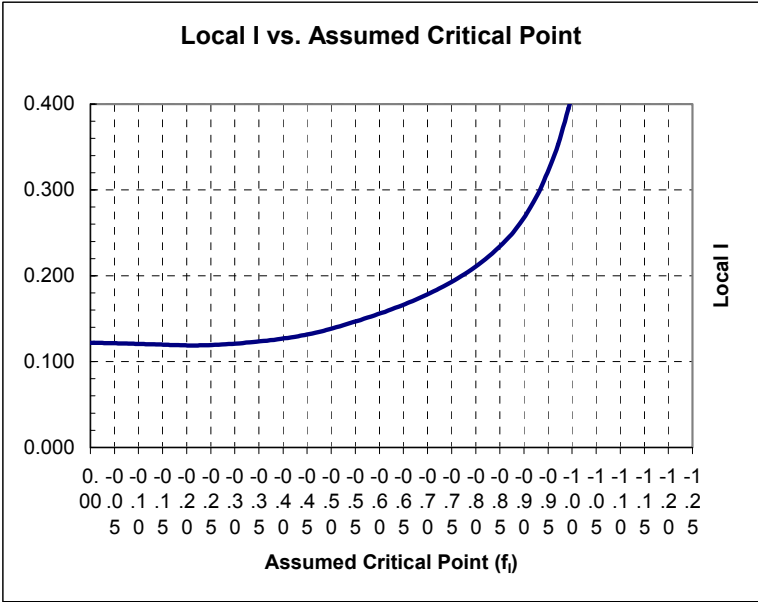


Table 42: Bevel Gear Pitting Resistance Geometry Factor (continued)

$C_i$	Inertial factor			1.0000
$f_l$	Assumed location of critical point on tooth (straight bevel)	in		-0.208532912
$\eta_l$	Local length of action within the contact ellipse (straight bevel)	in		2.2629
$z_o$	Distance along path of action in mean normal section from pitch line to point of maximum stress contact (straight bevel)	in		0.3642
$\rho_1, \rho_2$	Profile radius of curvature at point $f_l$ (straight bevel)	in	1.6412	
$\rho_o$	Relative radius of profile curvature (in Length of line of contact (straight bevel)	in		1.4303
$s$		in		1.6322
Term 1k1	Intermediate value (straight bevel)			9.3034
Term 1k2	Intermediate value (straight bevel)			0.0218
Term 2k1	Intermediate value (straight bevel)			3.1974
$\eta'_l{}^3$	Cube of local $\eta_l$ (straight bevel)			24.1108
$m_{Ni}$	Load sharing ratio (straight bevel)			0.4806
$I$	Geometry Factor (straight bevel)			0.1187
$I$	Geometry Factor (spiral bevel)			0.1187

## **APPENDIX C: SHAFT DESIGN CALCULATIONS**

## Summary of Results

**Table 43: Shafting Summary of Results**

### SHAFTING SUMMARY OF RESULTS

SHAFT_D	D	Outside diameter	in	8.55
SHAFT_di	d	Inside diameter	in	7.70
SHAFT_fb	$f_b$	Vibratory bending stress	psi	12275.73
SHAFT_nb	$n_b$	Bending factor of safety		1.16
SHAFT_Fts	$f_s$	Torsional shear stress	psi	10,023.6
SHAFT_nts	$n_s$	Torsional shear factor of safety		3.92
SHAFT_fa	$f_a$	Axial tension stress	psi	0.00
SHAFT_na	$n_a$	Axial tension factor of safety		0.00
SHAFT_W	$W_{\text{shaft}}$	Shaft weight	lb	14.98
SHAFT_MS	MS	Margin of Safety		1.00
<b>PASS</b>				
		Type of Shaft Analysis		0
SHAFT_n	n	Shaft speed	rpm	476.3
SHAFT_Nc	$N_c$	Critical speed	rpm	278,752.2
SHAFT_Ncsub	$N_{\text{sub}}$	Subcritical avoid speed	rpm	195,126.5
SHAFT_Ncsup	$N_{\text{sup}}$	Supercritical avoid speed	rpm	306,627.4
SHAFT_Type		Type of operation		0
SHAFT_Critical	<b>ACCEPTABLE SUBCRITICAL SPEED</b>			
SHAFT_Mmax	$M_{\text{max}}$	Maximum moment	lb in	259,285.7
SHAFT_T	T	Shaft torque	in lb	423,433.0
SHAFT_Fx	$F_x$	Shaft axial force	lb	0.0

## User Inputs and Selections

**Table 44: Shafting User Inputs and Selections**

### USER INPUTS AND SELECTIONS

SHAFT_DA	D <sub>A</sub>	Pitch diameter of gear A	in	10.00
SHAFT_DB	D <sub>B</sub>	Pitch diameter of gear B	in	10.00
SHAFT_nmin	n <sub>min</sub>	Minimum Margin of Safety		1.00
SHAFT_Kfb	K <sub>fb</sub>	Stress factor for bending		1.00
SHAFT_Kfs	K <sub>fs</sub>	Stress factor for sheer		1.00
SHAFT_Material				4
		Material Selected (see Database)		Aluminum Alloy T7075
SHAFT_Analysis				1
		Type of Shaft Analysis		Uniform shaft
SHAFT_Solid		Solid Shafting		0
				Hollow shaft
SHAFT_Wgear	W <sub>gear</sub>	Weight of gears	lb	0
SHAFT_n	n	Shaft speed	rpm	476.3
	ρ	Density	slugs/in <sup>3</sup>	0.283
	E	Modulus of Elasticity	psi	30.0E+6
SHAFT_MomentType		Type of Moment Diagram		1
SHAFT_FyA	F <sub>yA</sub>	Force of Gear A	lb	0.0
SHAFT_FyB	F <sub>yB</sub>	Force of Gear B	lb	0.0
SHAFT_FzA	F <sub>zA</sub>	Force of Gear A	lb	110,000.0
SHAFT_FzB	F <sub>zB</sub>	Force of Gear B	lb	0.0
SHAFT_xA	F <sub>xA</sub>	Axial Force	lb	0.0
SHAFT_xB	F <sub>xB</sub>	Axial Force	lb	0.0
SHAFT_Delta1	Δx <sub>1</sub>	Distance between members	in	3
SHAFT_Delta2	Δx <sub>2</sub>	Distance between members	in	11
SHAFT_Delta3	Δx <sub>3</sub>	Distance between members	in	0
SHAFT_TQ_A	T <sub>A</sub>	Torque at Gear A	in lb	423,433.0
SHAFT_TQ_B	T <sub>A</sub>	Torque at Gear B	in lb	
SHAFT_MRhp		Main Rotor HP		14,000.0

## Margin of Safety

Table 45: Shafting Margin of Safety Calculations

### SUMMARY FOR MARGIN OF SAFETY

D	Outside diameter	in	8.55
d	Inside diameter	in	7.70
$f_b$	Vibratory bending stress	psi	12,275.7
$n_b$	Bending factor of safety		1.16
$f_s$	Torsional shear stress	psi	10,023.6
$n_s$	Torsional shear factor of safety		3.9
$f_a$	Axial tension stress	psi	0.0
$n_a$	Axial tension factor of safety		0.0
$W_{\text{shaft}}$	Shaft weight	lb	14.98
n	Margin of Safety		1.00

PASS

### GEOMETRY LIMITS

D	Outside diameter	in	8.55
d	Inside diameter	in	7.70
$D_A$	Pitch diameter of gear A	in	10.00
$D_B$	Pitch diameter of gear B	in	10.00
$D_{\text{max}}$	Max permitted outside diameter	in	9.00
$D_{\text{min}}$	Min permitted outside diameter	in	0.50
$d_{\text{max}}$	Max permitted inside diameter	in	8.10
$d_{\text{min}}$	Min permitted inside diameter	in	0.00
$n_{\text{min}}$	Minimum Margin of Safety		1.00

### BENDING STRESS

$K_{fb}$	Stress factor for bending		1.00
$M_{\text{max}}$	Maximum moment	lb in	259,285.7
$f_b$	Vibratory bending stress	psi	12,275.7
$n_b$	Bending factor of safety		1.16



Table 45: Shafting Margin of Safety Calculations (continued)

## TORSIONAL SHEAR STRESS

$K_{fs}$	Stress factor for sheer		1.00
$T$	Shaft torque	in lb	423,433.0
$f_s$	Torsional shear stress	psi	10,023.6
$n_s$	Torsional shear factor of safety		3.92

## AXIAL TENSION STRESS

$F_x$	Axial force	lb	0.0
$f_a$	Axial tension stress	lb	0.0
$n_a$	Axial tension factor of safety	psi	0.00

## ALLOWABLE STRESSES

	Material Selected (see Database)		4
$S_{ut}$	Ultimate tensile strength	psi	86,000
$S_y$	Yield tensile strength	psi	78,600
$F_{ty}$	Tensile yield strength	psi	78,600
$F_{sy}$	Shear yield stress	psi	39,300
$F_{en}$	Endurance limit	psi	14,280

## Critical Speed (Uniform Shaft)

**Table 46: Shafting Critical Speed Calculations (Uniform Shaft)**

### CRITICAL SPEED SUMMARY

Type of Shaft Analysis			Uniform shaft
n	Shaft speed	rpm	476.3
N <sub>c</sub>	Critical speed	rpm	278,752.2
N <sub>sub</sub>	Subcritical avoid speed	rpm	195,126.5
N <sub>sup</sub>	Supercritical avoid speed	rpm	306,627.4
Type of operation		SUBCRITICAL	
ACCEPTABLE SUBCRITICAL SPEED			

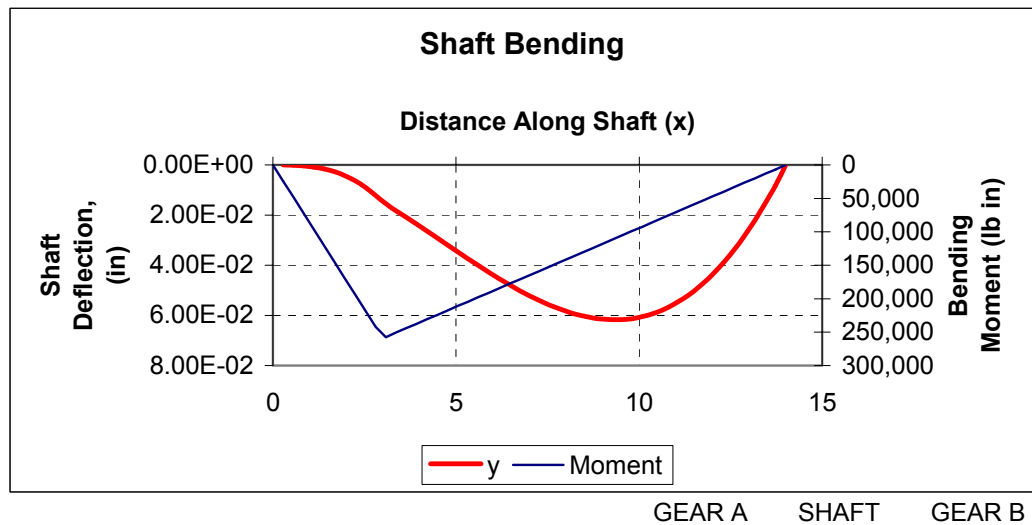


Table 46: Shafting Critical Speed Calculations (Uniform Shaft) (continued)

## GEOMETRY & PROPERTIES

L	Shaft length	in	14
D	Outside diameter	in	8.55
d	Inside diameter	in	7.70
I	Cross sectional moment of inertia	in <sup>4</sup>	90.32
M <sub>max</sub>	Maximum moment	lb in	259,285.7
m	Mass	slugs	20,232.5
W <sub>gear</sub>	Weight of gears	lb	0 1,982.8 0
n	Shaft speed	rpm	476.3
ω	Shaft speed	rad/s	49.9

## MATERIAL PROPERTIES

ρ	Density	slugs/in <sup>3</sup>	0.098
E	Modulus of Elasticity	psi	10.3E+6

## NUMERICAL ITERATION SETUP

p	Number of iteration points	50
dx	Change along x	in 0.28
d <sub>w</sub>	Segmented change in shaft weight	lb 39.66

## RAYLEIGH'S ENERGY METHOD

g	Gravity constant	in/sec <sup>2</sup>	386.4
T <sub>part</sub>	Intermediate value	lb in <sup>2</sup>	3.27E+00
V <sub>part</sub>	Intermediate value	lb in	6.82E+01
T	Kinetic energy	in lb	10.54
V	Potential energy	in lb	34.08
N <sub>c</sub>	Critical speed	rpm	856.49

## UNIFORM SHAFT METHOD

N <sub>c</sub>	Critical Speed for uniform shaft	rpm	278,752.2
N <sub>c</sub>	Critical Speed for uniform shaft (thin wall)	rpm	278,366.9

## Critical Speed (Nonuniform Shaft)

**Table 47: Shafting Critical Speed Calculations (Nonuniform Shaft)**

### CRITICAL SPEED SUMMARY

	Type of Shaft Analysis		Nonuniform shaft
n	Shaft speed	rpm	476.3
N <sub>c</sub>	Critical speed	rpm	856.5
N <sub>sub</sub>	Subcritical avoid speed	rpm	599.5
N <sub>sup</sub>	Supercritical avoid speed	rpm	942.1
	Type of operation	SUBCRITICAL	

**ACCEPTABLE SUBCRITICAL SPEED**

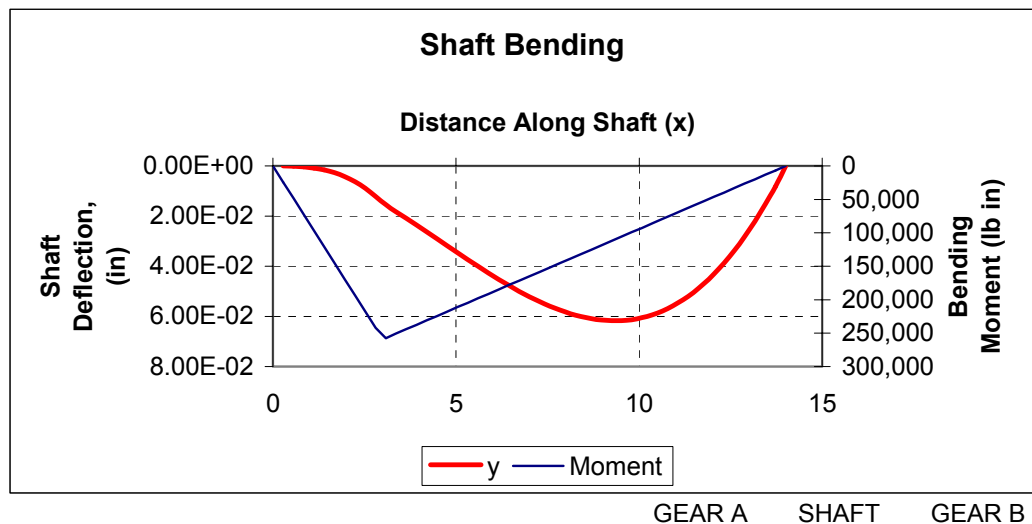


Table 47: Shafting Critical Speed Calculations (Nonuniform Shaft) (continued)

## GEOMETRY & PROPERTIES

L	Shaft length	in	14
D	Outside diameter	in	8.55
d	Inside diameter	in	7.70
I	Cross sectional moment of inertia	in <sup>4</sup>	90.32
M <sub>max</sub>	Maximum moment	lb in	259,285.7
m	Mass	slugs	20,232.5
W <sub>gear</sub>	Weight of gears	lb	0 1,982.8 0
n	Shaft speed	rpm	476.3
ω	Shaft speed	rad/s	49.9

## MATERIAL PROPERTIES

ρ	Density	slugs/in <sup>3</sup>	0.098
E	Modulus of Elasticity	psi	10.3E+6

## NUMERICAL ITERATION SETUP

p	Number of iteration points		50
dx	Change along x	in	0.28
d <sub>w</sub>	Segmented change in shaft weight	lb	39.66

## RAYLEIGH'S ENERGY METHOD

g	Gravity constant	in/sec <sup>2</sup>	386.4
T part	Intermediate value	lb in <sup>2</sup>	3.27E+00
V part	Intermediate value	lb in	6.82E+01
T	Kinetic energy	in lb	10.54
V	Potential energy	in lb	34.08
N <sub>c</sub>	Critical speed	rpm	856.49

## UNIFORM SHAFT METHOD

N <sub>c</sub>	Critical Speed for uniform shaft	rpm	278,752.2
N <sub>c</sub>	Critical Speed for uniform shaft (thin wall)	rpm	278,366.9

Table 47: Shafting Critical Speed Calculations (Nonuniform Shaft) (continued)

**LOADING FOR Mz**

	BEARING		GEAR		BEARING		
	R1	Dx1	A	Dx2	R2		
x		0		3		14	14
Dx			3		11		0
F		0		0		0	0
Mz		0		0		0	0
T		0		423433		0	0

**LOADING FOR My**

	BEARING		GEAR		BEARING		
	R1	Dx1	A	Dx2	R2		
x		0		3		14	14
Dx			3		11		0
F		-86428.57		110000		-23571.43	0
My		0		-259285.7		0	0
T		0		423433		0	0
Mmax		0		259,286		0	0
slope			3		11		0
xA	FALSE	FALSE	86428.57		-23571.43	#DIV/0!	FALSE
xB	FALSE	FALSE	FALSE	3	FALSE	FALSE	FALSE
	FALSE	FALSE	FALSE	FALSE	FALSE	FALSE	FALSE

Table 47: Shafting Critical Speed Calculations (Nonuniform Shaft) (continued)

	dx	x	M	C	y'	y	w of gears	wi	Ti part	Vi
		0	0		0	0.00	0			
1	0.28	0.28	24,200	2.60E-05	7.28E-06	1.63E-05	0	39.66	1.06E-08	6.47E-04
2	0.28	0.56	48,400	5.20E-05	2.91E-05	1.06E-04	0	39.66	4.46E-07	4.21E-03
3	0.28	0.84	72,600	7.80E-05	6.56E-05	3.43E-04	0	39.66	4.65E-06	1.36E-02
4	0.28	1.12	96,800	1.04E-04	1.17E-04	7.99E-04	0	39.66	2.53E-05	3.17E-02
5	0.28	1.4	121,000	1.30E-04	1.82E-04	1.55E-03	0	39.66	9.53E-05	6.15E-02
6	0.28	1.68	145,200	1.56E-04	2.62E-04	2.67E-03	0	39.66	2.82E-04	1.06E-01
7	0.28	1.96	169,400	1.82E-04	3.57E-04	4.23E-03	0	39.66	7.08E-04	1.68E-01
8	0.28	2.24	193,600	2.08E-04	4.66E-04	6.30E-03	0	39.66	1.57E-03	2.50E-01
9	0.28	2.52	217,800	2.34E-04	5.90E-04	8.95E-03	0	39.66	3.17E-03	3.55E-01
10	0.28	2.8	242,000	2.60E-04	7.24E-04	1.21E-02	0	39.66	5.82E-03	4.80E-01
11	0.28	3.08	257,400	2.77E-04	8.40E-04	1.54E-02	0	39.66	9.37E-03	6.09E-01
12	0.28	3.36	250,800	2.70E-04	9.06E-04	1.82E-02	0	39.66	1.31E-02	7.22E-01
13	0.28	3.64	244,200	2.62E-04	9.55E-04	2.09E-02	0	39.66	1.72E-02	8.27E-01
14	0.28	3.92	237,600	2.55E-04	1.00E-03	2.35E-02	0	39.66	2.20E-02	9.33E-01
15	0.28	4.2	231,000	2.48E-04	1.04E-03	2.63E-02	0	39.66	2.74E-02	1.04E+00
16	0.28	4.48	224,400	2.41E-04	1.08E-03	2.90E-02	0	39.66	3.34E-02	1.15E+00
17	0.28	4.76	217,800	2.34E-04	1.11E-03	3.18E-02	0	39.66	4.01E-02	1.26E+00
18	0.28	5.04	211,200	2.27E-04	1.14E-03	3.46E-02	0	39.66	4.74E-02	1.37E+00
19	0.28	5.32	204,600	2.20E-04	1.17E-03	3.73E-02	0	39.66	5.52E-02	1.48E+00
20	0.28	5.6	198,000	2.13E-04	1.19E-03	4.00E-02	0	39.66	6.35E-02	1.59E+00
21	0.28	5.88	191,400	2.06E-04	1.21E-03	4.27E-02	0	39.66	7.22E-02	1.69E+00
22	0.28	6.16	184,800	1.99E-04	1.22E-03	4.52E-02	0	39.66	8.10E-02	1.79E+00
23	0.28	6.44	178,200	1.92E-04	1.23E-03	4.76E-02	0	39.66	9.00E-02	1.89E+00
24	0.28	6.72	171,600	1.84E-04	1.24E-03	5.00E-02	0	39.66	9.89E-02	1.98E+00
25	0.28	7	165,000	1.77E-04	1.24E-03	5.21E-02	0	39.66	1.08E-01	2.07E+00

Table 47: Shafting Critical Speed Calculations (Nonuniform Shaft) (continued)

26	0.28	7.28	158,400	1.70E-04	1.24E-03	5.41E-02	0	39.66	1.16E-01	2.15E+00
27	0.28	7.56	151,800	1.63E-04	1.23E-03	5.59E-02	0	39.66	1.24E-01	2.22E+00
28	0.28	7.84	145,200	1.56E-04	1.22E-03	5.75E-02	0	39.66	1.31E-01	2.28E+00
29	0.28	8.12	138,600	1.49E-04	1.21E-03	5.89E-02	0	39.66	1.38E-01	2.34E+00
30	0.28	8.4	132,000	1.42E-04	1.19E-03	6.00E-02	0	39.66	1.43E-01	2.38E+00
31	0.28	8.68	125,400	1.35E-04	1.17E-03	6.09E-02	0	39.66	1.47E-01	2.41E+00
32	0.28	8.96	118,800	1.28E-04	1.14E-03	6.15E-02	0	39.66	1.50E-01	2.44E+00
33	0.28	9.24	112,200	1.21E-04	1.11E-03	6.17E-02	0	39.66	1.51E-01	2.45E+00
34	0.28	9.52	105,600	1.14E-04	1.08E-03	6.17E-02	0	39.66	1.51E-01	2.45E+00
35	0.28	9.8	99,000	1.06E-04	1.04E-03	6.13E-02	0	39.66	1.49E-01	2.43E+00
36	0.28	10.08	92,400	9.93E-05	1.00E-03	6.05E-02	0	39.66	1.45E-01	2.40E+00
37	0.28	10.36	85,800	9.22E-05	9.55E-04	5.93E-02	0	39.66	1.40E-01	2.35E+00
38	0.28	10.64	79,200	8.51E-05	9.06E-04	5.78E-02	0	39.66	1.32E-01	2.29E+00
39	0.28	10.92	72,600	7.80E-05	8.52E-04	5.58E-02	0	39.66	1.23E-01	2.21E+00
40	0.28	11.2	66,000	7.09E-05	7.95E-04	5.33E-02	0	39.66	1.13E-01	2.12E+00
41	0.28	11.48	59,400	6.38E-05	7.33E-04	5.04E-02	0	39.66	1.01E-01	2.00E+00
42	0.28	11.76	52,800	5.68E-05	6.67E-04	4.70E-02	0	39.66	8.78E-02	1.87E+00
43	0.28	12.04	46,200	4.97E-05	5.98E-04	4.31E-02	0	39.66	7.38E-02	1.71E+00
44	0.28	12.32	39,600	4.26E-05	5.24E-04	3.87E-02	0	39.66	5.94E-02	1.54E+00
45	0.28	12.6	33,000	3.55E-05	4.47E-04	3.37E-02	0	39.66	4.51E-02	1.34E+00
46	0.28	12.88	26,400	2.84E-05	3.65E-04	2.82E-02	0	39.66	3.15E-02	1.12E+00
47	0.28	13.16	19,800	2.13E-05	2.80E-04	2.21E-02	0	39.66	1.93E-02	8.75E-01
48	0.28	13.44	13,200	1.42E-05	1.91E-04	1.53E-02	0	39.66	9.31E-03	6.08E-01
49	0.28	13.72	6,600	7.09E-06	9.73E-05	8.19E-03	0	39.66	2.66E-03	3.25E-01
50	0.28	14	0	0.00E+00	1.66E-05	0.00E+00	0	39.66	0.00E+00	0.00E+00
	0		0	0.00E+00	0.00E+00	0.00E+00	0	39.66	0.00E+00	0.00E+00
T total									3.27E+00	
V total										6.82E+01



## Total Load and Moments

Table 48: Shafting Total Load and Moments Calculations

### TOTAL LOAD AND MOMENTS

	Type of Moment Diagram		Loading Selection		
			<b>1</b>	<b>BGB</b>	<b>1</b>
F <sub>yA</sub>	Force of Gear A	lb	2	BGBG	0.0
F <sub>yB</sub>	Force of Gear B	lb	3	GBGB	0.0
F <sub>zA</sub>	Force of Gear A	lb	4	GBBG	110,000.0
F <sub>zB</sub>	Force of Gear B	lb	<b>5</b>	<b>BGGB</b>	0.0
F <sub>xA</sub>	Axial Force	lb			0.0
F <sub>xB</sub>	Axial Force	lb			0.0
Δx <sub>1</sub>	Distance between members	in			3
Δx <sub>2</sub>	Distance between members	in			11
Δx <sub>3</sub>	Distance between members	in			0
T <sub>A</sub>	Torque at Gear A	in lb			423,433.0
T <sub>B</sub>	Torque at Gear B	in lb			-423,433.0
M <sub>max</sub>	Maximum moment	lb in			259,285.7
T	Shaft torque	in lb			423,433.0
F <sub>x</sub>	Shaft axial force				0

### LOADING FOR M<sub>z</sub>

	BEARING		GEAR		BEARING	
	R1	Dx1	A	Dx2	R2	
x	0		3		14	14
Dx		3		11		0
F	0		0		0	0
Mz	0		0		0	0
T	0		423433		0	0

### LOADING FOR M<sub>y</sub>

	BEARING		GEAR		BEARING	
	R1	Dx1	A	Dx2	R2	
x	0		3		14	14
Dx		3		11		0
F	-86428.57		110000		-23571.43	0
My	0		-259285.7		0	0
T	0		423433		0	0

M <sub>max</sub>	0		259285.7		0	0
------------------	---	--	----------	--	---	---

## Material Properties

Table 49: Shafting Material Properties Database

### MATERIAL DATABASE

			GEAR	SHAFT	GEAR		
			Aluminum Alloy T7075				
$S_{ut}$	Ultimate tensile strength	psi		86,000			
$S_y$	Yield tensile strength	psi		78,600			
$F_{sy}$	Shear yield stress	psi		39,300			
$S_{en}$	Endurance strength	psi		20,000			
$F_{en}$	Endurance limit	psi		14,280			
$k_a$	Surface factor			1.00			
$k_b$	Size factor			0.70			
$k_c$	Load factor			1.00			
$k_d$	Temperature factor			1.02			
$k_e$	Miscellaneous effects			1.00			
$k$	Total endurance factor			0.71			
$\rho$	Density (weight)	lb/in <sup>3</sup>		0.098			
$E$	Modulus of Elasticity	psi		10.3E+6			
			General Alluminum alloy	Aluminum Alloy 2011	Aluminum Alloy T7075	Steel AISI 4340	Titanium Forging (6 A1-4V)
$S_{ut}$	Ultimate tensile strength			47,000	86,000	250,000	135,821
$S_y$	Yield tensile strength			24,500	78,600	230,000	122,642
$F_{sy}$	Shear yield stress	0	0	12,250	39,300	115,000	61,321
$S_{en}$	Endurance strength	0	20,000	20,000	20,000	100,000	20,000
$F_{en}$	Endurance limit	0	14,280	14,280	14,280	71,400	14,280
$k_a$	Surface factor	1.00	1.00	1.00	1.00	1.00	1.00
$k_b$	Size factor	0.70	0.70	0.70	0.70	0.70	0.70
$k_c$	Load factor	1.00	1.00	1.00	1.00	1.00	1.00
$k_d$	Temperature factor	1.02	1.02	1.02	1.02	1.02	1.02
$k_e$	Miscellaneous effects	1.00	1.00	1.00	1.00	1.00	1.00
$k$	Total endurance factor	0.71	0.71	0.71	0.71	0.71	0.71
$\rho$	Density (weight)	0.283	0.098	0.098	0.098	0.283	0.161
$E$	Modulus of Elasticity	30.0E+6	10.3E+6	10.3E+6	10.3E+6	30.0E+6	15.5E+6

## **APPENDIX D: PLANETARY DRIVE CALCULATIONS**

## Design Calculations

**Table 50: Planetary Design Calculations**

### **JHL PLANETRARY XMNS DESIGN V3.5**

#### **PERFORMANCE FACTORS**

##### **POWER PLANT**

NASA High-Tech Engine

	Number of Engines		
HPeng_	Drive System Rated Power	8,773	8,804
	Maximum Continuous Power (MCP)	8,773	8,773
	Intermediate Rated Power (IRP)	10,397	10,397
HPeng_MRP	Maximum Rated Power (MRP)	11,130	11,130
	Contingency Power (CP)	11,512	11,512
RPMeng	Engine High Speed Output Shaft Speed	15,000	rpm

##### **MAIN ROTOR**

	Tip Speed	725 ft/s
MRdiam	Diameter	120.4 ft
MRrpm	Rotor System Speed (100% Speed)	115.0 rpm
MRPowerReq	Main Rotor Power Required	22,247.0 hp
		19346

##### **EFFICIENCY**

HP <sub>n</sub>	26,350.6 hp
Main Rotor	22,247.0 hp
Tail Rotor	3,200.0 hp
Accessories (all 3)	120.0 hp
Oil Cooler	40.0 hp
HP <sub>useable</sub>	25,607.0 hp
HP <sub>Loss</sub>	743.6 hp
Efficiency	97.18%

##### **TAIL ROTOR**

	Tip Speed	725 ft/s
TRdiam	Diameter	29.1 ft
TRrpm	Tail Rotor System Speed (100% Speed)	476.3 rpm
TRPowerReq	Tail Rotor Power Required	1,989.0 hp

HP<sub>Loss</sub>  
Efficiency

**EFFICIENCY 97.18%**

##### **OVERALL SPEEDS**

Engine High Speed Output Shaft Speed	15,000.0 rpm
Engine Gearbox Output Speed	5,587.7 rpm
Main Rotor Drive Shaft Speed	115.0 rpm
Tail Takeoff Drive Shaft Speed	2,264.5 rpm
Intermediate Tail Drive Shaft Speed	1,421.3 rpm
Tail Rotor Drive Shaft Speed	476.3 rpm

AccessPower	Accessory Takeoff Power	40.0 hp
OCPower	Oil Cooler HP	40.0 hp
OCRPM	Oil Cooler speed	2,000.0 rpm
AccessRPM	Accessory Speed	1,000.0 rpm
Nplanets1	Nplanets1	5.88
Nplanets2	Nplanets2	10.92
	Freewheeling Clutch	99.50%
	Spur or Helical Gear	99.50%
	Bevel Gear	99.50%
	Planetary Stage	99.25%

##### **OVERALL REDUCTION RATIOS**

ENGINE INPUT GEARBOX REDUX		
EngGBRedux	Engine Gearbox Reduction Ratio	2.684
	Bevel Accessory Takeoff	5.588
MAIN GEAR BOX REDUX		
		48.589
	Crown Bevel	4.859
Stage1Redux	1st Stage Reduction	3.744
Stage2Redux	2d Stage Reduction	2.671
	Overall Reduction Ratio	130.435

	TR TOTAL REDUX (from Crown)	2.414
IntTailRedux	Short Shaft Bevel Takeoff	0.508
	Intermediate Bevel Gear Takeoff	1.593
TRredux	Tail Rotor Gearbox Reduction Ratio	2.984

TR ACCESSORY REDUXS (from short shaft)	
Oil Cooler Spur Takeoff	1.132
Accessory Spur Takeoff	2.000

Table 50: Planetary Design Calculations (continued)

## JHL PLANETARY XMNS DESIGN V3.5

### ENGINE INPUT GEARBOXES OVERALL DESIGN

#### ENGINE OUTPUTS

	Gear Redux	RPM	TORQUE	Efficiency	HP <sub>in</sub>	HP <sub>loss</sub>	HP <sub>out</sub>	
L High Speed Engine Output Shaft		15,000	36,863.0		8,773.4		8,773.4	CW
C High Speed Engine Output Shaft		15,000	36,991.0		8,803.8		8,803.8	CW
R High Speed Engine Output Shaft		15,000	36,863.0		8,773.4		8,773.4	CW

#### L ENGINE INPUT GEARBOX

	Gear Redux	RPM	T <sub>design</sub> (into)	Efficiency	HP <sub>in</sub>	HP <sub>loss</sub>	HP <sub>out</sub>	
L High Speed Engine Output Shaft		15,000.0	36,863.0		8,773.4		8,773.4	CW
L Freewheeling Clutch		15,000.0	36,863.0	99.5%	8,773.4	43.9	8,729.5	CW
L Bevel Input Shaft		15,000.0	36,678.6		8,729.5		8,729.5	CW
L Bevel Input Pinion		15,000.0	36,678.6		8,729.5		8,729.5	CW
L Bevel Input Gear	2.68	5,587.7	98,461.9	99.5%	8,729.5	43.6	8,685.8	CCW
L Bevel Accessory Takeoff	5.59	1,000.0	844.5	99.5%	13.4	0.066667	13.3	CW
L Engine Gearbox Output Shaft		5,587.7	97,818.4		8,672.4		8,672.4	CW
		5,587.7	97,818.4	99.0%		87.6	8,672.4	

#### C ENGINE INPUT GEARBOX

	Gear Redux	RPM	T <sub>design</sub> (into)	Efficiency	HP <sub>in</sub>	HP <sub>loss</sub>	HP <sub>out</sub>	
C High Speed Engine Output Shaft		15,000.0	36,991.0		8,803.8		8,803.8	CW
C Freewheeling Clutch		15,000.0	36,991.0	99.5%	8,803.8	44.0	8,759.8	CW
C Helical Input Shaft		15,000.0	36,806.1		8,759.8		8,759.8	CW
C Helical Input Pinion		15,000.0	36,806.1		8,759.8		8,759.8	CW
C Helical Idler	1.00	15,000.0	36,806.1	99.5%	8,759.8	43.8	8,716.0	CCW
C Helical Input Gear	2.68	5,587.7	98,310.0	99.5%	8,716.0	43.6	8,672.4	CW
C Engine Gearbox Output Shaft		5,587.7	97,818.4		8,672.4		8,672.4	
		5,587.7	97,818.4	98.5%		131.4	8,672.4	

#### R ENGINE INPUT GEARBOX

	Gear Redux	RPM	T <sub>design</sub> (into)	Efficiency	HP <sub>in</sub>	HP <sub>loss</sub>	HP <sub>out</sub>	
R High Speed Engine Output Shaft		15,000.0	36,991.0		8,773.4		8,773.4	CW
R Freewheeling Clutch		15,000.0	36,863.0	99.5%	8,773.4	43.9	8,729.5	CW
R Bevel Input Shaft		15,000.0	36,678.6		8,729.5		8,729.5	CW
R Bevel Input Pinion		15,000.0	36,678.6		8,729.5		8,729.5	CW
R Bevel Input Gear	2.68	5,587.7	98,461.9	99.5%	8,729.5	43.6	8,685.8	CCW
R Bevel Accessory Takeoff	5.59	1,000.0	844.5	99.5%	13.4	0.066667	13.3	CW
R Engine Gearbox Output Shaft		5,587.7	97,818.4		8,672.4		8,672.4	CW
		5,587.7	97,818.4	99.0%		87.6	8,672.4	

Table 50: Planetary Design Calculations (continued)

**JHL PLANETRARY XMNS DESIGN V3.5****MAIN GEARBOX DESIGN****CROWN BEVEL**

	Gear Redux	RPM	TORQUE	Efficiency	HP <sub>in</sub>	HP <sub>loss</sub>	HP <sub>out</sub>	
L Engine Gearbox Output Shaft		5,587.7	97,818.4		8,672.4		8,672.4	CW
L Crown Bevel Pinion		5,587.7	97,818.4		8,672.4		8,672.4	CW
C Engine Gearbox Output Shaft		5,587.7	97,818.4		8,672.4		8,672.4	CW
C Crown Bevel Pinion		5,587.7	97,818.4		8,672.4		8,672.4	CW
R Engine Gearbox Output Shaft		5,587.7	97,818.4		8,672.4		8,672.4	CW
R Crown Bevel Pinion		5,587.7	97,818.4		8,672.4		8,672.4	CW
Crown Bevel		1,150.0	1,425,871.8	99.50%	26,017.3		26,017.3	CCW
from L Crown Bevel Input	4.86	1,150.0	475,290.6	99.50%	8,672.4	43.4	8,629.1	
from C Crown Bevel Input	4.86	1,150.0	475,290.6	99.50%	8,672.4	43.4	8,629.1	
from R Crown Bevel Input	4.86	1,150.0	475,290.6	99.50%	8,672.4	43.4	8,629.1	
Short Shaft Bevel Takeoff	0.51	2,264.5	91,910.5	99.50%	3,302.3	16.4	3,285.8	CW
1st Stage Sun Shaft		1,150.0	1,237,762.5		22,585.0		22,585.0	CCW
		1,150.0	1,237,762.5	99.44%		146.5	22,585.0	

**1ST STAGE PLANETARY GEAR**

	Gear Redux	RPM	TORQUE	Efficiency	HP <sub>in</sub>	HP <sub>loss</sub>	HP <sub>out</sub>	
Sun 1 Shaft		1,150.0	1,237,762.5		22,585.0		22,585.0	CCW
Spur Sun Gear 1		1,150.0	1,237,762.5		22,585.0		22,585.0	CCW
Per Mesh	Sun 1	1,150.0	210,389.9					CCW
Per Mesh	Planet 1	1,318.8	183,460.0	99.62%	3,838.9	14.4	3,824.5	CW
Per Mesh	Planet 1	1,318.8	183,460.0	99.62%	3,824.5	14.4	3,810.1	CW
Per Mesh	Ring 1	0.0	577,309.8					
Per Mesh	Carrier 1	3.74	307.2		3,810.1		3,810.1	CCW
Carrier 1 total		307.2	4,599,376.6		22,415.4		22,415.4	CCW
Sun 2 Shaft		307.2	4,599,376.6		22,415.4		22,415.4	CCW
Planet speed about post is	966.6	307.2	4,599,376.6	99.25%		169.6309	22,415.4	

**2nd STAGE PLANETARY GEAR**

	Gear Redux	RPM	TORQUE	Efficiency	HP <sub>in</sub>	HP <sub>loss</sub>	HP <sub>out</sub>	
Sun 2 Shaft		307.2	4,599,376.6		22,415.4		22,415.4	
Spur Sun Gear 2		307.2	4,599,376.6		22,415.4		22,415.4	
Per Mesh	Sun 2	307.2	421,153.0					CCW
Per Mesh	Planet 2	915.6	141,284.2	99.62%	2,052.5	7.7	2,044.8	CW
Per Mesh	Planet 2	915.6	141,284.2	99.62%	2,044.8	7.7	2,037.1	CW
Per Mesh	Ring 2	0.0	703,721.5					
Per Mesh	Carrier 2	2.67	115.0		2,037.1		2,037.1	CCW
Carrier 2 total		115.0	12,192,392.4		22,247.0		22,247.0	CCW
Main Rotor Shaft		115.0	12,192,392.4		22,247.0		22,247.0	CCW
Planet speed about post is	572.8	115.0	12,192,392.4	99.25%		168.3569	22,247.0	

Table 50: Planetary Design Calculations (continued)

## JHL PLANETRARY XMNS DESIGN V3.5

### TAIL ROTOR GEARBOX DESIGN

#### OIL COOLER GEARBOX

	Gear Redux	RPM	TORQUE	Efficiency	HP <sub>in</sub>	HP <sub>loss</sub>	HP <sub>out</sub>	
Short Shaft BevelTakeoff		2,264.5	91,453.2		3,285.8		3,285.8	+
Short Shaft		2,264.5	91,453.2		3,285.8		3,285.8	+
Short Shaft Spur Gear		2,264.5	91,453.2		3,285.8		3,285.8	+
Oil Cooler Spur Takeoff Gear	1.13	2,000.0	1,266.8	99.50%	40.2	0.2	40.0	
Accessory Spur Takeoff Pinion	2.00	1,000.0	844.6	99.50%	13.4	0.1	13.3	CCW
Tail Takeoff Shaft Segment		2,264.5	89,961.4		3,232.2		3,232.2	CCW
		2,264.5	89,961.4	99.99%		0.3	3,232.2	

#### INTERMEDIATE TAIL ROTOR GEARBOX

	Gear Redux	RPM	TORQUE	Efficiency	HP <sub>in</sub>	HP <sub>loss</sub>	HP <sub>out</sub>	
Tail Takeoff Shaft Segment		2,264.5	89,961.4		3,232.2		3,232.2	CCW
Intermediate Bevel Pinion		2,264.5	89,961.4		3,232.2		3,232.2	CCW
Intermediate Bevel Gear	1.59	1,421.3	143,332.6	99.50%	3,232.2	16.2	3,216.1	CW
Tail Intermediate Shaft Seg.		1,421.3	142,615.9		3,216.1		3,216.1	CW
		1,421.3	142,615.9	99.50%		16.2	3,216.1	

#### TAIL ROTOR GEARBOX

	Gear Redux	RPM	TORQUE	Efficiency	HP <sub>in</sub>	HP <sub>loss</sub>	HP <sub>out</sub>	
Tail Intermediate Shaft Seg.		1,421.3	142,615.9		3,216.1		3,216.1	CW
Tail Rotor GB Bevel Pinion		1,421.3	142,615.9		3,216.1		3,216.1	CW
Tail Rotor GB Bevel Gear	2.98	476.3	425,560.8	99.50%	3,216.1	16.1	3,200.0	CCW
Tail Rotor Drive Shaft		476.3	423,433.0		3,200.0		3,200.0	CCW
		476.3	423,433.0	99.50%		16.1	3,200.0	

## Weight Equations

**Table 51: Planetary Drive Weight Equations**

### **BOEING VERTOL**

	$a_{mr}$	MR adjustment factor	1
	$a_{tr}$	TR adjustment factor	0.9
	$HP_{mr}$	Drive sys rating	26,350.6
	$HP_{tr}$	TR HP required	3200
	$rpm_{mr}$	MR speed	115
	$rpm_{tr}$	TR speed	476.3
BO_z	$Z_{mr}$	Number of stages in main drive	4
BO_kt	$k_t$	Configuration factor	1
BO_W_mr	$W_{dsmr}$	Weight of MR drive sys	12,023.9
BO_W_tr	$W_{dstr}$	Weight of TR drive sys	1,337.5
BO_W_Dsys	$W_{ds}$	Weight of drive sys	13,361.4

### **RTL**

	$HP_{xmmr}$	Transmission rating	27,000.0	26,350.6
	$rpm_{mr}$	MR speed	115	
	$T_{mrgb}$	Ratio of Xmns rating to MR rpm	234.8	
	$HP_{tr}$	TR HP required	1,989.0	
	$rpm_{tr}$	TR speed	476.3	
	$T_{trgb}$	Ratio of TR hp to its rpm to $T_{mrgb}$	1.8	
RTL_ngb	$n_{gb}$	Number of gearboxes	7	
RTL_Ldr	$L_{dr}$	Horiz distance in ft b/w rotors	45	
RTL_ndsh	$n_{dsh}$	Number of drive shafts	10	
RTL_Wgb	$W_{gb}$	Weight of gearboxes	15,835.2	
RTL_Wdsh	$W_{dsh}$	Weight of drive shafts	784.9	
RTL_Wds	$W_{ds}$	Weight of drive sys	16,620.1	



## Modified Solid Rotor Volume Weight Estimation

**Table 52: Planetary Drive Solid Rotor Volume Weight Estimations**

### WEIGHT ESTIMATION (SOLID ROTOR VOLUME METHOD)

	Kplan	600		
	Kbv	600		
	Kspur	600		
	K	600		
<b>GEARBOX WEIGHT SUMMARY</b>				
Engine Input Gearbox Left		348.9 lb		
Engine Input Gearbox Center		424.5 lb		
Engine Input Gearbox Right		348.9 lb		
Oil Cooler Gearbox		4.9 lb		
Intermediate Tail Rotor Gearbox		431.8 lb		
Tail Rotor Gearbox		1,571.5 lb		
Main Rotor Gearbox		10,599.3 lb		
		13,729.8		
			G	0.25
<b>PLANETARY TOTAL WEIGHT</b>				
			Solid Rotor Volume	7,868.4 lbs
			Optimal Weight	7,785.5 lbs

**TOTAL GEARBOX WEIGHT 13,729.8 lb**

Name	m <sub>a</sub>	RPM	TQ	K	Vol	G	Weight	Sys Weight
<b>ENGINE INPUT GEARBOX LEFT</b>								
L Bevel Input Pinion		15,000.0	36,678.6	600	167.8	0.25	42.0	
L Bevel Input Gear	2.6844	5,587.7	98,461.9	600	1,209.3	0.25	302.3	344.3
L Bevel Input Gear		5587.743741	151.1	600	0.6	0.25		
L Bevel Accessory Takeoff	5.5877	1000	844.5	600	18.5	0.25	4.6	4.6
<b>ENGINE INPUT GEARBOX CENTER</b>								
C Helical Input Pinion		15000	36,806.1	600	245.4	0.25	61.3	
C Helical Idler	1	15000	36,806.1	600	245.4	0.25	61.3	122.7
C Helical Idler		15000	36,822.1	600	167.5	0.25		
C Helical Input Gear	2.6844	5587.743741	98,310.0	600	1,207.4	0.25	301.8	301.8
<b>ENGINE INPUT GEARBOX RIGHT</b>								
R Bevel Input Pinion		15,000.0	36,678.6	600	167.8	0.25	42.0	
R Bevel Input Gear	2.6844	5,587.7	98,461.9	600	1,209.3	0.25	302.3	344.3
R Bevel Input Gear		5587.743741	151.1	600	0.6	0.25		
R Bevel Accessory Takeoff	5.5877	1000	844.5	600	18.5	0.25	4.6	4.6
<b>CROWNWHEEL</b>								
L Crown Bevel Pinion		5587.743741	97,818.4	600	393.2	0.25	98.3	
from L Crown Bevel Input	4.8589	1150	475,290.6	600	9,282.3	0.25		98.3
C Crown Bevel Pinion		5587.743741	97,818.40701	600	393.2	0.25	98.3	
from C Crown Bevel Input	4.8589	1150	475,290.6013	600	9,282.3	0.25		98.3
R Crown Bevel Pinion		5587.743741	97,818.40701	600	393.2	0.25	98.3	
from R Crown Bevel Input	4.8589	1150	475,290.6013	600	9,282.3	0.25		98.3
Crown Bevel	4.8589	1150	475,290.6	600	9,282.3	0.25	2,320.6	2,320.6
Crown Bevel		1,150.0	180,979.9	600	1,791.2	0.25		
Short Shaft Bevel Takeoff	0.5078	2264.451662	91910.49964	600	462.0	0.25	115.5	115.5
<b>OIL COOLER GEARBOX</b>								
Short Shaft Spur Gear		2264.451662	1118.894589	600.0	7.0	0.25	1.8	
Oil Cooler Spur Takeoff Gear	1.1322	2000	1266.841356	600.0	9.0	0.25	2.3	2.3
Short Shaft Spur Gear		2264.451662	422.280452	600	2.1	0.25	0.5	
Accessory Spur Takeoff Pinion	2	1000	844.560904	600	8.4	0.25	2.1	2.1
Short Shaft Spur Gear	0	2264.451662	422.280452	600	2.111402	0.25	0.527851	0.5

Table 52: Planetary Drive Solid Rotor Volume Weight Estimations (continued)

**INTERMEDIATE TAIL ROTOR GEARBOX**

Intermediate Bevel Pinion		2264.451662	89961.37402	600	488.1	0.25	122.0	
Intermediate Bevel Gear	1.5933	1421.262355	143332.5678	600	1,239.0	0.25	309.7	431.8

**TAIL ROTOR GEARBOX**

Tail Rotor GB Bevel Pinion		1421.262355	142615.9049	600	634.7	0.25	158.7	
Tail Rotor GB Bevel Gear	2.984	476.3	425560.8167	600	5,651.4	0.25	1,412.8	1,571.5

**1ST STAGE PLANETARY GEAR**

Spur Sun Gear 1		1150	1237762.546	600		0.25		
Number of Planets	6							
Mo1	3.744							
ms1	0.872							
Spur Sun Gear 1		1,150.0	1,237,762.5	600	1,505.5	0.25	376.4	
Spur Planet 1 total weight		1318.807339	183459.9594	600	6,735.0	0.25	1,683.8	
					per planet	286.2		
Spur Ring 1		0.0	577,309.8	600.0	4,534.4	0.25	1,133.6	3,193.7

**2ND STAGE PLANETARY GEAR**

Spur Sun Gear 2		307.1581197	4599376.634	600		0.25		
Number of Planets	11							
Mo2	2.671							
ms1	0.3355							
Spur Sun Gear 2		307.2	4,599,376.6	600	5,588.5	0.25	1,397.1	
Spur Planet 1 total weight		307.1581197	4599376.634	600	6,868.6	0.25	1,717.1	
					per planet	157.2		
Spur Ring 1		0.0	421,153.0	600.0	6,241.4	0.25	1,560.3	4,674.6

## **Force Feed Oil Cooling**

**Table 53: Planetary Drive Force Feed Oil Cooling  
LUBRICATION ANALYSIS**

<b><u>SYMBOL</u></b>	<b><u>DESCRIPTION</u></b>	<b><u>UNITS</u></b>	<b><u>IN</u></b>	<b><u>MESH</u></b>	<b><u>OUT</u></b>
<b>MAIN GEARBOX</b>					
HP	Power	hp	26,017.3		25,483.7
$\eta_{\text{mesh}}$	efficiency			97.9%	
$P_{\text{loss}}$	Power dissipated	hp		533.7	
Q	heat generated	Btu/min		22,627.9	
$C_p$	Specific heat of oil	Btu/lb-°F		0.5	
	Oil flow design			2	
		lb/min		1005.684	
M	Oil flow	gal/min		134.0913	134.0913
		lb/min		900	
$M_{\text{manual}}$	Oil flow	gal/min		120	
		lb/min		1005.7	
$M_{\text{HLH}}$	HLH Design oil flow ( $\Delta T = +45^\circ\text{F}$ )	gal/min		134.1	
		lb/min		1508.5	
$M_{\text{rec}}$	Recommended oil flow	gal/min		201.1	
		gpm/hp		0.002	
	Rule of thumb	gpm		52.0347	
$\Delta T$	Temperature rise	°F		45.0	
$t_{\text{in}}$	Incoming oil temperature	°F		125	
$t_{\text{out}}$	Outgoing oil temperature	°F		170.0	
$t_{\text{oil}}$	Oil temperature (average)	°F		147.5	
<b>ENGINE INPUT GEARBOXES</b>					
HP	Power	hp	8,773.4		8,672.4
$\eta_{\text{mesh}}$	efficiency			98.8%	
$P_{\text{loss}}$	Power dissipated	hp		100.9	
Q	heat generated	Btu/min		4,278.8	
$C_p$	Specific heat of oil	Btu/lb-°F		0.5	
	Oil flow design			2	
		lb/min		190.1674	
M	Oil flow	gal/min		25.35565	32.16674
		lb/min		900	
$M_{\text{manual}}$	Oil flow	gal/min		120	
		lb/min		190.2	
$M_{\text{HLH}}$	HLH Design oil flow ( $\Delta T = +45^\circ\text{F}$ )	gal/min		25.4	
		lb/min		285.3	
$M_{\text{rec}}$	Recommended oil flow	gal/min		38.0	
		gpm/hp		0.002	
	Rule of thumb	gpm		17.5467	
$\Delta T$	Temperature rise	°F		45.0	
$t_{\text{in}}$	Incoming oil temperature	°F		125	
$t_{\text{out}}$	Outgoing oil temperature	°F		170.0	
$t_{\text{oil}}$	Oil temperature (average)	°F		147.5	

## Minimum Weight Solution

**Table 54: Planetary Drive Minimum Weight Solution  
MINIMIZED SOLUTION**

$W_1$	1st stage weight	3,145.9	
$W_2$	2nd stage weight	4,639.5	
$W_{total}$	Total Weight	7,785.5	
$M_{o1}$	1st stage redux ratio	3.7440	3.7440
$M_{o2}$	2nd stage redux ratio	2.6709	
$b_1$	# Stage 1 planets	5.883185321	
$b_2$	# Stage 2 planets	10.92091529	

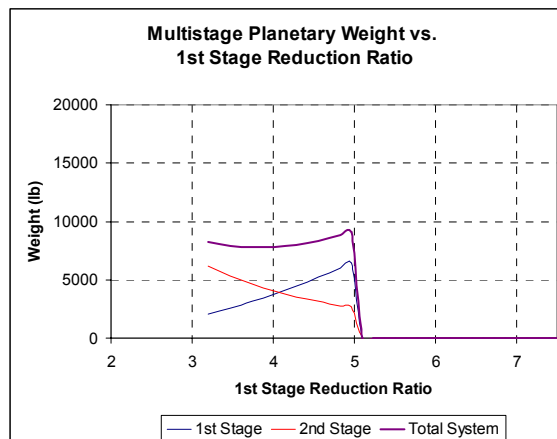
$M_o'$  10.00

Maximum Number of Planets

$m$	slope	2.7467
$c$	intercept	2.7333
$b_1$	# Stage 1 planets	6
$b_2$	# Stage 2 planets	11

Current Settings

$M_{o1}$	1st stage redux ratio	3.744
$M_{o2}$	2nd stage redux ratio	2.670940171
$G$	Application factor	0.25
$K_{planetary}$	K factor	600 lb/in <sup>2</sup>
$T_{sun1}$	Torque at 1st stage sun	1,219,239.2 in lb 12,192,392.4



## **APPENDIX E: SPLIT TORQUE DRIVE CALCULATIONS**

## Design Calculations

**Table 55: Split Torque Drive Design Calculations**

### **JHL SPLIT TORQUE XMNS DESIGN V3.5**

#### **PERFORMANCE FACTORS**

##### **POWER PLANT**

NASA High-Tech Engine

Number of Engines	3.00			
Drive System Rated Power	8,293	8,293	8,293	24,878.8
Maximum Continuous Power (MCP)	8,293	8,293	8,293 shp	
Intermediate Rated Power (IRP)	9,827	9,827	9,827 shp	
Maximum Rated Power (MRP)	10,521	10,521	10,521 shp	
Contingency Power (CP)	11,512	11,512	11,512 shp	
Engine High Speed Output Shaft Speed	15,000		rpm	

##### **MAIN ROTOR**

Tip Speed	725 ft/s	NumbBevInput
Diameter	120.4 ft	
Rotor System Speed (100% Speed)	115.0 rpm	NumbIdlers
Main Rotor Power Required	22,247.0 hp	

##### **DESIGN FACTORS**

#NAME?

# Bevel Input Split Per Path	2
# Engines	3
# Idlers per Input Spur	2

##### **TAIL ROTOR**

Tip Speed	725 ft/s	SpurCombRedux
Diameter	29.1 ft	IdlerRedux
Tail Rotor System Speed (100% Speed)	476.3 rpm	
Tail Rotor Power Required	1,989.0 hp	TRGBRedux
		IntTRGBRedux
		TakeoffBevRedux

##### **OVERALL REDUCTION RATIOS**

Spur Combiner	11.70
Spur Idler	3.29
Bevel Input	3.39
TR GB Redux	2.00
IntTRGB Redux	2.19
Takeoff Bevel Redux	0.64

##### **OVERALL SPEEDS**

High Speed Engine Output Shaft	15,000.0 rpm
Main Rotor Shaft	115.0 rpm
Tail Shaft	2,090.2 rpm
Intermediate Tail Shaft	952.6 rpm
Tail Rotor Shaft	476.3 rpm

**EFFICIENCY 97.90%**

##### **SHAFT DATA**

Tail Shaft	2,009.0 hp
IntTailShaft	2,009.0 hp
Main Rotor Shaft Torque	##### in lb
Tail Shaft Torque	60,578.1 in lb
Intermediate Tail Shaft Torque	132,256.3 in lb
Tail Rotor Shaft Torque	263,190.1 in lb

##### **MISCELLANEOUS**

HPloss	602.8 hp
Accessory Takeoff Power	40.0 hp
Accessory Speed	1,000.0 rpm
Freewheeling Clutch	99.50%
Spur or Helical Gear	99.50%
Bevel Gear	99.50%

Combiner pinions per combiner	12
Combiners per MR Shaft	2

Table 55: Split Torque Drive Design Calculations (continued)

## JHL SPLIT TORQUE XMNS DESIGN V3.5

### ENGINE OUTPUTS

	Gear Redux	RPM	TORQUE	Efficiency	HP <sub>in</sub>	HP <sub>loss</sub>	HP <sub>out</sub>
L High Speed Engine Output Shaft		15,000	34,844.3		8,292.9		8,292.9
C High Speed Engine Output Shaft		15,000	34,844.3		8,292.9		8,292.9
R High Speed Engine Output Shaft		15,000	34,844.3		8,292.9		8,292.9
					8,292.9	0.0	8,292.9

### BEVEL INPUT

	Gear Redux	RPM	TORQUE	Efficiency	HP <sub>in</sub>	HP <sub>loss</sub>	HP <sub>out</sub>
High Speed Engine Output Shaft		15,000.0	34,844.3		8,292.9		8,292.9
Freewheeling Clutch		15,000.0	34,844.3	99.5%	8,292.9	41.5	8,251.5
Bevel Input Shaft		15,000.0	34,670.1		8,251.5		8,251.5
Bevel Input Pinion		15,000.0	17,250.6		4,105.6		4,105.6
Bevel Input Gear	3.39	4,421.9	58,517.3	99.5%	4,105.6	20.5	4,085.1
Bevel Accessory Takeoff	4.42	1,000.0	2,533.7	99.5%	40.2	0.2	40.0
Bevel Output Shaft		4,421.9	58,224.7		4,085.1		4,085.1
	3.39			99.0%	24,878.8	248.2	24,630.6

### COMBINER BOX

	Gear Redux	RPM	TORQUE	Efficiency	HP <sub>in</sub>	HP <sub>loss</sub>	HP <sub>out</sub>
Bevel Output Shaft		4421.921	58,224.7		4,085.1		4,085.1
Input Spur		4421.921	58,224.7		4,085.1		4,085.1
Idler	3.29	1345.5	95,676.4	99.5%	2,042.6	10.2	2,032.3
Idler Shaft		1345.5	95,198.0		2,032.3		2,032.3
Combiner Pinion		1345.5	47,599.0		1,016.2		1,016.2
Spur Tail Takeoff Pinion	0.09	1345.5	47,527.4	99.5%	1,014.6	5.1	1,009.6
Combiner	11.70	115.0	6,126,830.4	99.50%	11,179.4	55.9	11,123.5
Main Rotor Shaft		115.0	12,192,392.4		22,247.0		22,247.0
	38.45	115.0	12,192,392.4	99.0%	24,510.6	244.5	24,266.1

Table 55: Split Torque Drive Design Calculations (continued)

#### Tail Takeoff Box

	Gear Redux	RPM	TORQUE	Efficiency	HP <sub>in</sub>	HP <sub>loss</sub>	HP <sub>out</sub>
Spur Tail Takeoff Pinion		1345.5	47,289.8		1,009.6		1,009.6
Takeoff Shaft		1345.5	94,579.5		2,019.1		2,019.1
Takeoff Bevel Pinion		1345.5	94,579.5		2,019.1		2,019.1
Takeoff Bevel Gear	0.64	2090.203	60,882.5	99.5%	2,019.1	10.1	2,009.0
Tail Shaft		2090.203	60,578.1		2,009.0		2,009.0
	0.64	2090.203	60,578.1	199.0%	1,009.6	-999.5	2,009.0

#### Intermediate TR Gearbox

	Gear Redux	RPM	TORQUE	Efficiency	HP <sub>in</sub>	HP <sub>loss</sub>	HP <sub>out</sub>
Tail Shaft		2090.203	60,578.1		2,009.0		2,009.0
Intermediate Tail Bevel Pinion		2090.203	60,578.1		2,009.0		2,009.0
Intermediate Tail Bevel Gear	2.19	952.6	132,920.9	99.5%	2,009.0	10.0	1,999.0
Intermediate Tail Shaft		952.6	132,256.3		1,999.0		1,999.0
	2.19	952.6	132,256.3	99.5%	2,009.0	10.0	1,999.0

#### Tail Rotor Gearbox

	Gear Redux	RPM	TORQUE	Efficiency	HP <sub>in</sub>	HP <sub>loss</sub>	HP <sub>out</sub>
Intermediate Tail Shaft		952.6	132,256.3		1,999.0		1,999.0
Tail Bevel Pinion		952.6	132,256.3		1,999.0		1,999.0
Tail Bevel Gear	2.00	476.3	264,512.6	99.5%	1,999.0	10.0	1,989.0
Tail Rotor Drive Shaft		476.3	263,190.1		1,989.0		1,989.0
	2.00	476.3	263,190.1	99.5%	1,999.0	10.0	1,989.0



## Weight Equations

**Table 56: Split Torque Weight Equations**

### **BOEING VERTOL**

	$a_{mr}$	MR adjustment factor	1
	$a_{tr}$	TR adjustment factor	0.9
	$HP_{mr}$	Drive sys rating	24,878.8
	$HP_{tr}$	TR HP required	1989
	$rpm_{mr}$	MR speed	115
	$rpm_{tr}$	TR speed	476.3
BO_z	$Z_{mr}$	Number of stages in main drive	24
BO_kt	$k_t$	Configuration factor	1
BO_W_mr	$W_{dsmr}$	Weight of MR drive sys	15,619.4
BO_W_tr	$W_{dstr}$	Weight of TR drive sys	914.3
BO_W_Dsys	$W_{ds}$	Weight of drive sys	16,533.7

### **RTL**

	$HP_{xmmr}$	Transmission rating	24,878.8
	$rpm_{mr}$	MR speed	115
	$T_{mrgb}$	Ratio of Xmns rating to MR rpm	216.3
	$HP_{tr}$	TR HP required	1,989.0
	$rpm_{tr}$	TR speed	476.3
	$T_{trgb}$	Ratio of TR hp to its rpm to $T_{mrgb}$	1.9
RTL_ngb	$n_{gb}$	Number of gearboxes	5
RTL_Ldr	$L_{dr}$	Horiz distance in ft b/w rotors	45
RTL_ndsh	$n_{dsh}$	Number of drive shafts	13
RTL_Wgb	$W_{gb}$	Weight of gearboxes	14,274.1
RTL_Wdsh	$W_{dsh}$	Weight of drive shafts	834.6
RTL_Wds	$W_{ds}$	Weight of drive sys	15,108.6

## Modified Solid Rotor Volume Weight Estimation

**Table 57: Split Torque Modified Solid Rotor Volume Weight Estimation**

### **SOLID ROTOR VOLUME FOR GEARBOXES**

Kplan	600
Kbv	600
Kspur	600
K	600
G	0.25

<b>TOTAL GB WEIGHT</b>	<b>13,325.1</b>
------------------------	-----------------

<u>Name</u>	<u>m<sub>G</sub></u>	<u>RPM</u>	<u>TQ</u>	<u>K</u>	<u>Vol</u>	<u>G</u>	<u>Weight</u>	<u>Component Weight</u>
<b>BEVEL INPUT GEARBOX</b>								
Bevel Input Pinion	0	15,000.0	17,250.6	600	74.5	0.25	18.6	111.7
Bevel Input Gear	3.392191	4,421.9	58,517.3	600	856.7	0.25	214.2	1,285.1
Bevel Input Gear		4421.921	573.0	600	2.3	0.25	214.1827	
Bevel Accessory Takeoff	4.421921	1000	2,533.7	600	45.8	0.201005	9.2	27.6
<b>COMBINER GEARBOX</b>								
Input Spur		4421.921	58,224.7	600	253.1	0.25	63.3	379.7
Idler	3.286452	1345.5	95,676.4	600	2,324.0	0.25	581.0	3,486.0
Combiner Pinion		1345.5	47,599.0	600	146.4	0.25	36.6	878.3
Combiner	11.7	115	6,126,830.4	600	10,079.0	0.25	2,519.7	5,039.5
<b>OC GEARBOX</b>								
Spur Tail Takeoff Pinion	0.08547	1345.5	47,527.4	600	2,012.0	0.25	503.0	1,006.0
Combiner	11.7	115	6,126,830.4					
<b>INTERMEDIATE TAIL ROTOR GEARBOX</b>								
Takeoff Bevel Pinion		1345.5	94,579.5	600	805.0	0.25	201.3	201.3
Takeoff Bevel Gear	0.643717	2090.203	60,882.5	600	333.6	0.25	83.4	83.4
<b>TAIL ROTOR GEARBOX</b>								
Tail Bevel Pinion		952.6	132,256.3	600	661.3	0.25	165.3	165.3
Tail Bevel Gear	2	476.3	264,512.6	600	2,645.1	0.25	661.3	661.3
								13,325.1

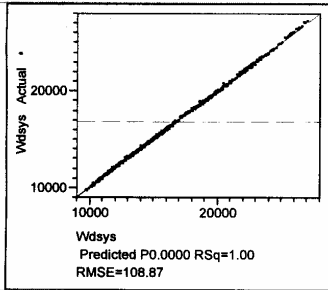
## **APPENDIX F: MODEL FIT FOR PLANETARY DRIVE**

# Table 58: RSE Model Fit for Planetary Drive

Fit Model

## Response Wdsys

### Actual by Predicted Plot



### Summary of Fit

RSquare	0.999304
RSquare Adj	0.999293
Root Mean Square Error	108.8652
Mean of Response	16815.12
Observations (or Sum Wgts)	2187

### Analysis of Variance

Source	DF	Sum of Squares	Mean Square	F Ratio	Prob > F
Model	35	3.68182e10	1.04824e9	88277.71	
Error	2151	25492871.9	11851.637		
C. Total	2186	3.68437e10		0.0000	

### Parameter Estimates

Term	Estimate	Std Error	t Ratio	Prob> t
Intercept	26125.942	316.6603	82.50	0.0000
Interm. TR Redux	-986.0615	39.44366	-25.00	<.0001
MR hp	1.0941462	0.006988	156.57	0.0000
MR rpm	-260.6584	3.080695	-84.61	0.0000
Planetary Redux	-133.6421	8.905187	-15.01	<.0001
TR GB Redux	-418.0653	19.72183	-21.20	<.0001
TR hp	-2.78e-12	0.050831	-0.00	1.0000
TR rpm	-20.32902	0.828631	-24.53	<.0001
Interm. TR Redux *Interm. TR Redux	150.49946	4.938227	30.48	<.0001
MR hp *Interm. TR Redux	-2.09e-11	0.000537	-0.00	1.0000
MR hp *MR hp	-0.000001	1.169e-7	-11.36	<.0001
MR rpm *Interm. TR Redux	-0.88001	0.174593	-3.89	0.0001
MR rpm *MR hp	-0.005508	0.000027	-205.1	0.0000
MR rpm *MR rpm	1.2261494	0.012346	99.32	0.0000
Planetary Redux *Interm. TR Redux	-4.986742	0.698371	-7.14	<.0001
Planetary Redux *MR hp	0.0132642	0.000107	123.45	0.0000
Planetary Redux *MR rpm	-0.741775	0.034919	-21.24	<.0001
Planetary Redux *Planetary Redux	7.5611567	0.197529	38.28	<.0001
TR GB Redux*Interm. TR Redux	48.129144	1.745927	27.57	<.0001
TR GB Redux*MR hp	-2.16e-11	0.000269	-0.00	1.0000
TR GB Redux*MR rpm	-0.340005	0.087296	-3.89	0.0001
TR GB Redux*Planetary Redux	-2.493371	0.349185	-7.14	<.0001
TR GB Redux*TR GB Redux	72.684085	1.234557	58.87	0.0000
TR hp *Interm. TR Redux	8.718e-14	0.004108	0.00	1.0000
TR hp *MR hp	1.477e-18	6.32e-7	0.00	1.0000
TR hp *MR rpm	4.78e-15	0.000205	0.00	1.0000
TR hp *Planetary Redux	0	0.000822	0.00	1.0000
TR hp *TR GB Redux	3.223e-14	0.002054	0.00	1.0000
TR hp *TR hp	7.218e-16	0.000007	0.00	1.0000
TR rpm *Interm. TR Redux	0.4455135	0.045056	9.89	<.0001
TR rpm *MR hp	3.864e-13	0.000007	0.00	1.0000
TR rpm *MR rpm	-0.003067	0.002253	-1.36	0.1735
TR rpm *Planetary Redux	-0.022494	0.009011	-2.50	0.0128
TR rpm *TR GB Redux	-0.169958	0.022528	-7.54	<.0001
TR rpm *TR hp	-3.28e-15	0.000053	-0.00	1.0000
TR rpm *TR rpm	0.0158758	0.000822	19.31	<.0001

### Effect Tests

Source	Nparm	DF	Sum of Squares	F Ratio	Prob > F
Interm. TR Redux	1	1	7406824	624.9621	<.0001
MR hp	1	1	290522520	24513.28	0.0000
MR rpm	1	1	84844603	7158.893	0.0000
Planetary Redux	1	1	2669185	225.2165	<.0001
TR GB Redux	1	1	5325646	449.3595	<.0001
TR hp	1	1	0	0.0000	1.0000
TR rpm	1	1	7133269	601.8805	<.0001
Interm. TR Redux *Interm. TR Redux	1	1	11007942	928.8119	<.0001
MR hp *Interm. TR Redux	1	1	0	0.0000	1.0000
MR hp *MR hp	1	1	1530632	129.1494	<.0001
MR rpm *Interm. TR Redux	1	1	179787	15.1698	0.0001
MR rpm *MR hp	1	1	498355578	42049.51	0.0000
MR rpm *MR rpm	1	1	116907682	9864.264	0.0000
Planetary Redux *Interm. TR Redux	1	1	604283	50.9873	<.0001
Planetary Redux *MR hp	1	1	180631807	15241.08	0.0000
Planetary Redux *MR rpm	1	1	5348237	451.2657	<.0001

Table 58: RSE Model Fit for Planetary Drive (continued)

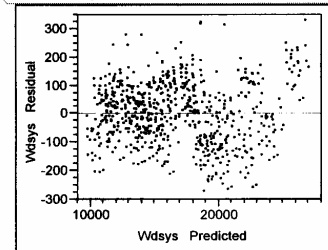
Fit Model

## Response Wdsys

## Effect Tests

Source	Nparm	DF	Sum of Squares	F Ratio	Prob > F
Planetary Redux *Planetary Redux	1	1	17365719	1465.259	<.0001
TR GB Redux*Intern. TR Redux	1	1	9006219	759.9135	<.0001
TR GB Redux*MR hp	1	1	0	0.0000	1.0000
TR GB Redux*MR rpm	1	1	179787	15.1698	0.0001
TR GB Redux*Planetary Redux	1	1	604283	50.9873	<.0001
TR GB Redux*TR GB Redux	1	1	41080423	3466.223	0.0000
TR hp *Intern. TR Redux	1	1	0	0.0000	1.0000
TR hp *MR hp	1	1	0	0.0000	1.0000
TR hp *MR rpm	1	1	0	0.0000	1.0000
TR hp *Planetary Redux	1	1	0	0.0000	1.0000
TR hp *TR GB Redux	1	1	0	0.0000	1.0000
TR hp *TR hp	1	1	0	0.0000	1.0000
TR rpm *Intern. TR Redux	1	1	1158755	97.7717	<.0001
TR rpm *MR hp	1	1	0	0.0000	1.0000
TR rpm *MR rpm	1	1	21971	1.8538	0.1735
TR rpm *Planetary Redux	1	1	73846	6.2309	0.0126
TR rpm *TR GB Redux	1	1	674548	56.9160	<.0001
TR rpm *TR hp	1	1	0	0.0000	1.0000
TR rpm *TR rpm	1	1	4418893	372.8508	<.0001

## Residual by Predicted Plot



## Scaled Estimates

Continuous factors centered by mean, scaled by range/2

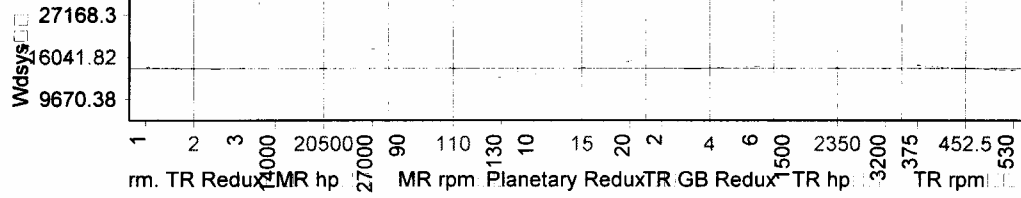
Term	Scaled Estimate	Std Error	t Ratio	Prob> t
Intercept	16041.818	9.015928	1779.28	0.0000
Intern. TR Redux	-139.5545	2.851087	-48.95	0.0000
MR hp	4113.0081	2.851087	1442.61	0.0000
MR rpm	-2381.079	2.851087	-835.15	0.0000
Planetary Redux	1266.9395	2.851087	444.37	0.0000
TR GB Redux	215.91698	2.851087	75.73	0.0000
TR hp	-1.23e-11	2.851087	-0.00	1.0000
TR rpm	-497.9408	2.851087	-174.65	0.0000
Intern. TR Redux *Intern. TR Redux	150.49946	4.938227	30.48	<.0001
MR hp *Intern. TR Redux	-1.36e-7	3.491854	-0.00	1.0000
MR hp *MR hp	-56.11995	4.938227	-11.36	<.0001
MR rpm *Intern. TR Redux	-13.6002	3.491854	-3.89	0.0001
MR rpm *MR hp	-716.0388	3.491854	-205.06	0.0000
MR rpm *MR rpm	490.45977	4.938227	99.32	0.0000
Planetary Redux *Intern. TR Redux	-24.93371	3.491854	-7.14	<.0001
Planetary Redux *MR hp	431.08606	3.491854	123.45	0.0000
Planetary Redux *MR rpm	-74.1775	3.491854	-21.24	<.0001
Planetary Redux *Planetary Redux	189.02892	4.938227	38.28	<.0001
TR GB Redux*Intern. TR Redux	96.258287	3.491854	27.57	<.0001
TR GB Redux*MR hp	-2.809e-7	3.491854	-0.00	1.0000
TR GB Redux*MR rpm	-13.6002	3.491854	-3.89	0.0001
TR GB Redux*Planetary Redux	-24.93371	3.491854	-7.14	<.0001
TR GB Redux*TR GB Redux	290.73634	4.938227	58.87	0.0000
TR hp *Intern. TR Redux	7.411e-11	3.491854	0.00	1.0000
TR hp *MR hp	8.162e-12	3.491854	0.00	1.0000
TR hp *MR rpm	8.126e-11	3.491854	0.00	1.0000
TR hp *Planetary Redux	0	3.491854	0.00	1.0000
TR hp *TR GB Redux	5.478e-11	3.491854	0.00	1.0000
TR hp *TR hp	5.215e-10	4.938227	0.00	1.0000
TR rpm *Intern. TR Redux	34.527297	3.491854	9.89	<.0001
TR rpm *MR hp	1.9466e-7	3.491854	0.00	1.0000
TR rpm *MR rpm	-4.754325	3.491854	-1.36	0.1735
TR rpm *Planetary Redux	-8.716262	3.491854	-2.50	0.0126
TR rpm *TR GB Redux	-26.34349	3.491854	-7.54	<.0001
TR rpm *TR hp	-2.16e-10	3.491854	-0.00	1.0000
TR rpm *TR rpm	95.35393	4.938227	19.31	<.0001

Table 58: RSE Model Fit for Planetary Drive (continued)

Fit Model

Response Wdsys

Prediction Profiler



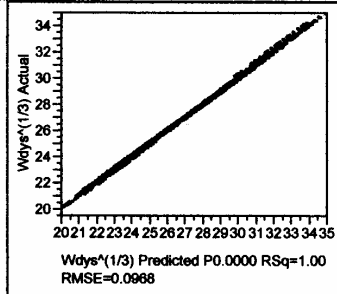
## **APPENDIX G: MODEL FIT FOR SPLIT TORQUE DRIVE**

Table 59: RSE Model Fit for Split Torque Drive

Fit Model

Response Wdys<sup>1/3</sup>(1/3)

Actual by Predicted Plot



Summary of Fit

RSquare	0.998954
RSquare Adj	0.998937
Root Mean Square Error	0.098838
Mean of Response	28.49931
Observations (or Sum Wgts)	2136

Analysis of Variance

Source	DF	Sum of Squares	Mean Square	F Ratio
Model	35	18806.116	537.318	57298.35
Error	2100	19.693	0.009378	Prob > F
C. Total	2135	18825.809		0.0000

Lack Of Fit

Source	DF	Sum of Squares	Mean Square	F Ratio
Lack Of Fit	2098	19.692835	0.009386	
Pure Error	2	0.000000	0.000000	Prob > F
Total Error	2100	19.692835		

Max RSq  
1.0000

Parameter Estimates

Term	Estimate	Std Error	t Ratio	Prob> t
Intercept	51.194464	0.234807	218.03	0.0000
MR HP	0.0008549	0.000008	113.34	0.0000
MR rpm	-0.286128	0.002713	-98.08	0.0000
Eng rpm	0.0003785	0.000008	49.25	0.0000
TR HP	0.0016302	0.000044	37.27	<.0001
TR GB Redux	0.032184	0.023389	1.38	0.1692
Spur Combiner Redux	-2.744049	0.013525	-202.9	0.0000
Idler Redux	-3.845215	0.038747	-99.24	0.0000
MR HP*MR HP	-3.961e-9	1.47e-10	-26.93	<.0001
MR HP*MR rpm	-0.000001	2.901e-8	-42.20	<.0001
MR rpm*MR rpm	0.000694	0.000011	62.64	0.0000
MR HP*Eng rpm	1.3581e-9	1.14e-10	11.88	<.0001
MR rpm*Eng rpm	-8.507e-7	3.191e-8	-26.66	<.0001
Eng rpm *Eng rpm	-1.93e-11	1.78e-10	-0.11	0.9134
MR HP*TR HP	-2.464e-8	6.74e-10	-36.59	<.0001
MR rpm*TR HP	-0.000001	1.866e-7	-8.00	<.0001
Eng rpm *TR HP	-1.659e-9	7.41e-10	-2.24	0.0252
TR HP *TR HP	-4.202e-8	6.152e-9	-6.83	<.0001
MR HP*TR GB Redux	-0.000003	3.816e-7	-8.90	<.0001
MR rpm*TR GB Redux	-0.000284	0.000106	-2.68	0.0073
Eng rpm *TR GB Redux	-8.777e-7	4.198e-7	-1.81	0.1098
TR HP *TR GB Redux	0.0000505	0.000002	20.46	<.0001
TR GB Redux*TR GB Redux	0.0170681	0.001977	8.63	<.0001
MR HP*Spur Combiner Redux	-0.000016	1.934e-7	-84.53	0.0000
MR rpm*Spur Combiner Redux	0.00482	0.000054	91.01	0.0000
Eng rpm *Spur Combiner Redux	-0.00001	2.127e-7	-47.21	0.0000
TR HP *Spur Combiner Redux	0.0000025	0.000001	2.01	0.0445
TR GB Redux*Spur Combiner Redux	-0.003713	0.000705	-5.27	<.0001
Spur Combiner Redux *Spur Combiner Redux	0.0785114	0.000493	155.27	0.0000
MR HP*Idler Redux	-0.000009	5.802e-7	-15.66	<.0001
MR rpm*Idler Redux	0.0077078	0.000162	47.52	0.0000
Eng rpm *Idler Redux	-0.000046	6.382e-7	-71.71	0.0000
TR HP *Idler Redux	0.0000105	0.000004	2.81	0.0050
TR GB Redux*Idler Redux	0.0044581	0.002115	2.11	0.0351
Spur Combiner Redux *Idler Redux	0.0897352	0.001081	83.00	0.0000
Idler Redux*Idler Redux	0.4121047	0.004432	92.99	0.0000



Table 59: RSE Model Fit for Split Torque Drive (continued)

Fit Model

Response Wdys^(1/3)

Effect Tests

Source	Nparm	DF	Sum of Squares	F Ratio	Prob > F
MR HP	1	1	120.46875	12846.52	0.0000
MR rpm	1	1	90.20164	9618.902	0.0000
Eng rpm	1	1	22.74965	2425.972	0.0000
TR HP	1	1	13.02919	1389.403	<.0001
TR GB Redux	1	1	0.01773	1.8911	0.1692
Spur Combiner Redux	1	1	386.02378	41164.71	0.0000
Idler Redux	1	1	92.35528	9848.561	0.0000
MR HP*MR HP	1	1	6.80222	725.3730	<.0001
MR HP*MR rpm	1	1	16.70164	1781.026	<.0001
MR rpm*MR rpm	1	1	36.79433	3923.666	0.0000
MR HP*Eng rpm	1	1	1.32295	141.0796	<.0001
MR rpm*Eng rpm	1	1	6.66401	710.6354	<.0001
Eng rpm *Eng rpm	1	1	0.00011	0.0118	0.9134
MR HP*TR HP	1	1	12.55514	1338.853	<.0001
MR rpm*TR HP	1	1	0.59969	63.9813	<.0001
Eng rpm *TR HP	1	1	0.04704	5.0159	0.0252
TR HP *TR HP	1	1	0.43763	46.8676	<.0001
MR HP*TR GB Redux	1	1	0.74236	79.1636	<.0001
MR rpm*TR GB Redux	1	1	0.06752	7.2002	0.0073
Eng rpm *TR GB Redux	1	1	0.02444	2.6059	0.1066
TR HP *TR GB Redux	1	1	3.92458	418.5087	<.0001
TR GB Redux*TR GB Redux	1	1	0.69893	74.5326	<.0001
MR HP*Spur Combiner Redux	1	1	67.00271	7145.019	0.0000
MR rpm*Spur Combiner Redux	1	1	77.66891	8282.439	0.0000
Eng rpm *Spur Combiner Redux	1	1	20.90294	2229.043	0.0000
TR HP *Spur Combiner Redux	1	1	0.03792	4.0441	0.0445
TR GB Redux*Spur Combiner Redux	1	1	0.26025	27.7529	<.0001
Spur Combiner Redux *Spur Combiner Redux	1	1	226.07964	24108.63	0.0000
MR HP*Idler Redux	1	1	2.30065	245.3363	<.0001
MR rpm*Idler Redux	1	1	21.18034	2258.624	0.0000
Eng rpm *Idler Redux	1	1	48.22748	5142.87	0.0000
TR HP *Idler Redux	1	1	0.07408	7.8996	0.0050
TR GB Redux*Idler Redux	1	1	0.04167	4.4440	0.0351
Spur Combiner Redux *Idler Redux	1	1	64.59434	6888.196	0.0000
Idler Redux*Idler Redux	1	1	81.06295	8646.505	0.0000

Residual by Predicted Plot

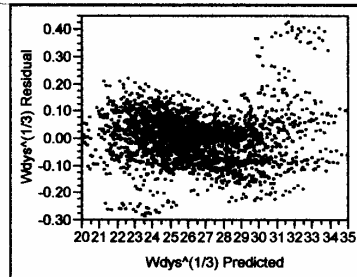
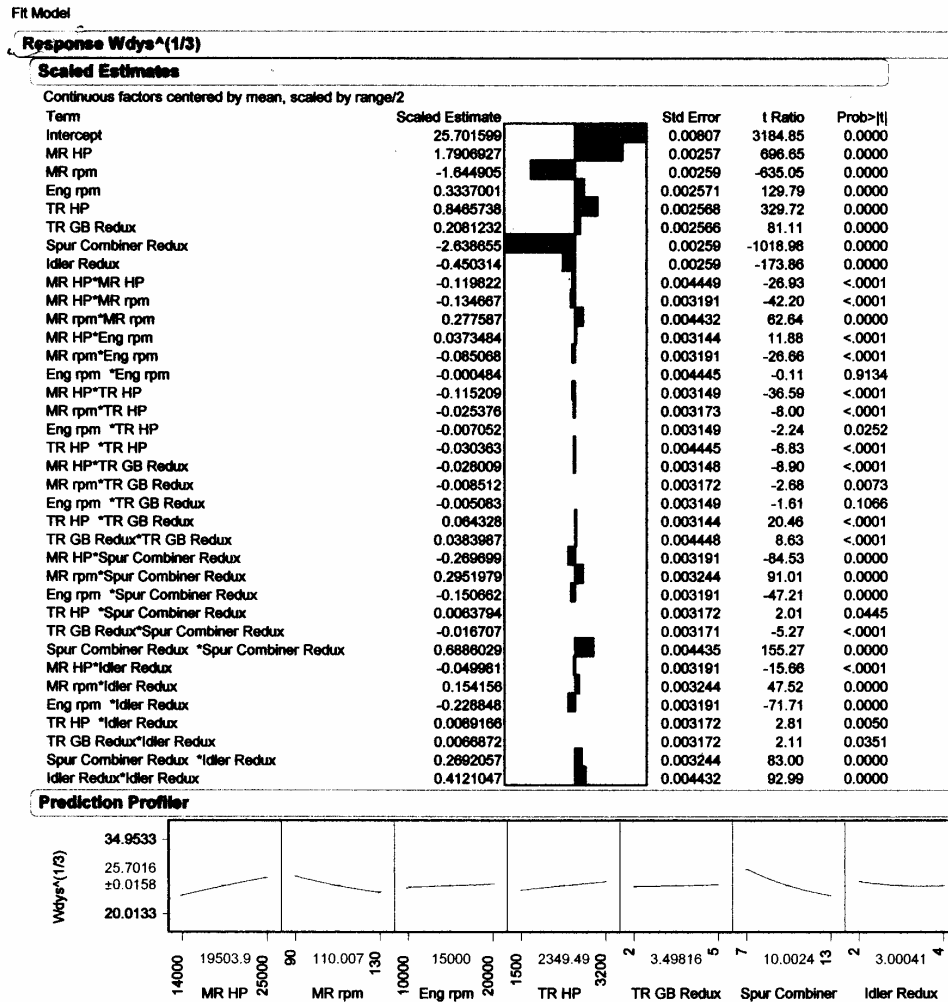


Table 59: RSE Model Fit for Split Torque Drive (continued)



## REFERENCES

American Gear Manufacturers Association, *AGMA 911-A94, Information Sheet-Design Guidelines for Aerospace Gearing*. Alexandria: AGMA, 1994.

American Gear Manufacturers Association, *AGMA Standard 2001-C95, Fundamental Rating Factors and Calculation Method for Involute Spur and Helical Gear Teeth*. Alexandria: AGMA, 1995.

American Gear Manufacturers Association, *AGMA Standard 908-B89, Information Sheet, Geometry Factors for Determining the Pitting Resistance and Bending Strength of Spur, Helical and Herringbone Gear Teeth*. Alexandria: AGMA, 1989.

American Gear Manufacturers Association, *ANSI/AGMA 2003-B97, Rating the Pitting Resistance and Bending Strength of Generated Straight Bevel, Zerol Bevel, and Spiral Bevel Gear Teeth*. Alexandria: AGMA, 1997.

Aviation Applied Technology Directorate, "Joint Heavy Lift Supplemental Package." November, 2004.

Dudley, Darle, Handbook of Practical Gear Design. Lancaster, Pennsylvania: Technomic, 1994.

Gmirya, Yuriy et al, "Design and Analysis of 5100 HP RDS-21 Demonstrator Gearbox." 60<sup>th</sup> Annual Forum Proceedings, vol 2. Alexandria: AHS International, 2004.

Hands Schuh, R., D. Lewicki, and R. Bossler, NASA TR 92-C-008 Experimental Testing of Prototype Face Gears for Helicopter Transmissions. Prepared for "Gearbox Configurations of the 90's" sponsored by the Institute of Mechanical Engineers Solihull, West Midlands, United Kingdom, October 28, 1992.

Headquarters, U.S. Army Material Command, AMC Pamphlet 706-201 Engineering Design Handbook: Helicopter Engineering (Part One: Preliminary Design). Alexandria, Virginia: GPO, 1974.

Johnson, Wayne, "Heavy Lift Rotorcraft Plans and Status." Ames Research Center: NASA, June 8, 2004.

Kirby, Michelle R., "An Overview of Response Surface Methodology" as presented in AE6373 lecture. Atlanta: Georgia Institute of Technology, August 25, 2004.

Litvin, F.L. et al, NASA/CR-2000-209909 Handbook on Face Gear Drives With a Spur Involute Pinion. NASA, March 2000.

Lynwander, Peter, Gear Drive Systems Design and Application. New York: Marcel Dekker, 1983.

Mack, J.C., USAAMRDL-TR-77-38: HLH Drive System. Philadelphia: Boeing Vertol, 1977.

NASA Research and Technology website,  
<http://www.grc.nasa.gov/WWW/RT1995/2000/2730h.htm>. November 1, 2005.

Reductor website, <http://www.reductor-pm.ru/eng/allpr.html>. September 14, 2005.

Shigley, Joseph and Charles Mischke, Mechanical Engineering Design, 5<sup>th</sup> ed. New York: McGraw-Hill, 1989.

Stepniewski, W.Z. and R.A. Shinn, NASA TR 82-A-10 A Comparative Study of Soviet vs. Western Helicopters: Part 2-Evaluation of Weight, Maintainability and Design Aspects of Major Components. Ames Research Center: AVRADCOM Research and Technology Laboratories, 1983.

Tishchenko, Marat N, “Mil Design Bureau Heavy-Lift Helicopters.” Presented at local chapters of the AHS in June 1996.

Wikipedia website, [http://en.wikipedia.org/wiki/Square-cube\\_law](http://en.wikipedia.org/wiki/Square-cube_law). 1 August, 2005.

Willis, R.J., “New Equations and Charts Pick Off Lightest-weight Gears,” Product Engineering v. 34, n.s. 2 (January 21, 1963): 64-75.